DISTRIBUTION AGREEMENT

In presenting this thesis or dissertation as a partial fulfillment of the requirements for an advanced degree from Emory University, I hereby grant to Emory University and its agents the non-exclusive license to archive, make accessible, and display my thesis or dissertation in whole or in part in all forms of media, now or hereafter known, including display on the world wide web. I understand that I may select some access restrictions as part of the online submission of this thesis or dissertation. I retain all ownership rights to the copyright of the thesis or dissertation. I also retain the right to use in future works (such as articles or books) all or part of this thesis or dissertation.

_____ _____

Daniel Rios Date

The Role of M Cells in the Development of the Mucosal Immune System

By
Daniel C. Rios
Doctor of Philosophy
Graduate Division of Biological and Biomedical Sciences
Immunology and Molecular Pathogenesis

_____
Ifor R. Williams
Advisor

_____
Timothy L. Denning
Committee Member

_____
Joshy Jacob
Committee Member

_____
David Weiss
Committee Member

_____
Jacob Kohlmeier
Committee Member

Accepted:

_____
Lisa A. Tedesco. Ph.D.
Dead of the James T. Laney School of Graduate Studies

_____
Date

The Role of M cells in the Development of the Mucosal Immune System

By

Daniel C. Rios

B.S. Brandeis University

Advisor: Ifor R. Williams, M.D., Ph.D.

An abstract of a dissertation submitted to the Faculty of the
Graduate School of Emory University in partial fulfillment
of the requirements for the degree of
Doctor of Philosophy

Graduate Division of Biological and Biomedical Sciences
Immunology and Molecular Pathogenesis
2016

Abstract

The Role of M Cells in the Development of the Mucosal Immune System

By

Daniel C. Rios

The mucosal immune system is tasked with the unique challenge of maintaining tolerance to beneficial commensal microbiota while simultaneously responding to and swiftly eliminating dangerous pathogens in the gut. The precise mechanisms underlying this duality have only begun to be unraveled.

We developed a novel mouse model of intestinal M cell deficiency based on a conditional knockout of the receptor for RANKL in intestinal epithelial cells. Using this first-of-its-kind model to study the role of M cells in the maintenance of homeostasis in intestinal tissues, we found two non-redundant roles for M cells in the development of the mucosal immune system. We observed that M cells were required for the sampling of large particulate antigen into Peyer's patches (PPs) in the gut. In the absence of M cells germinal center formation in PPs was delayed, resulting in a 10-14 day lag in the initiation of secretory IgA responses in the gut. These defects were not observed when M-cell-deficient mice were reared in the absence of commensal microbiota, indicating microbe-derived antigen sampled by M cells is the primary means of initiating IgA responses in the gut. Continuing these studies we sought to characterize other immune responses in the gut in the absence of M cells. We found, unexpectedly, that the frequency and function of group 3 innate lymphoid cells(ILC3s) in mice lacking PP M cells were reduced. The reduction in ILC3s combined with the delayed initiation of IgA responses in the gut resulted in an increased susceptibility of M cell deficient mice to systemic bacterial infections immediately after weaning. These results indicate that M cells are critical, non-redundant mediators of cross-talk between host and microbiota. Further characterization of M cells using this model system may provide potentially translatable insights in the mechanisms of disease pathogenesis in mucosal tissues.

The Role of M Cells in the Development of the Mucosal Immune System

By

Daniel C. Rios

B.S. Brandeis University

Advisor: Ifor R. Williams, M.D., Ph.D.

A dissertation submitted to the Faculty of the Graduate School of Emory University in partial fulfillment of the requirements for the degree of
Doctor of Philosophy

Graduate Division of Biological and Biomedical Sciences
Immunology and Molecular Pathogenesis
2016

Acknowledgements

First I would like to thank my advisor Dr. Ifor Williams for giving me the opportunity to work in his lab, for his insights into difficult questions, and encouragement. From the moment I joined his lab he treated me with the respect of a colleague and collaborator, not of a student. Under his guidance I was allowed to independently guide my research. This occasionally led me to dead end paths, but whenever I needed help he would always redirect me back to a productive line of investigation. His guidance shaped me into the scientist I am today.

I would also like to thank Professor Timothy Denning for the critical, sometimes devastatingly so, analysis of my work during our joint lab meetings. Your criticisms of my work forced me to constantly do better, and I thank you for that.

To the rest of my thesis committee - Professors Weiss, Jacob, and Kohlmeier – I would like to express my gratitude for their encouragement and their novel perspectives which allowed me to approach my research questions from directions.

I would like to thank my lab mates past and present, and the friends I made in grad school for providing companionship and solid foundation on which my research has thrived.

My time at Emory has provided me a fantastic education and the training to be a successful scientist. These were things that drew me here, but my time at Emory has also given me something that is not listed in any brochure. Geetha, without you these last seven years would have been totally unbearable. You are all things to me. You support me both emotionally and scientifically, you are my best friend, and the love of my life and for that I thank you.

Finally, I would like to thank my family. You have provided encouragement and support throughout my life, and without you I would not be here today.

Dedication

The work I do every day is dedicated to my parents. You gave me every opportunity to succeed, and to repay you I have seized those opportunities.

Table of Contents

List of Figures

(Listed in order of appearance in each chapter)

Introduction

Overview of the Mucosal Immune System

The systemic immune system is tasked with the duty to protect host organisms from infectious organisms and to facilitate clearance of toxic substances. Generally speaking this function is achieved by the ability of cells of the immune system to distinguish self from non-self. Substances recognized by the host immune system as non-self are either cleared or neutralized by a variety of immune mechanisms. This general paradigm of self vs. non-self, in contrast to the systemic immune system, does not hold true at mucosal sites, particularly in the intestinal tract.[1]

The cells of the mucosal immune system are constantly interacting with non-self antigen in the form of commensal microbiota. Despite this flood of non-self antigen the mucosal immune system is *not* in a constant state of inflammation. There are multiple redundant mechanisms in place at mucosal barriers that ensure maintenance of tolerance with the microbiota including anti-inflammatory cytokines, regulatory T cells, and physical barriers. Every cell type within the mucosa, both lymphoid and mesenchymal in origin, is dedicated in some way to maintaining immune homeostasis, while concomitantly retaining the possibility of initiating an inflammatory cascade should a potentially pathogenic threat be detected.

The mucosal immune system can be broken down into three component parts: the physical barrier created by intestinal epithelial cells, innate immune cells that support epithelial function and swiftly respond to potential pathogens and adaptive immune responses that allow for long-term immunity to potential pathogens. Individual cell types have a multitude of functional abilities and their precise role will be context dependent –

in certain immune states some populations of cells can be defined as beneficial, while in other states the same populations of cells can be deleterious.

Organization of the Mucosal Immune System

The mucosal immune system is divided into two unique compartments: the gut-associated lymphoid tissue (GALT) and the diffuse lamina propria. There are two types of GALT structures; large multifollicular bodies such as Peyer's patches (PPs) and small isolated lymphoid follicles. PPs are macroscopic aggregations of lymphoid cells comparable in size to peripheral lymph nodes (LN).[2] In mice PPs are located throughout the small intestine, while in humans PPs are concentrated in the terminal ileum. PPs have similar immunoarchitecture to lymph nodes –multiple large B cell follicles and peripheral T cell zones containing CD4 and CD8 T lymphocytes with antigen-presenting cells (APCs) interspersed throughout. One critical difference between PPs and LNs is that PPs lack afferent lymphatics. Instead of antigens entering PPs via afferent lymphatics, PPs have specialized epithelial cells, called M cells, which have the ability to sample particulate antigen and facilitate crosstalk between the contents of the gut and the mucosal immune system. [3] The cecal and colonic patches are similar in structure to PPs, but are located in the cecum and large intestine respectively. ILFs are also similar in structure to PPs but are much smaller in size, only contain a single follicle, and house relatively low frequencies of T cells. [4]

GALT structures are sites where mucosal immune responses are initiated and coordinated, but the lamina propria is where these immune responses are deployed. The lamia propria is the layer of stromal cells connecting the intestinal epithelium to

underlying muscle. The ephemeral nature of this connective tissue allows for a dense network of immune cells to reside within the lamina propria where they can carry out their various effector functions in response to antigen sampled and transported from the PP.

Physical Barrier

Similar to the epidermis, which physically separates self from non-self at the skin, the intestinal epithelial cells (IEC) are responsible for the physical segregation of self vs. non-self in the gut. The architecture of the intestinal epithelium of the small intestine has two component parts: crypts and villi. Crypts are where intestinal stem cells reside and from this niche all other types of intestinal epithelial cells originate. Villi are short finger-like projections that are designed to maximize total surface area for nutrient absorption. The predominant cell type of the intestinal epithelium is the basic absorptive enterocyte. Functionally, these cells are responsible for nutrient uptake and mediating physical separation of self and non-self. Adjacent enterocytes are linked by tight junction adhesion molecules such as occludin and claudins, which restrict the movement of bacteria past this layer.[5] Enterocytes are also able to produce a variety of antimicrobial peptides such as α - and β-defensins and the REG family of proteins that have bacteriostatic and bactericidal properties.[6]

Goblet cells are specialized epithelial cells that have the capacity to secrete large amounts of mucus [7]. The mucus layer present in the gut is essential to the maintenance of mucosal homeostasis; mice lacking goblet cells have high rates of postnatal mortality due to massive systemic bacterial infections.[8] Goblet cells are located throughout the small

and large intestine at a density ranging from 10-30 per villus depending on relative location in the intestine. Recently, goblet cells have been determined to have the ability to sample low molecular weight antigens in a process directly linked to mucus exocytosis.[9]

Paneth cells are a unique population of epithelial cells that reside in the crypt region. The role of Paneth cells is twofold: supporting the stem cell niche, and producing large quantities of antimicrobial products. Similar to goblet cells, mice lacking Paneth cells have extremely high rates of postnatal mortality due to severe defects in epithelial cell turnover.[10]

Finally there are M cells, which are a rare type of cells overlaying the GALT. M cells have several unique modifications relative to basic enterocytes: they lack a traditional brush border, which allows for particulate antigens to directly abut with their apical surface; they have a basolateral invagination which allows for lymphocytes and antigen-presenting cells to reside in very close proximity to the lumen of the small intestine; and they have the ability to sample large particulate antigens such as whole bacteria. M cells are found exclusively on the epithelium overlaying GALT in the region commonly referred to as the follicle-associated epithelium (FAE).[11]

Innate Barriers

Nearly every cell type of the innate immune system can be found in the mucosal immune system. The roles of these immune cells are fluid and can be described as "good" or "bad" depending on context. For example, neutrophils are important for swiftly responding to gut pathogens and for the restoration of barrier functions, but are also

deleterious mediators of inflammation in chronic diseases such as Crohn's disease and ulcerative colitis.[12] A similar framework can be used to describe essentially all cell types in the gut. Another notable example are macrophages, which are normally refractory to stimulation due in part to decreased expression of CD14 (LPS receptor), CD89, CD16, CD32 and CD64 (immunoglobulin receptors) [13, 14], but can become highly pro-inflammatory during mucosal insult, and are partially responsible for chronic mucosal immune pathologies. [15]

Dendritic cells (DCs) are also present throughout the lamina propria and are critical mediators linking the innate and adaptive immune system of the gut. Once they acquire antigen, migratory DCs are responsible for initiating adaptive immune responses in the gut. The precise phenotypic markers distinguishing DCs from macrophages, and tissue-resident from migratory cells in the gut remains an area of intense investigation. While few details can be fully agreed on, it is widely accepted that different populations of DCs and macrophages in the gut are highly specialized in their functions.[16] One critical feature of mucosal DCs is their ability to imprint a gut phenotype on target adaptive immune cells. This imprinting is achieved through context dependent antigen presentation. DCs have the ability to produce retinoic acid (RA) from vitamin A – antigen presentation in the presence of RA results in increased expression of the gut homing integrin α4β7 facilitating localization of cells to mucosal surfaces.[17]

Innate lymphoid cells (ILC) are a recently defined subset of lymphoid lineage cells that lack antigen specific receptors, but are functionally analogous to various traditional T cell subsets.[18] ILCs are defined by their capacity to produce particular sets of cytokines. Group 1 ILCs produce IFN-γ and TNF-α and are functionally similar to

CD8 T cells and Th1 CD4 T cells, Group 2 ILCs produce IL-4, IL-5, IL-9 and IL-13 akin to Th2 CD4 T cells [19] [20], and group 3 ILCs (ILC3s) can produce IL-17 and IL-22 and are comparable to Th17 / Th22 T cells.[21] In the gut, ILC3s predominate and are involved primarily in the maintenance of barrier integrity. ILC3s respond to the cytokine IL-23 produced by DCs that have received some form of Toll-like receptor (TLR) stimulation. IL-23 stimulation causes ILC3s to produce IL-22 and / or IL-17. IL-22 promotes epithelial cell turnover and the production of a range of previously described anti-microbial products while IL-17 initiates a sweeping pro-inflammatory cascade.[22]

Adaptive Immune Cells

The adaptive immune system of mucosal tissues can be defined by differences in cellular frequency and function relative to systemic immune compartments. IgA-secreting plasma cells, FoxP3+ T regulatory cells (Tregs), and Th17 cells are present at high densities throughout the small and large intestine, with Tregs found predominantly in the large intestine and Th17s predominantly found in the small intestine.

B cells responses in the gut are heavily skewed towards IgA production at mucosal sites due to high concentrations of transforming growth factor β (TGF-β) found in GALT structures[23] and the diffuse lamina propria. Traditional T-dependent IgA responses generate high affinity long-lived antibody responses while elevated levels of BAFF, APRIL and TACI support T-independent IgA responses.[24] Further discussion of IgA responses will be carried out in subsequent sections.

Tregs are thought to have several important roles for maintaining mucosal homeostasis. Elegant studies by Powrie identified a definitive role for Tregs in limiting

pathological immune responses against the microbiota .[25] Several reports have identified Tregs as the primary cellular source of TGF-β, which, as previously mentioned is key in generation of IgA immune responses and generally acts to limit all sources of cellular inflammation in the gut.[26] Studies of patients with ulcerative colitis or Crohn's disease have identified critical roles for these cells in limiting inflammation associated with these pathologies. Finally, one of the key regulatory functions of Tregs in the gut is mediating oral tolerance, an immune phenomenon by which food antigens fail to induce inflammatory immune responses. [27]

On the opposite end of the functional spectrum from Tregs lay Th17s, which exist primarily to initiate potent antibacterial, antifungal and antiparasitic immune responses. Gastrointestinal infection studies using mouse models in which IL-17 production is significantly reduced have uncovered a key role for IL-17-mediated protection during various pathologies. This key role in inflammatory responses is a double-edged sword as Th17s have also been identified as pathologic in a variety of immune disorders including ulcerative colitis, Crohn's disease and several models of autoimmunity. [28-30]

What is the Microbiota?

The human microbiota is defined as the ecological community of microorganisms that can be found on all surfaces of the human body, with bacteria being the dominant component. The highest density of bacteria can be found in the gastrointestinal tract where estimates place upwards to 10^{10} bacteria / gram feces. [31] Investigations into the role of the microbiota in health and disease began in earnest in the mid-to-late 1990s, although there are numerous anecdotes prior to this hinting at a potential role for bacteria

in the maintenance of mammalian homeostasis. Research into the microbiota has driven many discoveries in mucosal immunology paralleling the actual relationship between the microbiota and the mucosal immune system.

The mammalian intestinal microbiota is dominated by three bacterial phyla – Firmicutes, Bacteroidetes, and Proteobacteria – with numerous other bacterial phyla present as minor, but not insignificant, components. Estimates have identified as many as 1,000 unique bacterial species in the intestinal microbiota, but this number seems to depend on sampling and sequencing methodologies [32] Mucosal immunologists and microbiologists have attempted to classify individual members or community states of the microbiota as "good" or "bad" with limited success. Microbiota profiling of diverse human communities indicate that the makeup of the microbiota does indeed correlate to some disease states, however it is uncertain whether the composition of the microbiota is a cause or indicator of said disease states.[33] To further complicate matters, genetic and cultural factors appear to play significant roles in microbiota composition, indicating that a healthy microbiota for one individual may be pathologic in another individual. Despite the difficulties in discerning cause from effect in humans, mouse models have shed some light on the precise mechanisms by which the microbiota influences the mucosal immune system.

Segmented Filamentous Bacteria (SFB) are members of the *Firmicutes* bacterial phylum. In mice these bacteria are found preferentially in the terminal ileum of the small intestine, and appear to play important roles in the development of the adaptive mucosal immune system; colonization of ex-germ-free mice with SFB results in increased frequencies of Th17 T cells[34] and IgA[35] secreting B cells. Unlike all other non-pathogenic

members of the microbiota, SFB directly interact with epithelial cells under homeostatic conditions. SFB are literally anchored to epithelial cells thorough a "holdfast" structure in which one end of the bacteria is burrowed into an epithelial cell. Elegant studies in mice have identified that the population of Th17s induced after colonization with SFB are clonal in nature and SFB-reactive.[36] The mechanisms underlying the potent immunostimualtory nature of SFB are uncertain, but remain an active area of inquiry.

Recently a consortium of *Clostridia* has been identified as possessing immunomodulatory potential. Researchers in Japan identified a group of 13 members of the *Clostridia* family of bacteria, that when introduced to germ-free mice potently induced Foxp3+ regulatory T cells. This functional capacity was then linked to the production of the short chain fatty acid (SCFA) butyrate. These studies are notable because these bacteria were first isolated from human samples and then functionally studied in mice, indicating that this bacterial consortium may have potential therapeutic uses in humans suffering from chronic inflammatory disorders.[37, 38]

Finally bacteria from *Alcaligenes* genus have been determined to homeostatically reside directly in GALT structures of the mucosal immune system. Using a variety of techniques researchers found that these bacteria were able to reside within small intestine PP, some frequency of these bacteria were alive, and residence of this bacteria in PPs resulted in the induction of *Alcaligenes*-specific immune responses. These bacteria were also found in the GALT of non-human primates and humans indicating that they may play a fundamental role in the development of the mammalian mucosal immune system. [39] While the apparent niche of these bacteria is provocative, it is uncertain what

consequences PP colonization with *Alcaligenes* has on the development of the mucosal immune system.

Synergistic Development of the Mucosal Immune System and the Microbiota

At birth and during weaning the mucosal immune system is very poorly developed. There are two primary reasons for this; lack of complete colonization by commensal microbiota and protective immune functions of maternal breast milk. Longitudinal studies of the development of the murine mucosal immune system demonstrate that as mice transition away from breast milk and onto a solid food diet the density and maturation state of lymphoid cells at mucosal sites increases. Furthermore, this maturation does not occur in the absence of commensal microbiota under germ-free conditions.[40] In addition to the mucosal immune system maturing over time, the composition of the microbiota itself changes and matures over time. Thus the development of the mucosal immune system and the commensal microbiota are inextricably linked.[41]

It is clear that the microbiota and the mucosal immune system are entangled in a complicated interaction where any action affects both parties. What is unclear is what precise mechanisms underlie this entanglement. To date there have been four unique mechanisms of antigen sampling that have been show to directly facilitate crosstalk between the mucosal immune system and the commensal microbiota. M cells located on the follicle-associated epithelium (FAE) of GALT structures can sample particulate antigens such as whole bacteria. [42, 43] In the lamina propria certain populations of antigen presenting cells can directly sample the contents of the lumen by extending dendrites

between adjacent enterocytes while maintaining barrier integrity.[44] Goblet cells can sample low molecular weight antigen – a process that appears to be a result of fluid reflux that occurs after mucus secretion. [9] Lastly, absorptive enterocytes appear to have the ability to sample very low molecular weight antigen such as linear peptides and by products of bacterial metabolism, although it is debatable as to whether these processes should be considered antigen sampling or simply nutrient absorption.[45] However, a pressing question in the field of mucosal immunology is identification of the qualitative/quantitative differences in the downstream mucosal/systemic immune responses when certain mechanisms of antigen uptake are blocked.

Antigen Sampling in the Villous Epithelium

The primary function of the villous epithelium is nutrient uptake. However in addition to its primary function, there is evidence that several pathways of antigen sampling relevant to priming the immune system are active. Observations by Rescigno et al. in an *in vitro* model system demonstrated that under particular conditions it appeared that special populations of gut derived antigen presenting cells have the ability to sample antigens across a monolayer of intestinal epithelial cells.[44] Further in vivo studies using CX3CR1-GFP reporter mice found evidence that a similar process was taking place in the gut. GFP+ processes were observed to interdigitate between adjacent epithelial cells in the small intestine without disrupting expression of tight junction adhesion molecules indicating that this mechanism of sampling can occur under homeostatic conditions. Intragastric challenge of CX3CR1 deficient mice with fluorescently labeled bacteria (*E. coli and* non-invasive *Salmonella typhimurium)* resulted in reduced translocation of these

bacteria to the mesenteric lymph node.[46] The conclusion of these studies was that expression of CX3CR1 on DCs in the small intestine was necessary and sufficient for this manner of bacterial sampling.

Further scrutiny of these observations has raised concerns that this mechanism of sampling may have little impact in the actual functioning of the mucosal immune system. CX3CR1 has been recently identified as a marker of a special tissue resident population of lamina propria DCs that do not migrate to the draining mesenteric lymph node, and appear incapable of priming downstream immune responses.[47] A more recent study by McDole *et al.* allowed for the in vivo identification of resident lamina propria DCs and classical migratory DCs using a dual reporter system. This experimental system yielded the unexpected observation that it was migratory DCs, not the previously identified CX3CR1+ subpopulation that were acquiring luminal antigen. Furthermore, this second study used intravital microscopy on living tissue as opposed to confocal imaging on frozen sections, used in the initial study characterizing the importance of CX3CR1 in bacterial sampling. In this study by McDole *et al*., interdigitating DC processes were not observed in the small intestine; rather it appeared that DCs were acquiring antigen from goblet cells that were able to acquire low molecular weight antigen after mucus exocytosis.[9]

Studies of antigen sampling in the small intestine have yielded extremely confusing and contradictory results, probably for several reasons. Under normal, non-experimentally modified conditions, sampling of any given antigen is extremely unlikely due to the abundance of total antigen present in the lumen. Experimental setups, such as gastric loops or introductions of relatively large boluses of antigens and or fluids,

probably disrupt normal barrier mechanisms that prevent epithelial interactions from taking place. The mucus layer in the small intestine, although not as restrictive as that of the large intestine, largely prevents direct interaction between the cells of the lamina propria and the commensal microbiota. There has also been a dearth of evidence suggesting that any one of these processes can initiate an immune response. The overwhelming majority of these studies have focused on the capture of antigen while ignoring the downstream consequences of antigen acquisition. For these reasons it is unlikely that the antigen sampling processes in the small intestine described above play a role in the generation of homeostatic responses to the microbiota.

Antigen Sampling Across the FAE

The follicle-associated epithelium (FAE) of GALT structures has several modifications that promote sampling of large particulate antigen. A decreased frequency of goblet cells results in a relatively thin glycocalax and allows for more direct interactions between particulate antigens and epithelial cells.[48] But the primary distinguishing characteristic of the FAE relative to the normal villous epithelium is the presence of specialized antigen sampling epithelial cells termed M cells. M cells have the ability to directly sample large particulate antigen and smaller antigens in a variety of manners including clathrin-coated vesicle endocytosis [49], phagocytosis and fluid phase macropinocytosis.[50] Once a target antigen is acquired by an M cells it can be rapidly transferred to antigen-presenting cells that reside in an intraepithelial pocket on the basolateral side of the M cell.[51] Whereas antigen sampling in the villous epithelium is unlikely to play a large role in induction of mucosal immune responses, antigen sampling

across the FAE is a highly efficient process designed to orchestrate complex mucosal immune responses.

Development and Function of M cells

M cells are a unique population of epithelial cells found exclusively on the follicle-associated epithelium (FAE) of GALT structures. They share the polarized structural configuration of normal intestinal epithelial cells (IEC), but also retain several important structural and functional modifications relative to basic IEC. The two characteristic features of M cells are; decreased apical glycocalyx and a basolateral pocket-like invagination.

The apical surface of absorptive enterocytes is designed to maximize surface area for nutrient absorption while minimizing contact with large macromolecules. The total surface area of enterocytes is maximized by the presence of microvilli – microscopic membrane protrusions – while a glycocalyx – a continuous layer of heavily glycosylated proteins – prevents direct interactions between the apical surface of enterocytes and the microbiota. The apical surface of M cells lacks both of these structures and instead is characterized by irregular “microfolds” (the source of the “M” in M cells) and large areas of exposed plasma membrane. M cells are capable of various forms of antigen uptake including clathrin-mediated endocytosis of inert particles and large macromolecules, actin-dependent phagocytosis, and macropinocytosis.

The identities of proteins located on the apical surface of M cells remain poorly characterized, with one notable exception. GP2 is a GPI-anchored membrane protein that is highly expressed on the surface of M cells in the intestinal epithelium relative to other

intestinal epithelial cells, although it is also highly expressed on pancreatic acinar cells. Functionally GP2 is required for efficient M-cell sampling of bacteria expressing the $FimH^+$ bacterial adhesion protein.[52] Due to its M-cell specific expression pattern in the gut, protein staining for GP2 has become the gold standard of M cell identification *in vivo*. It is speculated that there are other proteins present on the surface of M cells which confer specificity to antigen acquisition, but these other hypothetical proteins have yet to be discovered. The glycosylation pattern of M cells differs from other enterocytes and it is thought that the glycan present on the surface of M cells may confer some broad specificity to antigen acquisition by M cells. In the small intestine M cells can be identified through use of the lectin UEA-I derived from the *Ulex europaeus* plant. This lectin binds to a unique alpha-1-2-fucose moiety present on M cells.[53] However the M-cell-specific expression pattern of this moiety is only present under homeostatic conditions. The introduction of various immunostimulatory compounds in the gut results in expression of the same alpha-1-2-fucose moiety on all intestinal epithelial cells.

Once M cells acquire antigen it is loaded into an endosomal vesicle, which is then rapidly trafficked to the basolateral pocket where it is released to the immune system. The exact processes that take place during transcytosis in an M cell are unclear, but it appears that limited processing takes place inside of M cells. Due to the deep basolateral invagination present on the basolateral surface of M cells, the total distance for endosomes to be transcytosed is very small (1-2 μm), and as such trafficking of antigens from the gut lumen to the cells residing in the basolateral pocket of M cells takes mere minutes.[11]

Until very recently the exact mechanism by which epithelial cells are induced to differentiate into M cells was unknown. LT-α -/- and LT-β-/- deficient mice lack development of secondary organized lymphoid tissues such as PPs, and as such lack the immunoarchitecture required for M cell development.[54] Recently RANKL, a TNF superfamily member, has been identified as the primary driver of M cell differentiation. Mice lacking either RANKL or RANK also lacked PP M cells, and administration of rRANKL to RANK-/- mice rescued PP M cell differentiation in these mice.[55] Identification of RANKL as a key factor in M cell differentiation allowed for a full differentiation analysis of M cells. Using a combination of in vivo and in vitro model systems, the Ets family transcription factor Spi-B was identified as the master regulator of M cell differentiation.[56]

While much progress has been made in M-cell biology, both in terms of development and function, the immunological consequences of M-cell-mediated antigen acquisition remain poorly understood. Based on their location, M cells have long been thought to play a key role in many mucosal processes, but lack of suitable models of M-cell deficiency have hampered direct investigation of these questions.

Generation and function of mucosal IgA responses

At mucosal sites the overwhelming majority of plasma cells secrete the IgA isotype of antibody. Enterocytes expressing the polymeric immunoglobulin receptor (pIgR) bind IgA and facilitate retrograde transport and secretion of IgA in the gut lumen.[57] However a definitive role for IgA in maintenance of homeostasis is elusive as

IgA-deficient mice and humans are mostly healthy with only subtle immune deficits and perturbations.

The primary functional role of secretory IgA in the gut is to limit direct interactions between the microbiota and the host immune system through a set of diverse processes collectively referred to as "immune exclusion".[58] Immune exclusion was initially thought to be absolute, with no interaction between the host and the microbiota. We now know that there is constant interaction between the host and the microbiota and that proper regulation of these interactions is required for homeostatic development of the mucosal immune system.

As IgA is first and foremost an antibody, the majority of its functional capabilities are determined through the sequence of its complementarity-determining region 3 (CDR3). IgA antibodies have been demonstrated to be able to bind and neutralize bacterial toxins [59] and viruses. [60] Additionally binding of IgA directly to bacteria appears to limit bacterial motility [61] and suppress expression of particular virulence factors [62] thus preventing infection by bacterial pathogens. Finally it appears that IgA may be able to act in a unique non-specific mechanism similar to antimicrobial peptides. IgA is coated with a dense array of glycans, which allows for direct interactions between IgA and bacterial glycans and confers functional activity independent of CDR3 specificity.[63]

Early studies of specific mucosal IgA responses indicated that these responses lacked traditional memory characteristics.[64] However further studies by Pabst *et al.* have demonstrated that contrary to prior belief, IgA responses do maintain at least some rudimentary form of memory. Through a novel deep-sequencing approach they demonstrated that the IgA repertoire before and after plasma cell depletion was

essentially the same.[65] There are multiple explanations for these findings that do not invoke true memory responses. For example, it is possible that since the composition of the microbiota was stable during plasma cell depletion, that the same IgA repertoire arose *de novo* after depletion. In a follow up study these alternative possibilities were directly addressed. The IgA repertoire of individual mice was determined longitudinally starting at weaning. They found that, unexpectedly, despite similar composition of microbiota between mice there was relatively little overlap of IgA variable sequences between mice. Furthermore they found a high degree of similarity in the sequence diversity of CDR3 regions between sorted IgA memory B cells and IgA-secreting plasma cells indicating that plasma cells were derived from memory cells, as opposed to constantly being generated *de novo.* [66]

While IgA responses are required for protection of the entire intestinal epithelium, they are only efficiently induced in GALT structures such as PP and ILF. A foundational study by Cebra et al demonstrated that PP were enriched for IgA-switched and pre-switched B cells relative to other lymphoid sites, indicating that the majority of IgA responses were generated here.[67] More recently studies by Lycke and colleagues have identified that PP are also involved in the synchronization of mucosal IgA responses. They found that after mucosal immunization B cell responses in individual PPs were unique and non-overlapping, however over time the B cell repertoire in all PPs became highly similar. The mechanism underlying this synchronization was germinal center B cells that were circulating between different PPs and linking individual GALT structures into a highly organized network.[68] T cell help also appears to be required for efficient generation of mucosal IgA response, as T cell deficient mice have significant reductions

in mucosal IgA production.[69] Interestingly mice lacking CD40, an important co-stimulatory receptor, have normal levels of mucosal IgA production despite absence of PP germinal centers.[70]

What is the Relationship Between M Cell antigen Sampling and the Development of the Mucosal Immune System?

There are several models in which PP, and by extension, M cells are missing. These models include the aforementioned LT-α -/- and LT-β -/- models, mice lacking NF-κB signaling, and common gamma chain mutants to name a few [71]. Recently our lab identified the RANKL-RANK axis (receptor activator of NF-κB) as critical for development of M cells. Mice lacking either the receptor or ligand demonstrated total loss of PP M cells, and complementation of RANKL-/- mice with recombinant RANKL rescued PP development. All of these currently described models share one common feature -- massive and systemic immune defects. Therefore it is a fruitless endeavor to attempt to study the downstream consequences of M cell antigen acquisition in any of these models. To address this question we developed a novel model of M cell deficiency in which any defects in the development of the immune system are due to the loss of M cells and not off-target effects.[72] Using this model we were able to elucidate several of the downstream consequences of M-cell antigen-sampling and gain valuable insight into the mechanistic workings of the mucosal immune system.

References

1 Iweala, O. I. & Nagler, C. R. Immune privilege in the gut: the establishment and maintenance of non-responsiveness to dietary antigens and commensal flora. *Immunol Rev* **213**, 82-100(2006).

2 Macpherson, A. J., McCoy, K. D., Johansen, F. E. & Brandtzaeg, P. The immune geography of IgA induction and function. *Mucosal Immunol* **1**, 11-22, (2008).

3 Mabbott, N. A., Donaldson, D. S., Ohno, H., Williams, I. R. & Mahajan, A. Microfold (M) cells: important immunosurveillance posts in the intestinal epithelium. *Mucosal Immunol* **6**, 666-677(2013).

4 Newberry, R. D. Intestinal lymphoid tissues: is variety an asset or a liability? *Curr Opin Gastroenterol* **24**, 121-128 (2008).

5 Snoeck, V., Goddeeris, B. & Cox, E. The role of enterocytes in the intestinal barrier function and antigen uptake. *Microbes Infect* **7**, 997-1004(2005).

6 Gill, N., Wlodarska, M. & Finlay, B. B. Roadblocks in the gut: barriers to enteric infection. *Cell Microbiol* **13**, 660-669, doi:10.1111/j.1462-5822.2011.01578.x (2011).

7 McCauley, H. A. & Guasch, G. Three cheers for the goblet cell: maintaining homeostasis in mucosal epithelia. *Trends Mol Med* **21**, 492-503 (2015).

8 Yang, Q., Bermingham, N. A., Finegold, M. J. & Zoghbi, H. Y. Requirement of Math1 for secretory cell lineage commitment in the mouse intestine. *Science* **294**, 2155-2158 (2001).

9 McDole, J. R. *et al.* Goblet cells deliver luminal antigen to CD103+ dendritic cells in the small intestine. *Nature* **483**, 345-349 (2012).

10 Salzman, N. H. & Bevins, C. L. Dysbiosis--a consequence of Paneth cell dysfunction.

Semin Immunol **25**, 334-341, doi:10.1016/j.smim.2013.09.006 (2013).

11 Kraehenbuhl, J. P. & Neutra, M. R. Epithelial M cells: differentiation and function. *Annu Rev Cell Dev Biol* **16**, 301-332 (2000).

12 Amulic, B., Cazalet, C., Hayes, G. L., Metzler, K. D. & Zychlinsky, A. Neutrophil function: from mechanisms to disease. *Annu Rev Immunol* **30**, 459-489 (2012).

13 Smythies, L. E. *et al.* Human intestinal macrophages display profound inflammatory anergy despite avid phagocytic and bacteriocidal activity. *J Clin Invest* **115**, 66-75 (2005).

14 Smith, P. D. *et al.* Intestinal macrophages lack CD14 and CD89 and consequently are down-regulated for LPS- and IgA-mediated activities. *J Immunol* **167**, 2651-2656 (2001).

15 Rugtveit, J. *et al.* Respiratory burst of intestinal macrophages in inflammatory bowel disease is mainly caused by CD14+L1+ monocyte derived cells. *Gut* **37**, 367-373 (1995).

16 Mowat, A. M. & Agace, W. W. Regional specialization within the intestinal immune system. *Nat Rev Immunol* **14**, 667-685 (2014).

17 Iwata, M. *et al.* Retinoic acid imprints gut-homing specificity on T cells. *Immunity* **21**, 527-538 (2004).

18 Eberl, G., Colonna, M., Di Santo, J. P. & McKenzie, A. N. Innate lymphoid cells. Innate lymphoid cells: a new paradigm in immunology. *Science* **348**, (2015).

19 Bernink, J. H. *et al.* Human type 1 innate lymphoid cells accumulate in inflamed mucosal tissues. *Nat Immunol* **14**, 221-229 (2013).

20 Moro, K. *et al.* Innate production of T(H)2 cytokines by adipose tissue-associated c-Kit(+)Sca-1(+) lymphoid cells. *Nature* **463**, 540-544 (2010).

21 Sanos, S. L. *et al.* RORgammat and commensal microflora are required for the differentiation of mucosal interleukin 22-producing NKp46+ cells. *Nat Immunol* **10**, 83-

91 (2009).

22 Bernink, J. H. *et al.* Interleukin-12 and -23 Control Plasticity of CD127(+) Group 1 and Group 3 Innate Lymphoid Cells in the Intestinal Lamina Propria. *Immunity* **43**, 146-160 (2015).

23 van Vlasselaer, P., Punnonen, J. & de Vries, J. E. Transforming growth factor-beta directs IgA switching in human B cells. *J Immunol* **148**, 2062-2067 (1992).

24 Cerutti, A. The regulation of IgA class switching. *Nat Rev Immunol* **8**, 421-434 (2008).

25 Mottet, C., Uhlig, H. H. & Powrie, F. Cutting edge: cure of colitis by CD4+CD25+ regulatory T cells. *J Immunol* **170**, 3939-3943 (2003).

26 Cong, Y., Feng, T., Fujihashi, K., Schoeb, T. R. & Elson, C. O. A dominant, coordinated T regulatory cell-IgA response to the intestinal microbiota. *Proc Natl Acad Sci U S A* **106**, 19256-19261 (2009).

27 Hadis, U. *et al.* Intestinal tolerance requires gut homing and expansion of FoxP3+ regulatory T cells in the lamina propria. *Immunity* **34**, 237-246 (2011).

28 Happel, K. I. *et al.* Divergent roles of IL-23 and IL-12 in host defense against Klebsiella pneumoniae. *J Exp Med* **202**, 761-769 (2005).

29 Huang, W., Na, L., Fidel, P. L. & Schwarzenberger, P. Requirement of interleukin-17A for systemic anti-Candida albicans host defense in mice. *J Infect Dis* **190**, 624-631(2004).

30 Burkett, P. R., Meyer zu Horste, G. & Kuchroo, V. K. Pouring fuel on the fire: Th17 cells, the environment, and autoimmunity. *J Clin Invest* **125**, 2211-2219 (2015).

31 Turnbaugh, P. J. *et al.* The human microbiome project. *Nature* **449**, 804-810 (2007).

32 Flint, H. J., Scott, K. P., Louis, P. & Duncan, S. H. The role of the gut microbiota in nutrition and health. *Nat Rev Gastroenterol Hepatol* **9**, 577-589 (2012).

33 Manichanh, C., Borruel, N., Casellas, F. & Guarner, F. The gut microbiota in IBD. *Nat Rev Gastroenterol Hepatol* **9**, 599-608 (2012).

34 Ivanov, II *et al.* Induction of intestinal Th17 cells by segmented filamentous bacteria. *Cell* **139**, 485-498 (2009).

35 Talham, G. L., Jiang, H. Q., Bos, N. A. & Cebra, J. J. Segmented filamentous bacteria are potent stimuli of a physiologically normal state of the murine gut mucosal immune system. *Infect Immun* **67**, 1992-2000 (1999).

36 Yang, Y. *et al.* Focused specificity of intestinal TH17 cells towards commensal bacterial antigens. *Nature* **510**, 152-156 (2014).

37 Chiba, T. & Seno, H. Indigenous clostridium species regulate systemic immune responses by induction of colonic regulatory T cells. *Gastroenterology* **141**, 1114-1116 (2011).

38 Atarashi, K. *et al.* Induction of colonic regulatory T cells by indigenous Clostridium species. *Science* **331**, 337-341 (2011).

39 Obata, T. *et al.* Indigenous opportunistic bacteria inhabit mammalian gut-associated lymphoid tissues and share a mucosal antibody-mediated symbiosis. *Proc Natl Acad Sci U S A* **107**, 7419-7424 (2010).

40 Olszak, T. *et al.* Microbial exposure during early life has persistent effects on natural killer T cell function. *Science* **336**, 489-493 (2012).

41 Matamoros, S., Gras-Leguen, C., Le Vacon, F., Potel, G. & de La Cochetiere, M. F. Development of intestinal microbiota in infants and its impact on health. *Trends Microbiol* **21**, 167-173 (2013).

42 Owen, R. L. Uptake and transport of intestinal macromolecules and microorganisms by

M cells in Peyer's patches--a personal and historical perspective. *Semin Immunol* **11**, 157-163 (1999).

43 Neutra, M. R., Mantis, N. J. & Kraehenbuhl, J. P. Collaboration of epithelial cells with organized mucosal lymphoid tissues. *Nat Immunol* **2**, 1004-1009, (2001).

44 Rescigno, M. *et al.* Dendritic cells express tight junction proteins and penetrate gut epithelial monolayers to sample bacteria. *Nat Immunol* **2**, 361-367 (2001).

45 Yoshida, M. *et al.* Human neonatal Fc receptor mediates transport of IgG into luminal secretions for delivery of antigens to mucosal dendritic cells. *Immunity* **20**, 769-783 (2004).

46 Niess, J. H. *et al.* CX3CR1-mediated dendritic cell access to the intestinal lumen and bacterial clearance. *Science* **307**, 254-258 (2005).

47 Pabst, O. & Bernhardt, G. The puzzle of intestinal lamina propria dendritic cells and macrophages. *Eur J Immunol* **40**, 2107-2111, doi:10.1002/eji.201040557 (2010).

48 Owen, R. L. & Jones, A. L. Epithelial cell specialization within human Peyer's patches: an ultrastructural study of intestinal lymphoid follicles. *Gastroenterology* **66**, 189-203 (1974).

49 Frey, A. *et al.* Role of the glycocalyx in regulating access of microparticles to apical plasma membranes of intestinal epithelial cells: implications for microbial attachment and oral vaccine targeting. *J Exp Med* **184**, 1045-1059 (1996).

50 Bockman, D. E. & Cooper, M. D. Pinocytosis by epithelium associated with lymphoid follicles in the bursa of Fabricius, appendix, and Peyer's patches. An electron microscopic study. *Am J Anat* **136**, 455-477 (1973).

51 Neutra, M. R., Phillips, T. L., Mayer, E. L. & Fishkind, D. J. Transport of membrane-

bound macromolecules by M cells in follicle-associated epithelium of rabbit Peyer's patch. *Cell Tissue Res* **247**, 537-546 (1987).

52 Hase, K. *et al.* Uptake through glycoprotein 2 of FimH(+) bacteria by M cells initiates mucosal immune response. *Nature* **462**, 226-230 (2009).

53 Mantis, N. J., Frey, A. & Neutra, M. R. Accessibility of glycolipid and oligosaccharide epitopes on rabbit villus and follicle-associated epithelium. *Am J Physiol Gastrointest Liver Physiol* **278**, G915-923 (2000).

54 Koni, P. A. *et al.* Distinct roles in lymphoid organogenesis for lymphotoxins alpha and beta revealed in lymphotoxin beta-deficient mice. *Immunity* **6**, 491-500 (1997).

55 Knoop, K. A. *et al.* RANKL is necessary and sufficient to initiate development of antigen-sampling M cells in the intestinal epithelium. *J Immunol* **183**, 5738-5747 (2009).

56 Kanaya, T. *et al.* The Ets transcription factor Spi-B is essential for the differentiation of intestinal microfold cells. *Nat Immunol* **13**, 729-736 (2012).

57 Kaetzel, C. S., Robinson, J. K., Chintalacharuvu, K. R., Vaerman, J. P. & Lamm, M. E. The polymeric immunoglobulin receptor (secretory component) mediates transport of immune complexes across epithelial cells: a local defense function for IgA. *Proc Natl Acad Sci U S A* **88**, 8796-8800 (1991).

58 Pabst, O. New concepts in the generation and functions of IgA. *Nat Rev Immunol* **12**, 821-832 (2012).

59 Mantis, N. J., McGuinness, C. R., Sonuyi, O., Edwards, G. & Farrant, S. A. Immunoglobulin A antibodies against ricin A and B subunits protect epithelial cells from ricin intoxication. *Infect Immun* **74**, 3455-3462 (2006).

60 Hutchings, A. B. *et al.* Secretory immunoglobulin A antibodies against the sigma1 outer

capsid protein of reovirus type 1 Lang prevent infection of mouse Peyer's patches. *J Virol* **78**, 947-957 (2004).

61 Cullender, T. C. *et al.* Innate and adaptive immunity interact to quench microbiome flagellar motility in the gut. *Cell Host Microbe* **14**, 571-581 (2013).

62 Forbes, S. J., Bumpus, T., McCarthy, E. A., Corthesy, B. & Mantis, N. J. Transient suppression of Shigella flexneri type 3 secretion by a protective O-antigen-specific monoclonal IgA. *MBio* **2**, e00042-00011 (2011).

63 Perrier, C., Sprenger, N. & Corthesy, B. Glycans on secretory component participate in innate protection against mucosal pathogens. *J Biol Chem* **281**, 14280-14287 (2006).

64 Hapfelmeier, S. *et al.* Reversible microbial colonization of germ-free mice reveals the dynamics of IgA immune responses. *Science* **328**, 1705-1709 (2010).

65 Lindner, C. *et al.* Age, microbiota, and T cells shape diverse individual IgA repertoires in the intestine. *J Exp Med* **209**, 365-377 (2012).

66 Lindner, C. *et al.* Diversification of memory B cells drives the continuous adaptation of secretory antibodies to gut microbiota. *Nat Immunol* **16**, 880-888 (2015).

67 Craig, S. W. & Cebra, J. J. Peyer's patches: an enriched source of precursors for IgA-producing immunocytes in the rabbit. *J Exp Med* **134**, 188-200 (1971).

68 Bergqvist, P. *et al.* Re-utilization of germinal centers in multiple Peyer's patches results in highly synchronized, oligoclonal, and affinity-matured gut IgA responses. *Mucosal Immunol* **6**, 122-135 (2013).

69 Macpherson, A. J. *et al.* A primitive T cell-independent mechanism of intestinal mucosal IgA responses to commensal bacteria. *Science* **288**, 2222-2226 (2000).

70 Bergqvist, P., Stensson, A., Lycke, N. Y. & Bemark, M. T cell-independent IgA class

switch recombination is restricted to the GALT and occurs prior to manifest germinal center formation. *J Immunol* **184**, 3545-3553 (2010).

71 Mebius, R. E. Organogenesis of lymphoid tissues. *Nat Rev Immunol* **3**, 292-303 (2003).

72 Rios, D. *et al.* Antigen sampling by intestinal M cells is the principal pathway initiating mucosal IgA production to commensal enteric bacteria. *Mucosal Immunol* (2015).

Chapter 1

Antigen Sampling by Intestinal M cells is the Principal Pathway Initiating Mucosal IgA Production to Commensal Enteric Bacteria

Rios D[1], Wood MB[1], Li J[1], Chassaing B[2], Gewirtz AT[2], Williams IR[1]

[1]Department of Pathology and Laboratory Medicine, Emory University School of Medicine, Atlanta, Georgia, USA.
[2]Center for Inflammation, Immunity and Infection, Institute for Biomedical Sciences, Georgia State University, Atlanta, Georgia, USA

Published in Mucosal Immunology epub ahead of print Nov 25 2015

Abstract

Secretory IgA (SIgA) directed against gut resident bacteria enables the mammalian mucosal immune system to establish homeostasis with the commensal gut microbiota after weaning. Germinal centers (GCs) in Peyer's patches (PPs) are the principal inductive sites where naive B cells specific for bacterial antigens encounter their cognate antigens and receive T-cell help driving their differentiation into IgA-producing plasma cells. We investigated the role of antigen sampling by intestinal M cells in initiating the SIgA response to gut bacteria by developing mice in which receptor activator of nuclear factor-κB ligand (RANKL)-dependent M-cell differentiation was abrogated by conditional deletion of *Tnfrsf11a* in the intestinal epithelium. Mice without intestinal M cells had profound delays in PP GC maturation and emergence of lamina propria IgA plasma cells, resulting in diminished levels of fecal SIgA that persisted into adulthood. We conclude that M-cell-mediated sampling of commensal bacteria is a required initial step for the efficient induction of intestinal SIgA.

Introduction

IgA antibodies have a major role in maintaining homeostasis at mucosal surfaces including the gastrointestinal tract.[1, 2] Peyer's patches (PPs) are critical inductive sites in the mammalian small intestine where naive B cells are initially activated by exogenous luminal antigens and then differentiate with T-cell help into IgA plasmablasts that circulate in the blood before preferentially homing to the intestinal lamina propria to become resident IgA-secreting plasma cells.[3, 4] High local concentrations of transforming growth factor-β and retinoic acid, and the presence of interleukin-21-producing follicular helper T cells are all factors that promote IgA class switching in PPs.[5, 6] Many of the dimeric IgA antibodies produced by lamina propria IgA-secreting plasma cells are transcytosed across the epithelial layer and bind to commensal enteric bacteria after reaching the lumen.[7] Secretory IgA (SIgA) directed against bacterial antigens has a variety of effects that help to shape gut microbial populations including immune exclusion from the inner mucus layer, inhibition of bacterial motility, impairment of bacterial fitness and neutralization of toxins.[2, 8, 9] Commensal bacteria resident in the small intestine are more efficient than those in the cecum and colon at eliciting a robust host SIgA response that leads to coating of the bacteria with SIgA detectable by bacterial flow cytometry. The increased SIgA coating of small intestinal bacteria by SIgA correlates with enhanced priming of B cells to bacterial antigens in the small intestinal gut-associated lymphoid tissue (GALT) [10] In addition, high levels of bound IgA on gut resident bacteria may flag those commensal bacteria with a propensity to elicit a strong host immune response and induce colitis, leading to intestinal pathology.[11] The meager

SIgA response of germ-free mice supports the concept that the commensal microbiota is the major stimulus that elicits the normal homeostatic SIgA response.[12, 13]

Several distinct antigen-sampling mechanisms are used to transport luminal antigens across the intestinal epithelium to initiate an adaptive immune response.[14]Antigen-sampling cells include M cells found in the follicle-associated epithelium overlying PPs and isolated lymphoid follicles, [15] macrophages and dendritic cells that directly sample luminal antigens by sending transepithelial dendrites between or through epithelial cells[16, 17, 18] and goblet cells that can provide a conduit for low-molecular-weight antigens to traverse the epithelial layer and reach mononuclear phagocytes in the lamina propria.[19] However, the relative contributions of these various antigen-sampling pathways to the SIgA response to antigens from commensal bacteria are not known.

M cells are specialized phagocytic epithelial cells with several adaptations that facilitate their ability to efficiently sample particulate antigens. Blunted microvilli and an attenuated glycocalyx allow antigens to come in close proximity to the apical surface of M cells, whereas a basolateral invagination allows for positioning of antigen-presenting cells (APCs) and lymphocytes in very close proximity to the lumen.[20] M cell antigen sampling can occur either through clathrin-coated endocytic vesicles[21] for larger antigens or via fluid phase pinocytosis for smaller antigens.[22, 23] Antigens acquired by M cells through their apical surface are rapidly shuttled via vesicular transport to the basolateral membrane where they are released, enabling uptake by APCs and processing for presentation to T cells and transport to follicular dendritic cells present within the B-cell follicles. Differentiation of M cells from uncommitted precursors in intestinal crypts is

dependent on receptor activator of nuclear factor-κB ligand (RANKL)-expressing subepithelial stromal cells that are normally restricted to organized lymphoid structures such as PPs and isolated lymphoid follicles.[24, 25]

We previously showed that intestinal M cells are absent in PPs from RANKL-deficient mice.[25] However, the critical involvement of RANKL–RANK signaling in multiple facets of immune system development including lymph node formation[26] and medullary thymic epithelial cell differentiation[27] detracts from the value of global RANKL or RANK knockout mice as models to investigate how loss of intestinal M cells perturbs mucosal immune responses. To restrict the effects of interrupting the RANKL–RANK signaling axis to the intestinal epithelium, we generated a conditional knockout mouse in which *Tnfrsf11a* (the gene encoding RANK) is only deleted in intestinal epithelial cells. These $RANK^{\Delta IEC}$ mice represent a first-of-its-kind model system in which intestinal M-cell-mediated antigen uptake is ablated, whereas other RANKL–RANK-dependent developmental events required for normal immune system function are not impacted. Our analysis of the SIgA response in the intestine of $RANK^{\Delta IEC}$ mice demonstrates the pivotal role M cells have in facilitating sampling of the commensal microbiota by GALT, which initiates SIgA production and is, in turn, key to the maintenance of homeostasis in epithelial tissues richly colonized by the commensal microbiota.

Materials and Methods

Conditional RANK knockout mice. Mice with a conditional allele of *Tnfrsf11a* (the gene encoding RANK) featuring loxP sites flanking exons 2 and 3 were produced at inGenious Targeting Laboratory (Stony Brook, NY). Mice carrying this floxed allele were donated to The Jackson Laboratory Mouse Repository (http://jaxmice.jax.org/strain/027495.html); the official strain designation is B6.Cg-Tnfrsf11a$^{tm1.1Irw}$/J. Mice with the floxed allele were bred to villin-cre mice (Tg(Vil-cre)997Gum/J strain; The Jackson Laboratory, Bar Harbor, ME), to produce mice homozygous for the floxed RANK allele that also carried the villin-cre transgene (villin-cre RANK$^{F/F}$ genotype; also designated RANK$^{\Delta IEC}$ and referred to as 'M-less'). Most experimental mice used in experiments originated from breeding pairs of male RANK$^{\Delta IEC}$ mice and female RANK$^{F/F}$, and consisted of a mix of RANK$^{\Delta IEC}$ mice and RANK$^{F/F}$ littermates used as controls. Litters were weaned at 21 days after birth. All animal studies were reviewed and approved by the Emory University Institutional Animal Care and Use Committee.

Germ-free conditional RANK knockout mice. Germ-free rederivation of the RANK$^{\Delta IEC}$ mouse strain was done at Taconic (Germantown, NY). Rederived mice confirmed to be germ-free at Taconic were shipped to the germ-free mouse facility at Georgia State University, to establish a breeding colony. The germ-free status of the isolators used for these studies was verified on a regular basis by quantitative PCR with primers for 16S rDNA sequences. For conventionalization experiments, germ-free mice were transferred from isolators to conventional housing and initially exposed to drinking water containing fecal bacteria from conventionally housed specific pathogen-free mice

in the same mouse facility. The studies done in this facility using germ-free and gnotobiotic $RANK^{\Delta IEC}$ and $RANK^{F/F}$ mice were reviewed and approved by the Georgia State Institutional Animal Care and Use Committee.

Immunofluorescence staining of M cells. For whole mount preparations, PPs were isolated directly into cold Dulbecco's modified Eagle's media and then incubated for 10 min at room temperature in 1% *N*-acetyl cysteine followed by vigorous vortexing to dissociate the mucus layer. The PPs were fixed in 4%paraformaldehyde for 30min at 20°C. For frozen section preparations, PPs were cut transversely through the dome area, embedded in optimal cutting temperature compound, and sectioned with a cryostat as previously described.[24] Both whole mounts and cryosections were incubated overnight at 4°C with anti-GP2 antibody (2F11-C3; MBL, Woburn, MA) and rhodamine-UEA-I (Vector Labs, Burlingame, CA) in TBB buffer (PerkinElmer, Waltham, MA) containing 0.25% saponin. The whole mounts and sections were washed for 10min with TBB with 0.25% saponin and incubated with Alexa647-conjugated polyclonal goat anti-rat antibody (Invitrogen, Grand Island, NY) for 3h at 20°C. DAPI (4',6-diamidino-2-phenylindole; Sigma-Aldrich, St. Louis, MO) was added to the frozen sections as a nuclear counterstain. Whole mounts and frozen sections were mounted in ProLong Gold antifade reagent (Invitrogen) and held for 1h at 4°C in the dark before image acquisition using a Nikon (Melville, NY) 80i epifluorescence microscope.

Immunofluorescence staining of GCs and IgA-secreting cells. For analysis of PP GCs, horizontal sections of PPs were stained overnight at 4°C with FITC- or phycoerythrin (PE)-conjugated anti-IgD (11-26c; eBioscience, San Diego, CA), allophycocyanin (APC)-conjugated anti-GL7 (GL-7; eBioscience), and FITC-conjugated anti-CD21/35

(7G6; BD Biosciences, San Jose, CA). Lamina propria IgA-secreting cells were detected with FITC-conjugated anti-IgA (C10-3; BD Biosciences) and the location of the epithelium was defined using APC-conjugated anti-EpCAM (G8.8; eBioscience).

Enteroid cultures for *in vitro* induction of M-cell differentiation. Small intestinal crypts from the distal 10 cm of the small intestine were isolated and cultured in Matrigel (Corning, Tewksbury, MA) to generate three-dimensional enteroids using a modified version of published methods.[42, 43] After 3 days of culture, the media above the Matrigel was replaced and half the wells were supplemented with 100ngml^{-1} of soluble mouse RANKL (Peprotech, Rocky Hill, NJ) for 3 days to induce M-cell differentiation.

Quantitative real-time PCR analysis of gene expression in enteroids. The Matrigel droplet containing enteroids was incubated with 500µl of Cell Recovery Solution (Corning) for 1h at 4°C. Once the Matrigel was depolymerized, the cell pellet was washed and used for extraction of RNA. cDNA was synthesized with the iScript cDNA synthesis kit (Bio-Rad, Hercules, CA). Quantitative PCR was performed on a CFX Connect thermal cycler (Bio-Rad) using iTaq Universal SYBR Green Supermix (Bio-Rad) and primers for three M-cell-associated genes. The relative expression of the M-cell-associated genes was determined by normalization to*Gapdh* using the comparative Ct method.

LGG culture and labeling. LGG provided by Dr Andrew Neish (Emory University) was grown overnight under anaerobic conditions with no shaking in MRS broth (BD Biosciences). To label the bacteria, 1×10^{10} washed bacteria were incubated in a total volume of 20ml of phosphate-buffered saline (PBS) with 50µgml^{-1} NHS-fluorescein (Thermo Fisher Scientific, Waltham, MA) for 30min at 20°C with constant agitation. The

FITC-labeled bacteria were washed three times in PBS. Before gavage, the concentration of bacteria was determined using a Bacteria Counting Kit (Invitrogen) on a FACSCalibur flow cytometer (BD Biosciences).

Quantification of PP uptake of fluorescent bacteria or beads. Aliquots of 1×10^9 FITC-labeled LGG bacteria or 1×10^{11} 0.2-μm diameter polystyrene nanoparticles (Fluoresbrite YG; Polysciences, Warrington, PA) were administered by gavage to 6- to 8-week-old mice using a 20-gauge gavage needle in a total volume of 400μl. Mice given LGG bacteria were pretreated 5min before gavage with 100μl of 10% w/v sodium bicarbonate, to neutralize stomach acid. Multiple PPs were isolated either 6h (LGG bacteria) or 24h (nanoparticles) after gavage and snap frozen in optimal cutting temperature compound. Cryosections of PPs from mice administered nanoparticles were immediately counterstained with DAPI ($5\mu g ml^{-1}$in PBS). Cryosections of PPs from mice given FITC-labeled LGG bacteria were fixed for 20min in acetone at −20°C and mounted in 10μl of ProLong Gold antifade reagent. The sections were imaged on a Nikon Eclipse 80i epifluorescence microscope to allow manual counting of uptake events.

Preparation of cell suspensions for flow cytometry. PPs and mesenteric lymph nodes were isolated and mechanically dissociated in ice-cold RPMI-1640 (Corning). The resulting cell suspensions were passed through a 70-μm mesh cell strainer. To prepare intestinal lamina propria cells, PPs were excised from the small intestine, the opened PP-free tissue was thoroughly washed in ice-cold PBS to remove luminal contents, and the small intestine was cut into 10 equal-sized pieces. The intestinal pieces were incubated for 15min in PBS with 0.5mM EDTA and 10mM HEPES in a shaking incubator at 37°C, and then strained though a large metal mesh strainer to remove epithelial cells. This step

was repeated at until no epithelial cells were visible in the supernatant. The intestinal fragments were washed thoroughly with PBS to remove the EDTA, minced exactly 30 times with a small scissors in an microfuge tube and incubated in 20ml of RPMI-1640 supplemented with 10% fetal bovine serum, 0.25mgml^{-1} Collagenase D (Roche, Indianapolis, IN), 0.25mgml^{-1}Collagenase Fraction IV (MP Biomedicals, Santa Ana, CA), and 40μgml^{-1} DNase I (Roche) for 20min at 37°C with constant agitation. After digestion, intestinal fragments were shaken vigorously by hand for 30s and passed through a 100-μm mesh cell strainer. The cell suspension was sedimented at 1,000*g* for 10min and the resuspended pellet was further purified from the interface of a 30%/100%Percoll density gradient.

Flow cytometry analysis. The directly conjugated monoclonal antibodies used to stain cells for flow cytometry included PE-anti-mouse CD138 (281-2; BD Biosciences), FITC-anti-mouse IgA (C10-3; BD Biosciences), eFluor 450-anti-mouse IgD (11-25c; eBioscience), APC-anti-GL7 (GL7; eBioscience), FITC-anti-mouse PD-1 (294.1a12; BioLegend, San Diego, CA), PE-anti-mouse CXCR5 (L138D7; BioLegend), Brilliant Violet 605-anti-mouse B220 (RA3-6B2; BioLegend), PE-Cy7-anti-mouse CD19 (1D3; Tonbo Biosciences, San Diego, CA), APC-Cy7 anti-mouse CD45.2 (104; Tonbo Biosciences), and VF450-anti-mouse CD4 (RM4-5; Tonbo Biosciences). Live/dead cell discrimination for all antibody panels was done with Fixable Viability Dye eFluor 506 (eBioscience). Staining was carried out for 15min at 20°C in PBS with 1% bovine serum albumin and 0.02% NaN_3. After staining, all cells were fixed for 20min at 20°C in BD Fix/Perm buffer. To stain for intracellular IgA, cells were permeabilized for 20min at 20°C in BD Perm/Wash buffer and then stained for 15min at 20°C in BD Perm/Wash

buffer. Stained cells were analyzed on an LSRII cytometer (BD Biosciences). Post-acquisition analysis of data files was done with FlowJo v9.3.1 software (Ashland, OR).

Processing of fecal pellets to yield fecal supernatant and fecal bacteria. Fresh fecal pellets were collected, weighed, and diluted 1:10 (w/v) in PBS with 1mM EDTA. The suspension was vortexed for up to 15min, to allow complete liquefaction, followed by centrifugation at 400*g* at 4°C for 5min. The turbid supernatant was centrifuged a second time at 12,000*g* for 10min at 4°C. The supernatant from this spin was used to determine the fecal IgA concentration by a sandwich enzyme-linked immunosorbent assay method using a IgA, κ-isotype control monoclonal antibody (BD Biosciences) as a standard, as previously described.[25] Fecal supernatants were stored at −80°C after preparation and all supernatants from a single experiment were analyzed by enzyme-linked immunosorbent assay at the same time. The concentration of IgA in serum samples was determined by the same enzyme-linked immunosorbent assay method. The remaining pellet containing fecal bacteria was fixed overnight in 4%paraformaldehyde. The fixed bacterial suspension was washed twice in PBS with 1%bovine serum albumin and 0.02% NaN_3, and stored in a 10% glycerol solution at −80°C until the bacteria were analyzed for bound IgA by flow cytometry.

Oral immunization with horse spleen ferritin. Five-week-old $RANK^{\Delta IEC}$ mice and $RANK^{F/F}$ littermates were orally immunized with horse spleen ferritin (Sigma) using a modification of a previously described method.[30] Ferritin was added to the drinking water on days 0–2 and then again on days 7–9. Fecal samples were collected 2 weeks after the first day of immunization and were processed to prepare fecal supernatants by the same methods used to do measurements of total fecal IgA content. Serial dilutions of fecal

supernatant from individual mice were tested for ferritin-specific fecal IgA by enzyme-linked immunosorbent assay using wells coated with ferritin. Bound anti-ferritin IgA antibody was detected with horseradish peroxidase-conjugated goat anti-mouse IgA (Southern Biotech, Birmingham, AL) followed by use of optEIA (BD Biosciences) as substrate.

Flow cytometric analysis of IgA bound to fecal bacteria. The density of fixed fecal bacteria in stored samples was estimated on the basis of OD600. The equivalent of 1×10^6 live bacteria derived from a fresh *in vitro* culture was incubated in a solution containing $1 mg ml^{-1}$ rat serum, 1.5% bovine serum albumin, and $0.5 \mu g ml^{-1}$ of PE-anti-IgA (mA-6E1; eBioscience) for 30min at 20°C in the dark. A PE-labeled rat IgG1 antibody (R3-34; BD Biosciences) was used as an isotype control. Bacterial suspensions were analyzed on an LSRII cytometer (BD Biosciences) using FSC-H and FSC-W to gate on bacterial events. The percentage of bacteria with bound IgA was determined using gates established by analysis of fecal bacteria from B-cell-deficient $JH^{-/-}$ mice (Taconic) without any bound IgA.

Analysis of fecal microbiota composition by 16S sequencing. Fecal pellets from co-housed littermate $RANK^{\Delta IEC}$ and $RANK^{F/F}$ mice were collected at 3, 7, 20, 30, and 40 days after weaning. DNA was extracted and amplified with forward 515F and reverse 806R primers flanking the V4 variable region as previously described.[44] Pooled products from four independent PCRs on each sample were purified and sequenced using an Illumina MiSeq sequencer. QIIME software was used to assign OTUs and perform rarefaction analysis.[45]

Conditional RANK Knockout Mice. Mice with a conditional allele of *Tnfrsf11a* (the

gene encoding RANK) were produced at inGenious Targeting Laboratory (Stony Brook, NY). Homologous recombination in a hybrid 129 x C57BL/6 ES cell line was used to flank exons 2 and 3 of *Tnfrsf11a* with loxP sites. This strategy was used because a previously reported *Tnfrsf11a* null allele featured deletion of just these 2 exons[1]. The neo resistance selection cassette used to select for integration of the floxed allele was flanked by FRT sites, allowing its subsequent deletion using a flippase (FLP)- expressing transgenic mouse line. Mice carrying this floxed *Tnfrsf11a* allele were donated to the The Jackson Laboratory Mouse Repository (http://jaxmice.jax.org/strain/027495.html); the official strain designation is B6.Cg-Tnfrsf11a$^{tm1.1Irw}$/J. The floxed *Tnfrsf11a* allele was validated by using CMV-cre mice (Tg(CMV-cre)1Cgn strain; The Jackson Laboratory) to delete the floxed exons in the germ line, allowing generation of mice homozygous for the deleted allele that reproduced the expected skeletal and lymphoid organ abnormalities of mice with a full knockout of *Tnfrsf11a*.[1,2] The floxed *Tnfrsf11a* allele was backcrossed to C57BL/6 mice to yield mice with >99% C57BL/6 background genes as evaluated by an array-based SNP analysis (Taconic). Mice with the floxed allele were also bred to villin-cre mice (Tg(Vil-cre)997Gum/J strain; The Jackson Laboratory) to produce mice homozygous for the floxed RANK allele that also carried the villin-cre transgene (villin-cre $RANK^{F/F}$ genotype; also designated $RANK^{\Delta IEC}$ and referred to as "M-less"). Most experimental mice used in experiments originated from breeding pairs of male $RANK^{\Delta IEC}$ mice and female $RANK^{F/F}$ and consisted of a mix of $RANK^{\Delta IEC}$ mice and $RANK^{F/F}$ littermates used as controls. Litters were weaned at 21 days after birth. All animal studies were reviewed and approved by the Emory University Institutional Animal Care and Use Committee.

Validation of Genomic Deletion in RANK$^{\Delta IEC}$ RANKΔIEC Mice and Genotyping of Mice.A PCR reaction using 3 primers was used to confirm cre recombinase-mediated deletion of exons 2 and 3 of the *Tnfrsf11a* gene in DNA from enterocytes from RANK$^{\Delta IEC}$ RANKΔIEC mice. Primer 1 (5'-TGTCCCACTGACACAGGAGA-3') is a sense primer that anneals 5' to the loxP site located upstream of the second exon. Primer 2 (5'AGCTCACAACGCACAAAACA-3') is an antisense primer that anneals 3' of the same loxP site. Primer 3 (5'- GAGTTCAAGGCCAACCTGAG-3') is antisense primer that anneals 3' of the loxP site located downstream of the third exon. Primers 1 and 2 amplify a 469 bp product from the floxed locus. Primers 1 and 3 amplify a 392 bp product after successful excision of the floxed region by cre recombinase. Primers 1 and 2 alone were routinely used to genotype mice for the floxed *Tnfrsf11a* allele since the wild type allele yielded a smaller product (290 bp) than the floxed allele (469 bp). Primer 3 was used in conjunction with primers 1 and 2 to genotype mice to be used as breeders to rule out the presence of a fully deleted RANK allele transmitted through the germ line. Mice were genotyped for the villin-cre transgene using 3 primers: 5'-AGGGAGGTCGAGGCTAAAGA-3' (a sense primer that anneals within the villin promoter), 5'-GACCGACGATGAAGCATGT-3' (an antisense primer that anneals to the cre recombinase gene), and 5'-CCTTTGACTTGGGCATTCAG-3' (an antisense primer that anneals to the endogenous villin gene). Mice with the villin-cre transgene yielded two products with sizes of 725 bp (from transgene) and 349 bp (from endogenous villin gene), while mice lacking this transgene yielded only the 349 bp product. Genomic DNA amplifications were done using 35 cycles of PCR with denaturation at 94 ^{o}C, annealing at

58 ^{o}C, and extension at 72 ^{o}C.

Enteroid Cultures for In Vitro Induction of M Cell Differentiation. Small intestinal crypts were isolated and cultured in Matrigel (Corning) to generate three- dimensional enteroids using a modified version of published methods.[3,4] Intact crypts were isolated from the distal 10 cm of the small intestine by incubation in 5 mM EDTA for 20 min followed by manual disruption in a buffer containing 54.9 mM D-sorbitol and 43.4 mM sucrose to lift off the epithelium. The epithelial fraction was filtered through a 70 μm nylon mesh filter, and the crypts were sedimented at 200 g for 4 min. The crypts were resuspended in 50 μl of Matrigel per well of a 24-well plate. The Matrigel droplet was overlaid with a base media consisting of 50:50 DMEM:Ham's F-12 (Corning), 1% N-2 Plus Media Supplement (R&D Systems), 2% B-27 serum-free supplement (Life Technologies), 1% penicillin/streptomycin (Corning) and 10 mM HEPES (Life Technologies) that was further supplemented with 100 ng/ml murine Noggin (Peprotech), 50 ng/ml murine EGF (Peprotech) and conditioned media from R-spondin 2-transfected HEK293T cells.[5] After 3 days of culture, the media above the Matrigel was replaced and half the wells were supplemented with 100 ng/ml of soluble mouse RANKL (Peprotech) for 3 days to induce M cell differentiation.

Quantitative Real-Time PCR Analysis of Gene Expression in Enteroids. The Matrigel droplet containing enteroids was incubated with 500 μL of Cell Recovery Solution (Corning) for 1 hr at 4^{o}C. Once the Matrigel was depolymerized, the cell pellet was washed 3 times with 1 ml of PBS. The RNeasy Mini Kit (Qiagen) was used for extraction of RNA from the cell pellet. RNA concentration was determined using a NanoDrop 1000 (NanoDrop Instruments). cDNA was synthesized with the iScript cDNA

synthesis kit (Bio-Rad). qPCR was performed on a CFX Connect thermal cycler (BioRad) using iTaq Universal SYBR Green Supermix (Bio-Rad) and primers for 3 M cell-associated genes: *Spib* (5'- GCCCACACTTAAGCTGTTTGTA-3' and 5'-CTGTCCAGCCCCATGTAGAG-3'); *Gp2* (5'- CTGCTACCTCGAAGGGGACT-3' and 5'-CATTGCCAGAGGGAAGAACT-3'); *Anxa5* (5'-ATCCTGAACCTGTTGACATCCC-3' and 5'-AGTCGTGAGGGCTTCATCATA-3'). The relative expression of the M-cell associated genes was determined by normalization to *Gapdh* (5'-TTCACCACCATGGAG AAGGC-3' and 5'-GGCATGGACTGTGGTCATGA-3') using the comparative Ct method.

Measurement of Follicle Area in Peyer's Patch Sections. Horizontal sections of PP were stained with FITC-conjugated anti-IgD (11-26c; eBioscience). The major radius and minor radius of individual follicles were measured by image analysis with ImageJ software (http://rsb.info.nih.gov/ij/) and used to calculate the area.

Histological Analysis of Intestinal Tissue Mouse small intestine tissue was fixed with 10% formalin and embedded in paraffin. Five micron tissue sections were stained with Alcian blue followed by 0.5% periodic acid and Schiff's reagent (all staining reagents from Thermo Scientific) to visualize mucin in goblet cells and Paneth cell granules.

Measurement of Serum Immunoglobulins. The concentrations of serum IgG, IgA and IgM were determined by a sandwich ELISA method using IgG, IgA and IgM isotype control mAbs (BD Biosciences) as standards as previously described.[6]

Statistical analysis. Differences between the mean values for groups were analyzed by a two-tailed Student's *t*-test using Prism (GraphPad Software, La Jolla, CA). A *P*-value <0.05 was considered significant.

Supplementary Experimental Procedures

Conditional RANK Knockout Mice. Mice with a conditional allele of Tnfrsf11a (the gene encoding RANK) were produced at inGenious Targeting Laboratory (Stony Brook, NY). Homologous recombination in a hybrid 129 x C57BL/6 ES cell line was used to flank exons 2 and 3 of Tnfrsf11a with loxP sites. This strategy was used because a previously reported Tnfrsf11a null allele featured deletion of just these 2 exons. [46] The neo resistance selection cassette used to select for integration of the floxed allele was flanked by FRT sites, allowing its subsequent deletion using a flippase (FLP)- expressing transgenic mouse line. Mice carrying this floxed Tnfrsf11a allele were donated to the The Jackson Laboratory Mouse Repository (http://jaxmice.jax.org/strain/027495.html); the official strain designation is B6.Cg-Tnfrsf11atm1.1Irw/J. The floxed Tnfrsf11a allele was validated by using CMV-cre mice (Tg(CMV-cre)1Cgn strain; The Jackson Laboratory) to delete the floxed exons in the germ line, allowing generation of mice homozygous for the deleted allele that reproduced the expected skeletal and lymphoid organ abnormalities of mice with a full knockout of *Tnfrsf11a*. [46, 47] The floxed Tnfrsf11a allele was backcrossed to C57BL/6 mice to yield mice with >99% C57BL/6 background genes as evaluated by an array-based SNP analysis (Taconic). Mice with the floxed allele were also bred to villin-cre mice (Tg(Vil-cre)997Gum/J strain; The Jackson Laboratory) to produce mice homozygous for the floxed RANK allele that also carried the villin-cre transgene (villin-cre RANKF/F genotype; also designated RANKΔIEC and referred to as “M-less”). Most experimental mice used in experiments originated from breeding pairs of male RANKΔIEC mice and female RANKF/F and consisted of a mix of RANKΔIEC mice and RANKF/F littermates used as controls. Litters were weaned at 21 days after birth. All

animal studies were reviewed and approved by the Emory University Institutional Animal Care and Use Committee.

Validation of Genomic Deletion in RANKΔIEC Mice and Genotyping of Mice. A PCR reaction using 3 primers was used to confirm cre recombinase-mediated deletion of exons 2 and 3 of the Tnfrsf11a gene in DNA from enterocytes from RANKΔIEC mice. Primer 1 (5'-TGTCCCACTGACACAGGAGA-3') is a sense primer that anneals 5' to the loxP site located upstream of the second exon. Primer 2 (5'-AGCTCACAACGCACAAAACA-3') is an antisense primer that anneals 3' of the same loxP site. Primer 3 (5'- GAGTTCAAGGCCAACCTGAG-3') is antisense primer that anneals 3' of the loxP site located downstream of the third exon. Primers 1 and 2 amplify a 469 bp product from the floxed locus. Primers 1 and 3 amplify a 392 bp product after successful excision of the floxed region by cre recombinase. Primers 1 and 2 alone were routinely used to genotype mice for the floxed Tnfrsf11a allele since the wild type allele yielded a smaller product (290 bp) than the floxed allele (469 bp). Primer 3 was used in conjunction with primers 1 and 2 to genotype mice to be used as breeders to rule out the presence of a fully deleted RANK allele transmitted through the germ line. Mice were genotyped for the villin-cre transgene using 3 primers: 5'-AGGGAGGTCGAGGCTAAAGA-3' (a sense primer that anneals within the villin promoter), 5'-GACCGACGATGAAGCATGT-3' (an antisense primer that anneals to the cre recombinase gene), and 5'-CCTTTGACTTGGGCATTCAG-3' (an antisense primer that anneals to the endogenous villin gene). Mice with the villin-cre transgene yielded two products with sizes of 725 bp (from transgene) and 349 bp (from endogenous villin gene), while mice lacking this transgene yielded only the 349 bp product. Genomic DNA

amplifications were done using 35 cycles of PCR with denaturation at 94 ^{o}C, annealing at 58 ^{o}C, and extension at 72 ^{o}C.

Enteroid Cultures for In Vitro Induction of M Cell Differentiation. Small intestinal crypts were isolated and cultured in Matrigel (Corning) to generate threedimensional enteroids using a modified version of published methods.[48,49] Intact crypts were isolated from the distal 10 cm of the small intestine by incubation in 5 mM EDTA for 20 min followed by manual disruption in a buffer containing 54.9 mM D-sorbitol and 43.4 mM sucrose to lift off the epithelium. The epithelial fraction was filtered through a 70 μm nylon mesh filter, and the crypts were sedimented at 200 g for 4 min. The crypts were resuspended in 50 μl of Matrigel per well of a 24-well plate. The Matrigel droplet was overlaid with a base media consisting of 50:50 DMEM:Ham's F-12 (Corning), 1% N-2 Plus Media Supplement (R&D Systems), 2% B-27 serum-free supplement (Life Technologies), 1% penicillin/streptomycin (Corning) and 10 mM HEPES (Life Technologies) that was further supplemented with 100 ng/ml murine Noggin (Peprotech), 50 ng/ml murine EGF (Peprotech) and conditioned media from R-spondin 2-transfected HEK293T cells.[50] After 3 days of culture, the media above the Matrigel was replaced and half the wells were supplemented with 100 ng/ml of soluble mouse RANKL (Peprotech) for 3 days to induce M cell differentiation.

Quantitative Real-Time PCR Analysis of Gene Expression in Enteroids. The Matrigel droplet containing enteroids was incubated with 500 μL of Cell Recovery Solution (Corning) for 1 hr at 4^{o} C. Once the Matrigel was depolymerized, the cell pellet was washed 3 times with 1 ml of PBS. The RNeasy Mini Kit (Qiagen) was used for extraction of RNA from the cell pellet. RNA concentration was determined using a

NanoDrop 1000 (NanoDrop Instruments). cDNA was synthesized with the iScript cDNA synthesis kit (Bio-Rad). qPCR was performed on a CFX Connect thermal cycler (BioRad) using iTaq Universal SYBR Green Supermix (Bio-Rad) and primers for 3 M cell-associated genes: Spib (5'- GCCCACACTTAAGCTGTTTGTA-3' and 5'-CTGTCCAGCCCCATGTAGAG-3'); Gp2 (5'- CTGCTACCTCGAAGGGGACT-3' and 5'-CATTGCCAGAGGGAAGAACT-3'); Anxa5 (5'-ATCCTGAACCTGTTGACATCCC-3' and 5'-AGTCGTGAGGGCTTCATCATA-3'). The relative expression of the M-cell associated genes was determined by normalization to Gapdh (5'-TTCACCACCATGGAG AAGGC-3' and 5'-GGCATGGACTGTGGTCATGA-3') using the comparative Ct method.

Measurement of Follicle Area in Peyer's Patch Sections Horizontal sections. of PP were stained with FITC-conjugated anti-IgD (11-26c; eBioscience). The major radius and minor radius of individual follicles were measured by image analysis with ImageJ software (http://rsb.info.nih.gov/ij/) and used to calculate the area.

Histological Analysis of Intestinal Tissue. Mouse small intestine tissue was fixed with 10% formalin and embedded in paraffin. Five micron tissue sections were stained with Alcian blue followed by 0.5% periodic acid and Schiff's reagent (all staining reagents from Thermo Scientific) to visualize mucin in goblet cells and Paneth cell granules.

Measurement of Serum Immunoglobulins. The concentrations of serum IgG, IgA and IgM were determined by a sandwich ELISA method using IgG, IgA and IgM isotype control mAbs (BD Biosciences) as standards as previously described.

Results

Conditional deletion of RANK in the intestinal epithelium results in the absence of PP M cells

A villin-cre transgene was bred to mice homozygous for a floxed allele of RANK ($RANK^{F/F}$), to generate mice lacking RANK expression in the intestinal epithelium (designated $RANK^{\Delta IEC}$) (Supplementary Figure S1 online). Whole mounts and cross-sections of intestinal PPs from adult $RANK^{F/F}$ and $RANK^{\Delta IEC}$ mice were stained with anti-GP2 antibody to detect M cells (Figure 1a–d). The PP domes of $RANK^{F/F}$ mice typically contained 150–200 GP2-expressing M cells. In contrast, no $GP2^{+}$ cells were detected in $RANK^{\Delta IEC}$ mice. Absorptive enterocytes, goblet cells, and Paneth cells differentiated normally in the small intestine of $RANK^{\Delta IEC}$ mice (Supplementary Figure S2). To further evaluate the penetrance of the intestinal M-cell differentiation defect in $RANK^{\Delta IEC}$ mice, we used an *in vitro* model of RANKL-stimulated M-cell differentiation in enteroid cultures similar to that described by de Lau *et al.*[28] Addition of RANKL to enteroid cultures established from $RANK^{F/F}$ mice led to robust induction of M-cell-specific genes including *Spib* and *Gp2* after 3 days compared with unstimulated cultures (Figure 1e). In contrast, RANKL was unable to induce M-cell-specific genes in enteroids from $RANK^{\Delta IEC}$ mice. Thus, the villin-cre transgene-mediated deletion of the *Tnfrsf11a* gene encoding RANK was fully penetrant in uncommitted crypt enterocytes and completely abrogated differentiation of the M-cell lineage.

PPs in $RANK^{\Delta IEC}$ mice are deficient in uptake of particulate antigens

To assess the impact of the absence of M cells in $RANK^{\Delta IEC}$ mice on uptake of particulate antigens from the intestinal lumen, $RANK^{\Delta IEC}$ and $RANK^{F/F}$ mice were

gavage-fed particulate antigens known to be taken up into PPs via M cells. The uptake of fluorescent 0.2μm polystyrene beads or fluorescently labeled *Lactobacillus rhamnosus* strain GG (LGG) bacteria was measured by counting the number of beads or bacteria observed in sections of the PP dome (Figure 2). Numerous 0.2μm polystyrene beads were detected within the PPs of $RANK^{F/F}$ mice 24h after gavage (Figure 2a,c). In $RANK^{\Delta IEC}$ mice, uptake of polystyrene beads into PPs was reduced by over 90%, although not completely eliminated (Figure 2a,d). We speculate that the low level of residual sampling of polystyrene beads in $RANK^{\Delta IEC}$ mice is mediated by one or more of the M-cell-independent antigen uptake pathways. Examination of the uptake of fluorescein isothiocyanate (FITC)-labeled LGG bacteria 6h after gavage revealed a more pronounced uptake deficit in the $RANK^{\Delta IEC}$ mice (with <1% of the uptake in $RANK^{F/F}$ mice), with the vast majority of sections examined showing no bacterial uptake at all (Figure 2b,e,f). The substantially larger size of the LGG bacteria compared with the 0.2μm beads is likely responsible for the greater dependence on M cells for bacterial uptake into PPs.

Germinal center development is delayed in the PP follicles of $RANK^{\Delta IEC}$ mice

In wild-type adult mice, all PP follicles contain active germinal centers (GCs), with GC development occurring rapidly after mice are weaned from their mothers.[29] To determine whether loss of M cells and M-cell-mediated particulate antigen uptake affected the maturation of PP follicles, we compared the size of PP follicles in $RANK^{F/F}$ and $RANK^{\Delta IEC}$ mice at 1 and 3 weeks after weaning by measuring the follicular area in sections. $RANK^{\Delta IEC}$ mice showed a significant reduction in the size of the B-cell follicles at 1 week after weaning (Supplementary Figure 3). Follicle size increased between 1 and

3 weeks after weaning in both groups, with the follicles remaining smaller in $RANK^{\Delta IEC}$ mice compared with $RANK^{F/F}$ littermates. To directly assess the formation of GCs within these follicles, we stained PP sections with anti-GL7, a marker of GC B cells, and anti-IgD to define the borders of the GCs (Figure 3a–d). In PP follicles from $RANK^{F/F}$ mice, a few IgD^{-} cells in the center of the follicle were already $GL7^{+}$ at 1 week after weaning and by 3 weeks after weaning almost all follicles had easily appreciated clusters of $GL7^{+}$ cells within the IgD^{-} GC area. In contrast, only a minority of the PP follicles in $RANK^{\Delta IEC}$ mice had clusters of $GL7^{+}$cells within the IgD^{-} area of the follicle at 3 weeks after weaning. Analysis of PP cell suspensions by flow cytometry confirmed that fewer $CD19^{+}IgD^{-}$ $GL7^{hi}$ GC B cells and $CD4^{+}$ $PD\text{-}1^{hi}$ $CXCR5^{+}$ follicular helper T cells are present in the PPs of $RANK^{\Delta IEC}$ mice at 2 weeks after weaning (Figure 3e,f and Supplementary Figure 3). By 6 weeks after weaning, the density of $GL7^{+}$ GC B cells and $CD21/35^{+}$ follicular dendritic cells was comparable in $RANK^{\Delta IEC}$ and $RANK^{F/F}$ mice (Supplementary Figure 4). Thus, GC formation in PP follicles is delayed in $RANK^{\Delta IEC}$ mice lacking M cells.

The density of lamina propria IgA-secreting plasma cells and the concentration of fecal IgA are reduced in $RANK^{\Delta IEC}$ mice

GCs in PP follicles are known to be major inductive sites where B-cells class switch to IgA and differentiate into IgA-secreting plasma cells that home to the intestinal lamina propria. We investigated whether the impaired antigen uptake into PPs of $RANK^{\Delta IEC}$ mice was associated with a deficiency in cells producing SIgA (Figure 4). By 1 week after weaning, groups of IgA^{+} antibody-secreting cells (ASCs) were present at the base of small intestinal villi in $RANK^{F/F}$ mice; at 4 weeks after weaning, a high density of

IgA^+ ASCs was found throughout the villi (Figure 4a,b). In contrast, only rare scattered IgA^+ ASCs were present in the lamina propria of $RANK^{\Delta IEC}$ mice 1 week after weaning (Figure 4c). By 4 weeks after weaning, the density of IgA^+ ASCs in $RANK^{\Delta IEC}$ mice had increased (Figure 4d), but remained lower than that observed in $RANK^{F/F}$ littermates (Figure 4b). Flow cytometry of small intestine lamina propria cell suspensions was performed at 1 and 4 weeks after weaning, to quantify the extent of IgA plasma cell differentiation (Figure 4eand Supplementary Figure 5). Very few IgA^+ $CD138^+$ plasma cells were detected in $RANK^{\Delta IEC}$ mice at 1 week after weaning. At 4 weeks after weaning, a population of IgA^+ $CD138^+$ cells was present in $RANK^{\Delta IEC}$ mice but the frequency of these cells remained less than that in $RANK^{F/F}$ littermates. There were no significant differences in frequencies of IgA^+ plasma cells at any time points in the mesenteric lymph node or spleen (Supplementary Figure 5). As most of the IgA produced by IgA^+ ASCs in the intestinal lamina propria is transcytosed across the epithelium and released into the lumen as SIgA, we also compared the concentration of fecal IgA in control and mutant mice at multiple time points beginning 4 days before weaning (Figure 5a). As neonatal mice transition from mother's milk to mouse chow as their primary food source, the concentration of fecal IgA drops to a nadir reached around 1 day after weaning. Tracking the production of fecal IgA at daily time points revealed that by 4 days post weaning there was a significant increase above baseline in fecal IgA production in all $RANK^{F/F}$ mice (Figure 5b). In contrast, there was not a significant uptick in fecal IgA production in any $RANK^{\Delta IEC}$ mice until at least 7 days after weaning. In M-cell-deficient $RANK^{\Delta IEC}$ mice, fecal IgA levels were lower throughout the first 5 weeks after weaning compared with $RANK^{F/F}$ littermates (Figure 5a). Although fecal IgA levels did

progressively increase in $RANK^{\Delta IEC}$ mice, the rate of this increase and the plateau concentration of fecal IgA reached in adults were significantly decreased compared with $RANK^{F/F}$ controls (Figure 5c). Although most of the IgA produced in the intestinal lamina propria ends up as SIgA, we also investigated whether serum IgA levels were affected in $RANK^{\Delta IEC}$ mice. $RANK^{\Delta IEC}$ mice also had significantly lower serum IgA levels than $RANK^{F/F}$ mice at 1 week after weaning but this difference was no longer apparent by 3 weeks after weaning (Supplementary Figure 6). The concentrations of serum IgM and IgG were equivalent in both genotypes at all time points tested.

$RANK^{\Delta IEC}$ mice display an impaired SIgA response to oral immunization with a protein antigen

To determine whether the absence of intestinal M cells in $RANK^{\Delta IEC}$ mice diminished their capacity to mount an antigen-specific SIgA response following oral exposure to a foreign protein antigen, 5-week-old $RANK^{\Delta IEC}$ and $RANK^{F/F}$ littermates were immunized with horse spleen ferritin.[30] Ferritin was added to their drinking water on days 0–2 and then again on days 7–9. Two weeks after the initial immunization, a ferritin-specific fecal IgA response was readily detected in $RANK^{F/F}$ mice but anti-ferritin IgA levels in $RANK^{F/F}$ littermates were still comparable to unimmunized controls (Supplementary Figure 7).

Enteric bacteria in fecal samples from $RANK^{\Delta IEC}$ mice have less bound SIgA

A significant portion of the normal SIgA repertoire in the intestine is directed against antigens found on enteric bacteria[7]. We prepared suspensions of fecal bacteria from $RANK^{\Delta IEC}$, $RANK^{F/F}$, and $JH^{-/-}$ mice, and measured the amount of IgA bound to individual bacteria by flow cytometry with a labeled secondary anti-IgA monoclonal

antibody (Figure 6). As expected, bound IgA was not detected on fecal bacteria from $JH^{-/-}$ mice (data not shown). At 4 weeks after weaning, the fraction of fecal bacteria coated by IgA and the average amount of bound IgA per bacterium were both decreased in $RANK^{\Delta IEC}$ samples compared with $RANK^{F/F}$ controls.

Effect of delayed and decreased SIgA production by $RANK^{\Delta IEC}$ mice on composition of the fecal microbiota

As production of SIgA is one of the pivotal host immune responses involved in establishing homeostasis with the gut microbiota, we investigated whether the absence of M cells and the associated SIgA deficit in $RANK^{\Delta IEC}$ mice resulted in perturbations in the composition of the gut microbiota. Fecal samples from co-housed littermate $RANK^{\Delta IEC}$ and $RANK^{F/F}$ mice were collected at 3, 7, 20, 30, and 40 days after weaning. Illumina (San Diego, CA) sequencing of 16S rRNA amplimers revealed no substantive shifts at the family level in the types of bacteria present in the two genotypes of mice and a comparable amount of alpha diversity (Supplementary Figure 8).

Impaired induction of SIgA after conventionalization of germ-free $RANK^{\Delta IEC}$ mice

SIgA responses in the intestine of germ-free mice are markedly suppressed due to the absence of the microbiota that normally provides the dominant source of antigens eliciting this response.[31, 32] Conventionalization of previously germ-free mice normally results in a rapid rebound of the SIgA response.[3] To examine the impact of loss of intestinal M cells on fecal IgA responses in the germ-free condition and after conventionalization, we established a germ-free colony of $RANK^{\Delta IEC}$ mice housed with $RANK^{F/F}$ littermates. Both groups produced equally low concentrations of fecal IgA after weaning and the IgA concentrations rose slightly to reach a plateau around 4 weeks after

weaning that was far below the typical fecal IgA concentration detected in conventionally housed mice (Figure 7a). When groups of germ-free $RANK^{\Delta IEC}$ mice and $RANK^{F/F}$ controls were acutely conventionalized at the time of weaning with the microbiota present in the specific pathogen-free mouse colony, the M-cell-deficient mice exhibited significantly decreased fecal IgA responses at 4 and 6 weeks after weaning (Figure 7b). This deficit in fecal IgA production recapitulated the fecal IgA phenotype observed in the original specific pathogen-free colony (Supplementary Figure 5) and confirmed that the absence of antigen-sampling M cells is sufficient to seriously compromise the rapid host SIgA response elicited by conventionalization of germ-free mice.

Discussion

One of the cardinal features of mucosal immunity in mammals is the synthesis and transepithelial transport of large amounts of SIgA that contribute to maintaining homeostasis with the enteric microbiota.[4, 33] Endogenous SIgA production normally begins shortly after weaning, coincident with a shift from breast milk to solid food as the main nutrition source and accelerated colonization of the intestine by commensal bacteria. The initial endogenous SIgA response is dominated by IgA antibodies with few, if any, mutations in their variable regions and low avidity for the bacteria in the lumen.[34] As the mucosal immune system matures, most of the SIgA antibodies secreted in the intestine carry mutations concentrated in the complementarity-determining regions of VH and VL domains. These mutations occur as a result of T-cell-dependent somatic mutation in GCs and lead to increased avidity of the antibodies for target antigens. B-cell clones responding to foreign antigens that persist can undergo additional rounds of somatic mutation in GALT GCs contributing to further increases in antibody affinity.[35]

A major source of antigens driving SIgA production in the intestine is the commensal enteric flora. As a result, germ-free mice have a markedly attenuated SIgA response.[31, 36] Furthermore, SIgA production in germ-free mice can be restored to near normal levels over the course of several weeks after conventionalization with bacterial species that can establish stable residence in the intestine.[3] For the host immune system to mount an IgA response to antigens originating with the commensal microbiota, bacterial antigens must cross the epithelium and reach APCs that display the antigens enabling stimulation and expansion of reactive B cells and T cells. This antigen sampling process can potentially involve either soluble antigens or whole bacteria. The relative

contributions to the overall SIgA response of the main cellular pathways that participate in *in vivo* sampling of antigens from the intestinal lumen (i.e., M cells, mononuclear phagocytes, and goblet cells) have not been established.[14] A series of technical limitations have made it impractical or impossible to selectively eliminate just one of these antigen sampling pathways *in vivo* in the intestine. For example, mice lacking any intestinal goblet cells die shortly after weaning due to severe problems with establishment of the normal mucus barrier.[37] Although some knockout mouse strains either lack or have induced defects in specific DC and macrophage subsets, there is not yet an established model with a complete absence of all mononuclear phagocyte subsets. The absence of suitable mouse models featuring complete abrogation of individual intestinal antigen sampling pathways has hampered efforts to assess the individual contributions of each cellular pathway.

We sought to develop mice with selective absence of intestinal M cells by drawing on previous work that established the dependence of intestinal M-cell differentiation on RANKL–RANK signaling.[25] Cre-mediated deletion of a floxed *Tnfrsf11a* gene restricted to enterocytes yielded mice in which RANKL-directed differentiation of intestinal M cells from uncommitted precursors in follicle-associated crypts did not occur. The functional consequence of the absence of M cells in these 'M-less' mice was a profound deficit in the uptake of several types of model particulate antigens (0.2μm beads and bacteria) into PPs, confirming that M cells are responsible for the vast majority of uptake of these classes of antigens into GALT structures. The other major cell types responsible for intestinal antigen sampling (mononuclear phagocytes and goblet cells) remain functionally intact in these mice, which enabled us to investigate

whether loss of the M-cell antigen-sampling pathway alone interfered with specific types of mucosal immune responses.

Seminal work by Craig and Cebra[38] identified PPs as a rich source of lymphocyte precursors capable of differentiating into IgA-secreting plasma cells in the intestinal lamina propria after adoptive transfer. Although M-cell-mediated antigen sampling is restricted to GALT structures such as PPs, the other major antigen sampling mechanisms described in the intestine are also functional in GALT structures and could therefore contribute to inducing IgA responses at these sites. The substantial deficit in the post-weaning SIgA response observed in the $RANK^{\Delta IEC}$ mouse model proves that antigen sampling by GALT M cells is pivotal for the efficient early generation of IgA responses. A closely correlated feature of the deficient inductive environment in PPs from $RANK^{\Delta IEC}$ mice was delayed appearance of recognizable GCs within the B-cell follicles. The decreased amount of total fecal IgA secreted into the intestinal lumen of $RANK^{\Delta IEC}$ mice also correlated well with flow cytometry results showing a decreased amount of IgA bound to fecal bacteria. $RANK^{\Delta IEC}$ mice also displayed a defect in the induction of fecal IgA responses to a newly introduced oral protein antigen, confirming that lack of intestinal M cells results in a generalized defect in the rapid induction of IgA responses to foreign antigens encountered in the gut lumen.

When the normal commensal microbiota was eliminated as a potential source of antigens inducing the SIgA response by studying germ-free $RANK^{\Delta IEC}$ mice, the weak residual SIgA response was not significantly different from that of the control $RANK^{F/F}$ littermates. Thus, the normal SIgA response of mice that briskly develops following weaning depends on sampling of the commensal microbiota by M cells. The availability

of this efficient M-cell-mediated antigen-sampling pathway is one of the major factors responsible for the high frequency of precursors to mature IgA-secreting plasma cells in PPs compared with the blood and peripheral lymph nodes.[38]

We also found that the extent of the fecal IgA deficit observed in $RANK^{\Delta IEC}$ mice compared with $RANK^{F/F}$ controls was partially attenuated as the mice progressed toward adulthood. Several factors likely contribute to this narrowing of the difference between the two genotypes over time. As antigen sampling is not impaired at the non-intestinal mucosal sites in $RANK^{\Delta IEC}$ mice, normal initiation of IgA responses occurs at these other mucosal sites. Not all IgA plasma cells induced within a single mucosal tissue end up homing back to effector sites in the same mucosal tissue. The partial overlap in the homing mechanisms used for IgA plasma cells to return to the various mucosal tissues allows some IgA plasma cells induced in non-intestinal mucosal tissues to end up localizing to the intestine.[1, 39, 40]Another factor in narrowing the gap between the two genotypes is further expansion of the initial clones of memory B cells and plasma cells that reach the intestine. As IgA-producing B cells can re-enter GCs to proliferate further and undergo receptor diversification,[35] we speculate that the few IgA-secreting plasma cells that initially seed the lamina propria of $RANK^{\Delta IEC}$ mice have the potential to be amplified in PPs, leading to increases in the number of lamina propria plasma cells and the amount of SIgA even if the diversity of the resulting IgA repertoire remains substantially constricted compared with wild-type mice as a consequence of decreased transport of commensal microbiota antigens into the inductive sites via M cells. Finally, some of the SIgA normally present in feces initially enters the gastrointestinal tract as a constituent of bile. Hepatocytes and biliary epithelial cells expressing the polymeric

immunoglobulin receptor can transcytose dimeric IgA and deliver this SIgA into the gut lumen to add to the IgA transcytosed across the intestinal epithelium by enterocytes.[41]

Our findings support a fundamental role for M cells in driving SIgA responses that are targeted toward commensal bacteria. Despite the scarcity of M cells relative to other cell types in the intestinal epithelium and underlying lamina propria, M cells have a critical and non-redundant role in establishment of normal secretory immunity at inductive GALT sites.

Acknowledgements

We thank Dr. Tim Denning for valuable suggestions and advice. We also thank Dr Lucie Etienne-Mesmin from the Gewirtz lab for assisting with husbandry of the germ-free RANK$^{\Delta IEC}$ mice and Dr. Andrew Neish for providing the *LGG* bacterial strain. This work was supported by grants from the NIH (DK64730 to I.R.W., AI111388 to I.R.W. and A.T.G., and DK64399 supporting the Imaging Core Facility of the Emory Digestive Diseases Research Development Center) and the Crohn's & Colitis Foundation of America (Senior Research Award to I.R.W.). D.R. was supported in part by a Research Supplement to Promote Diversity in Health-Related Research from the NIH.

References

1. Brandtzaeg, P. Secretory IgA: designed for anti-microbial defense. *Front. Immunol.* 4, 222 (2013).
2. Gutzeit, C., Magri, G. & Cerutti, A. Intestinal IgA production and its role in host-microbe interaction. *Immunol. Rev.* 260, 76–85 (2014).
3. Cebra, J.J., Periwal, S.B., Lee, G., Lee, F. & Shroff, K.E. Development and maintenance of the gut-associated lymphoid tissue (GALT): the roles of enteric bacteria and viruses. *Dev. Immunol.* 6, 13–18 (1998).
4. Macpherson, A.J., McCoy, K.D., Johansen, F.E. & Brandtzaeg, P. The immune geography of IgA induction and function. *Mucosal Immunol.* 1, 11–22 (2008).
5. Cerutti, A. The regulation of IgA class switching. *Nat. Rev. Immunol.* 8, 421–434 (2008).
6. Cao, A.T., Yao, S., Gong, B., Nurieva, R.I., Elson, C.O. & Cong, Y. Interleukin (IL)-21 promotes intestinal IgA response to microbiota. *Mucosal Immunol.* 8, 1072–1082 (2015).
7. Benckert, J. *et al*. The majority of intestinal IgA+ and IgG+ plasmablasts in the human gut are antigen-specific. *J. Clin. Invest.* 121, 1946–1955 (2011).
8. Peterson, D.A., McNulty, N.P., Guruge, J.L. & Gordon, J.I. IgA response to symbiotic bacteria as a mediator of gut homeostasis. *Cell Host Microbe* 2, 328–339 (2007).
9. Cullender, T.C. *et al*. Innate and adaptive immunity interact to quench microbiome flagellar motility in the gut. *Cell Host Microbe* 14, 571–581 (2013).
10. Bunker, J.J. *et al*. Innate and adaptive humoral responses coat distinct commensal bacteria with immunoglobulin A. *Immunity* 43, 541–553 (2015).
11. Palm, N.W. *et al*. Immunoglobulin A coating identifies colitogenic bacteria in inflammatory bowel disease. *Cell* 158, 1000–1010 (2014).

12. Shroff, K.E., Meslin, K. & Cebra, J.J. Commensal enteric bacteria engender a self-limiting humoral mucosal immune response while permanently colonizing the gut. *Infect. Immun.* 63, 3904–3913 (1995).
13. Macpherson, A.J., Gatto, D., Sainsbury, E., Harriman, G.R., Hengartner, H. & Zinkernagel, R.M. A primitive T cell-independent mechanism of intestinal mucosal IgA responses to commensal bacteria. *Science* 288, 2222–2226 (2000).
14. Schulz, O. & Pabst, O. Antigen sampling in the small intestine. *Trends Immunol.* 34, 155–161 (2013).
15. Mabbott, N.A., Donaldson, D.S., Ohno, H., Williams, I.R. & Mahajan, A. Microfold (M) cells: important immunosurveillance posts in the intestinal epithelium. *Mucosal Immunol.* 6, 666–677 (2013).
16. Rescigno, M. *et al*. Dendritic cells express tight junction proteins and penetrate gut epithelial monolayers to sample bacteria. *Nat. Immunol.* 2, 361–367 (2001).
17. Chieppa, M., Rescigno, M., Huang, A.Y. & Germain, R.N. Dynamic imaging of dendritic cell extension into the small bowel lumen in response to epithelial cell TLR engagement. *J. Exp. Med.* 203, 2841–2852 (2006).
18. Farache, J. *et al*. Luminal bacteria recruit CD103+ dendritic cells into the intestinal epithelium to sample bacterial antigens for presentation. *Immunity*38, 581–595 (2013).
19. McDole, J.R. *et al*. Goblet cells deliver luminal antigen to CD103+ dendritic cells in the small intestine. *Nature* 483, 345–349 (2012).
20. Owen, R.L. & Jones, A.L. Epithelial cell specialization within human Peyer's patches: an ultrastructural study of intestinal lymphoid follicles.*Gastroenterology* 66, 189–203 (1974).

21. Neutra, M.R., Phillips, T.L., Mayer, E.L. & Fishkind, D.J. Transport of membrane-bound macromolecules by M cells in follicle-associated epithelium of rabbit Peyer's patch. *Cell Tissue Res.* 247, 537–546 (1987).

22. Bockman, D.E. & Cooper, M.D. Pinocytosis by epithelium associated with lymphoid follicles in the bursa of Fabricius, appendix, and Peyer's patches. An electron microscopic study. *Am. J. Anat.* 136, 455–477 (1973).

23. Owen, R.L. Sequential uptake of horseradish peroxidase by lymphoid follicle epithelium of Peyer's patches in the normal unobstructed mouse intestine: an ultrastructural study. *Gastroenterology* 72, 440–451 (1977).

24. Taylor, R.T. *et al*. Lymphotoxin-independent expression of TNF-related activation-induced cytokine by stromal cells in cryptopatches, isolated lymphoid follicles, and Peyer's patches. *J. Immunol.* 178, 5659–5667 (2007).

25. Knoop, K.A. *et al*. RANKL is necessary and sufficient to initiate development of antigen-sampling M cells in the intestinal epithelium. *J. Immunol.* 183, 5738–5747 (2009).

26. Dougall, W.C. *et al*. RANK is essential for osteoclast and lymph node development. *Genes Dev.* 13, 2412–2424 (1999).

27. Hikosaka, Y. *et al*. The cytokine RANKL produced by positively selected thymocytes fosters medullary thymic epithelial cells that express autoimmune regulator. *Immunity* 29, 438–450 (2008).

28. de Lau, W. *et al*. Peyer's patch M cells derived from Lgr5(+) stem cells require SpiB and are induced by RankL in cultured 'miniguts'. *Mol. Cell. Biol.* 32, 3639–3647 (2012).

29. Kramer, D.R. & Cebra, J.J. Early appearance of 'natural' mucosal IgA responses and germinal centers in suckling mice developing in the absence of maternal antibodies. *J. Immunol.* 154, 2051–2062 (1995).

30. Weisz-Carrington, P., Roux, M.E., McWilliams, M., Phillips-Quagliata, J.M. & Lamm, M.E. Organ and isotype distribution of plasma cells producing specific antibody after oral immunization: evidence for a generalized secretory immune system. *J. Immunol.* 123, 1705–1708 (1979).

31. Benveniste, J., Lespinats, G. & Salomon, J. Serum and secretory IgA in axenic and holoxenic mice. *J. Immunol.* 107, 1656–1662 (1971).

32. Crabbe, P.A., Bazin, H., Eyssen, H. & Heremans, J.F. The normal microbial flora as a major stimulus for proliferation of plasma cells synthesizing IgA in the gut. The germ-free intestinal tract. *Int. Arch. Allergy Appl. Immunol.* 34, 362–375 (1968).

33. Mestecky, J. The common mucosal immune system and current strategies for induction of immune responses in external secretions. *J. Clin. Immunol.* 7, 265–276 (1987).

34. Lindner, C. *et al*. Age, microbiota, and T cells shape diverse individual IgA repertoires in the intestine. *J. Exp. Med.* 209, 365–377 (2012).

35. Bergqvist, P. *et al*. Re-utilization of germinal centers in multiple Peyer's patches results in highly synchronized, oligoclonal, and affinity-matured gut IgA responses. *Mucosal Immunol.* 6, 122–135 (2013).

36. Hapfelmeier, S. *et al*. Reversible microbial colonization of germ-free mice reveals the dynamics of IgA immune responses. *Science* 328, 1705–1709 (2010).

37. Yang, Q., Bermingham, N.A., Finegold, M.J. & Zoghbi, H.Y. Requirement of Math1 for secretory cell lineage commitment in the mouse intestine. *Science*294, 2155–2158 (2001).

38. Craig, S.W. & Cebra, J.J. Peyer's patches: an enriched source of precursors for IgA-producing immunocytes in the rabbit. *J. Exp. Med.* 134, 188–200 (1971).

39. Mestecky, J., McGhee, J.R., Michalek, S.M., Arnold, R.R., Crago, S.S. & Babb, J.L. Concept of the local and common mucosal immune response. *Adv. Exp. Med. Biol.* 107, 185–192 (1978).

40. Kunkel, E.J. & Butcher, E.C. Plasma-cell homing. *Nat. Rev. Immunol.* 3, 822–829 (2003).

41. Brown, W.R. & Kloppel, T.M. The liver and IgA: immunological, cell biological and clinical implications. *Hepatology* 9, 763–784 (1989).

42. Sato, T. & Clevers, H. Primary mouse small intestinal epithelial cell cultures.*Methods Mol. Biol.* 945, 319–328 (2013).

43. Mahe, M.M. *et al*. Establishment of gastrointestinal epithelial organoids. *Curr. Protoc. Mouse Biol.* 3, 217–240 (2013).

44. Chassaing, B., Ley, R.E. & Gewirtz, A.T. Intestinal epithelial cell toll-like receptor 5 regulates the intestinal microbiota to prevent low-grade inflammation and metabolic syndrome in mice. *Gastroenterology* 147, 1363–1377 (2014).

45. Caporaso, J.G. *et al*. QIIME allows analysis of high-throughput community sequencing data. *Nat. Methods* 7, 335–336 (2010).

46. Li, J. et al. RANK is the intrinsic hematopoietic cell surface receptor that controls osteoclastogenesis and regulation of bone mass and calcium metabolism. Proc. Natl.

Acad. Sci. U. S. A. 97: 1566-1571 (2000).

47.Dougall, W.C. et al. RANK is essential for osteoclast and lymph node development. Genes Dev. 13: 2412-2424 (1999).

48. Sato, T., Clevers, H. Primary mouse small intestinal epithelial cell cultures. Methods Mol. Biol. 945: 319-328 (2013).

49.Mahe, M.M. et al. Establishment of gastrointestinal epithelial organoids. Curr. Protoc. Mouse Biol. 3: 217-240 (2013). 5. Bell, S.M., Schreiner, C.M., Wert, S.E., Mucenski, M.L., Scott, W.J., Whitsett, J.A. Rspondin 2 is required for normal laryngeal-tracheal, lung and limb morphogenesis. Development 135: 1049-1058 (2008).

50. Bell, S.M., Schreiner, C.M., Wert, S.E., Mucenski, M.L., Scott, W.J., Whitsett, J.A. Rspondin 2 is required for normal laryngeal-tracheal, lung and limb morphogenesis. Development 135: 1049-1058 (2008).

Figure 1

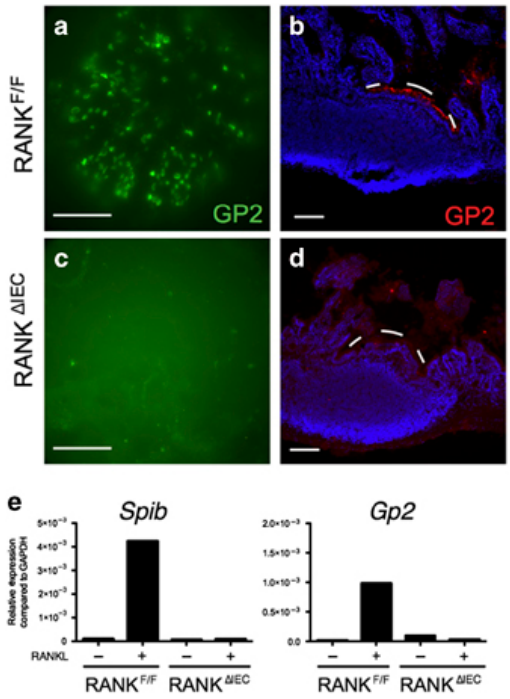

RANKΔIEC mice lack Peyer's patch (PP) M cells.

Representative images showing the distribution of GP2+ M cells in PPs from $RANK^{F/F}$ and RANKΔIEC mice as observed on whole mounts (a,c) and cryosections (b,d). The white dashes in (b) and (d) form an arc just above the apical surface of the follicle-associated epithelium (FAE). Bar = 100μM. (e) Enteroid cultures of crypt cells from $RANK^{F/F}$ and RANKΔIEC mice were cultured for 3 days in the presence or absence of RANKL. The level of expression of M-cell-associated genes Spib and Gp2 was determined by quantitative PCR and the results normalized to Gapdh. Data are representative of three experiments done with independently derived enteroid cultures. See also Supplementary Figure 1 for additional information on the floxed RANK allele and Supplementary Figure 2 for a histologic comparison of goblet cell and Paneth cell differentiation in $RANK^{F/F}$ and $RANK^{\Delta IEC}$ mice.

Figure 2

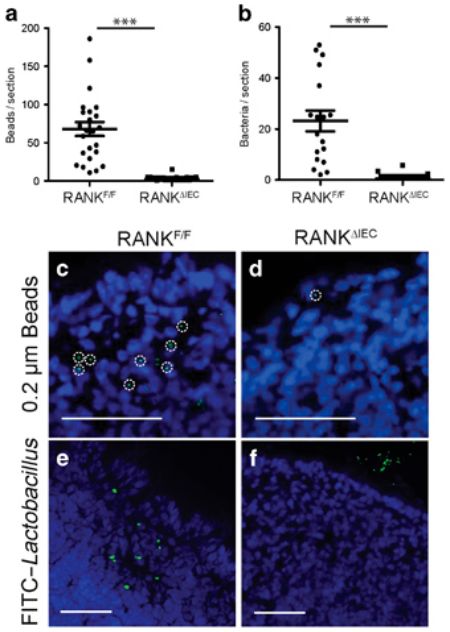

Peyer's patches (PPs) lacking M cells have reduced capacity to phagocytose particulate antigens.

$RANK^{F/F}$ and $RANK^{\Delta IEC}$ mice were gavage fed with either 1 × 1011 0.2-µm diameter fluorescein isothiocyanate (FITC)-labeled polystyrene beads (a) or 1 × 109 colony-forming unit (CFU) FITC-labeled L. rhamnosus strain GG (LGG) (b), followed by excision of the PPs after 6h (a) or 24h (b). Individual points on the scatter plots represent the number of beads or bacteria manually counted in cryosections of a single PP follicle (a) or the entire PP (b). (c,d) Representative images showing 0.2µm diameter beads within PPs from $RANK^{F/F}$ (c) and RANKΔIEC (d) mice. The dashed circles show individual phagocytic cells containing multiple beads. (e,f) Representative images showing FITC-LGG within PPs from $RANK^{F/F}$(e) and RANKΔIEC (f) mice. Bar = 100µM. Data from each group are summarized as mean±s.e.m. and are representative of two experiments with three mice per group. ***P<0.001 (t-test)

Figure 3

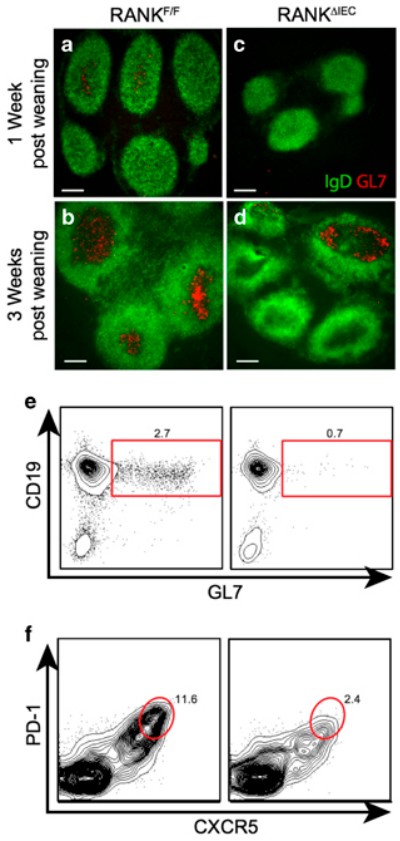

Germinal center (GC) formation is delayed in Peyer's patches (PPs) lacking M cells. Representative images of horizontal sections of PPs from $RANK^{F/F}$ and $RANK^{\Delta IEC}$ mice at 1 week (a,c) and 3 weeks (b,d) after weaning, showing the density of $GL7^+$ GC B cells within the IgD^- region of follicles. Bars =100μM. (e,f) Representative flow plots of PP lymphocytes from $RANK^{F/F}$ RANKF/F and $RANK^{\Delta IEC}$ mice at 2 weeks after weaning, stained for CD19 and GL7 to detect GC B cells (e) or PD-1 and CXCR5 to detect follicular helper T (Tfh) cells (f). Cells analyzed were gated on live $CD45^+$ singlets that were also $B220^+$ (e) or $CD4^+$ (f). Data are representative of two experiments with three mice per group. See also Supplementary Figures 3 and 4.

Figure 4

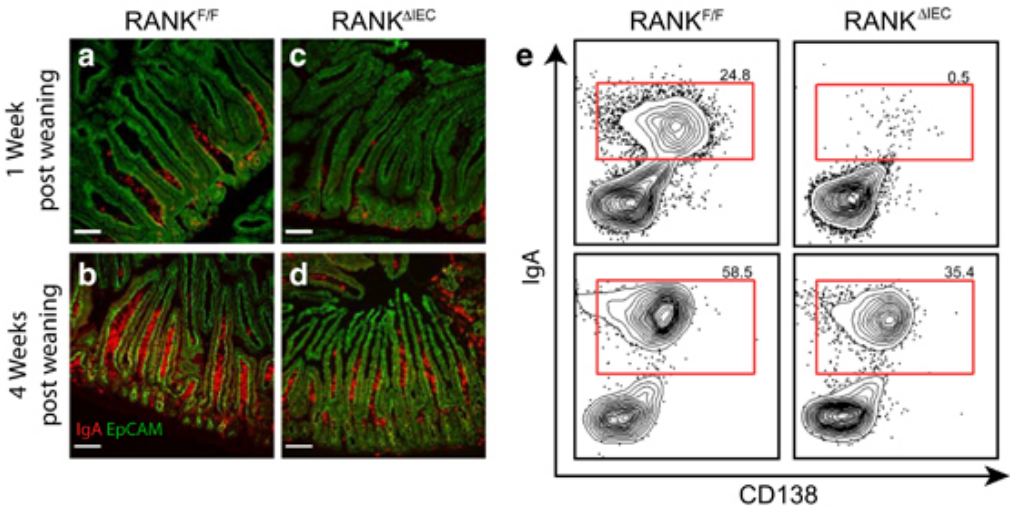

Frequency of lamina propria IgA$^+$ plasma cells is reduced in RANK$^{\Delta IEC}$ mice. Representative cryosections of small intestine from RANK$^{F/F}$ (a,b) or RANK$^{\Delta IEC}$ mice (c,d) at 1 week (a,c) or 4 weeks (b,d) after weaning were stained with anti-EpCAM (green) and anti-IgA (red). Bars = 100μM. (e) Representative flow plots from cells isolated from small intestinal lamina propria at 1 and 4 weeks after weaning. Cells analyzed were gated on live CD45$^+$ singlets that were also B220$^-$ and IgD$^-$. Data are representative of two experiments with three mice per group. See also Supplementary Figure 5.

Figure 5

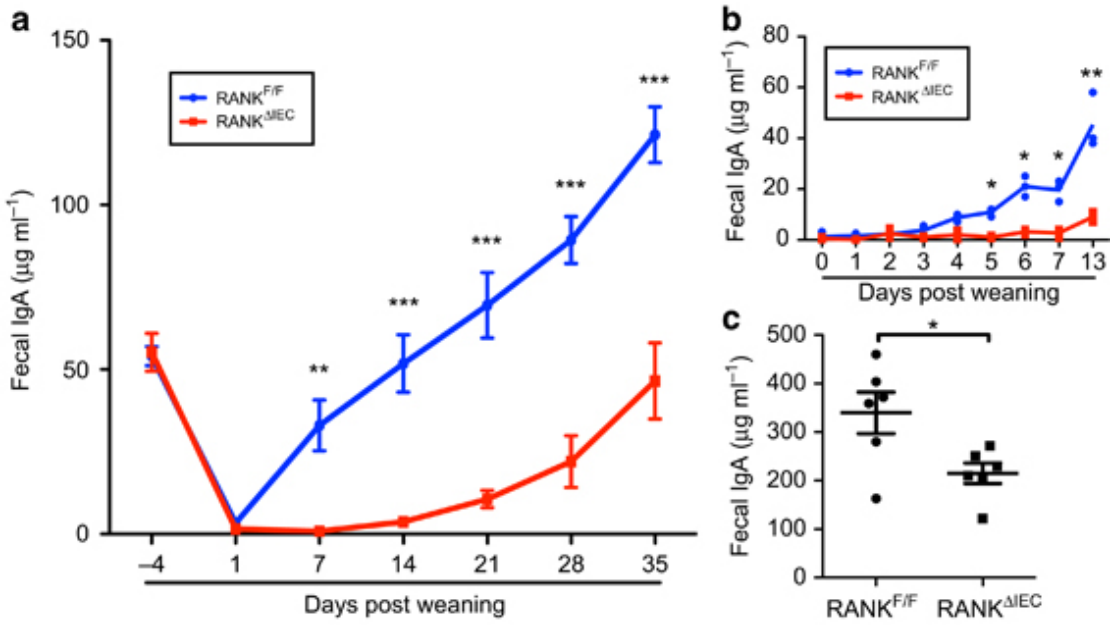

Production of fecal IgA is delayed and reduced in RANK$^{\Delta IEC}$ mice.

(a) Fecal IgA concentrations of RANK$^{F/F}$ and RANK$^{\Delta IEC}$ mice were determined at multiple time points starting at 4 days before weaning. Data are summarized as mean±s.e.m. and are representative of four experiments with four mice of each genotype. (b) Fecal IgA concentrations of RANK$^{F/F}$ and RANK$^{\Delta IEC}$ mice at daily time points beginning at weaning. Data are representative of two experiments with three mice of each genotype. (c) Fecal IgA concentrations in adult mice 8–10 weeks after weaning. Data are summarized as mean±s.e.m. and are from a single experiment with six mice of each genotype. *P<0.05, **P<0.01 (t-test). See also Supplementary Figure 6.

Figure 6

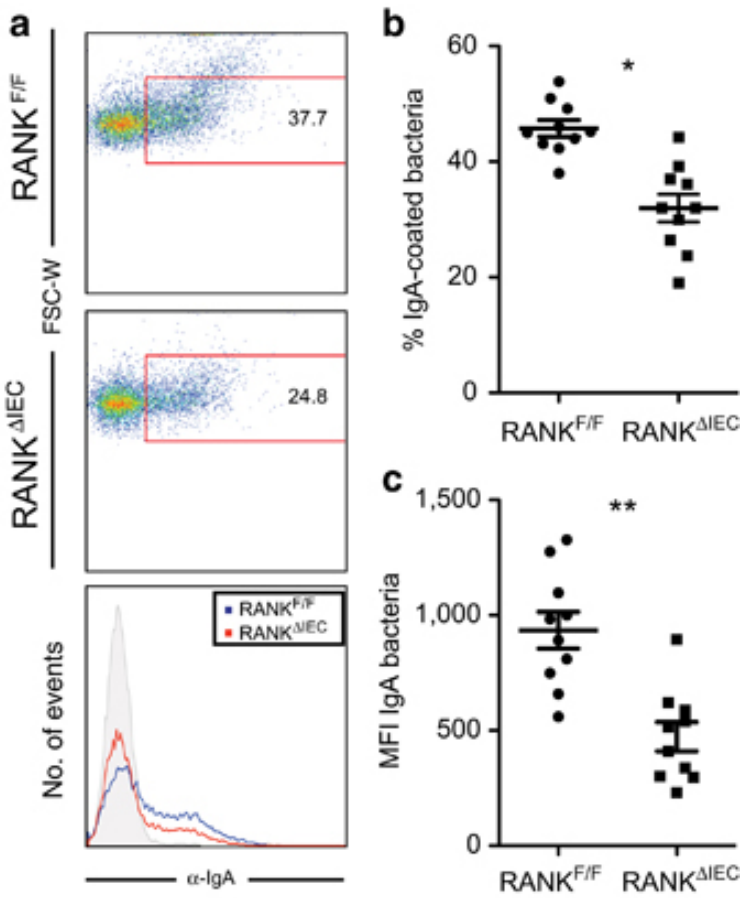

In vivo IgA coating of commensal microbiota is decreased in RANK$^{\Delta IEC}$ mice.

(a) Representative flow plots of fecal bacteria isolated from RANK$^{F/F}$ and RANK$^{\Delta IEC}$ mice 4 weeks after weaning and stained with anti-IgA. (b,c) The percentage of IgA+ fecal bacteria (b) and the mean fluorescence intensity of IgA binding (c) were determined using fecal bacteria from RANK$^{F/F}$ and RANK$^{\Delta IEC}$ mice. Data are summarized as mean±s.e.m. and are from 1 experiment with 10 mice per group. *P<0.05, **P<0.01 (t-test).

Figure 7

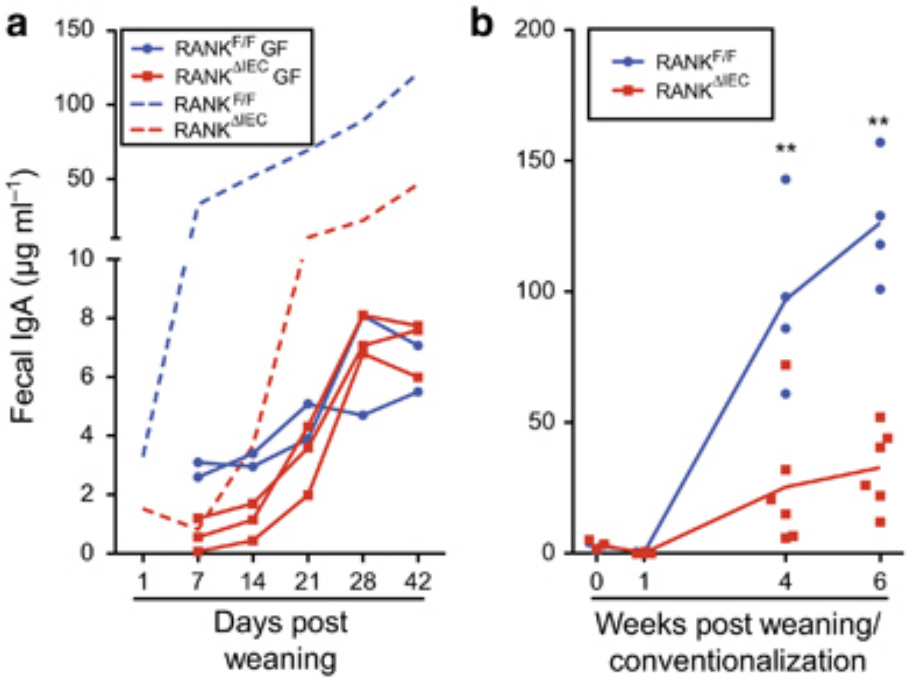

M cells are required to initiate IgA responses to the intestinal microbiota.

(a) The solid lines show fecal IgA concentrations in individual RANK$^{F/F}$ and RANK$^{\Delta IEC}$ littermates housed in a germ-free isolator from birth through 9 weeks of age. Data are from one of two litters that yielded similar results. The dashed lines show for comparison purposes the mean fecal IgA concentrations for RANK$^{F/F}$ and RANK$^{\Delta IEC}$ littermates housed under standard specific pathogen-free (SPF) conditions (data from Figure 5). (b) A single germ-free litter consisting of four RANK$^{F/F}$ mice and six RANK$^{\Delta IEC}$ mice was conventionalized by exposure to SPF fecal microbiota at weaning. The concentration of fecal IgA was determined at weaning and several time points after weaning. $^{**}P<0.01$ (unpaired *t*-test). See also Supplementary Figure 9.

Supplementary Figure 1

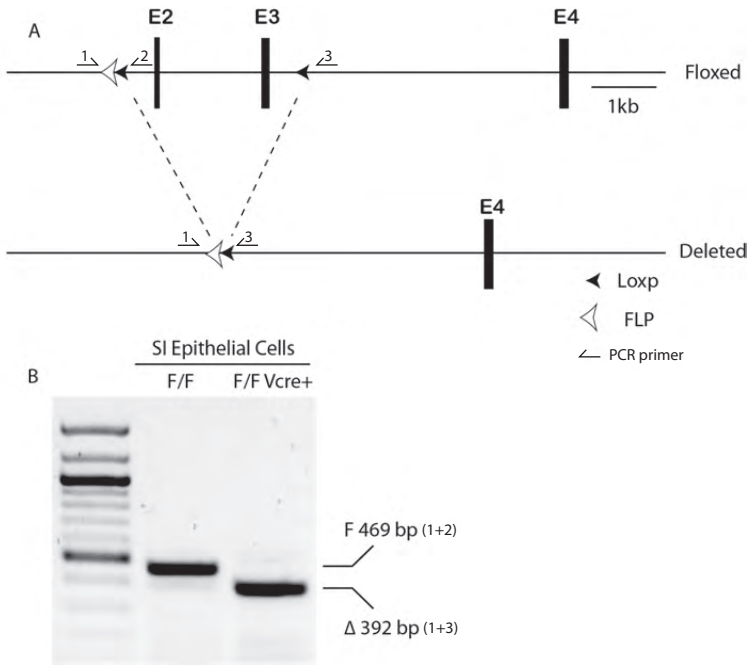

Generation of a Conditional RANK Knockout Allele

(A) LoxP sites were inserted before and after exons 2 and 3 of the RANK gene by homologous recombination in ES cells. When crossed with a transgenic mouse expressing Cre recombinase under the villin promoter, exons 2 and 3 of the RANK gene are deleted in intestinal epithelial cells resulting in a nonfunctional receptor. (B) DNA isolated from small intestinal epithelial cells was amplified by PCR using a sense primer (#1) and two antisense primers (#2 and #3). A 469 bp amplimer was obtained from $RANK^{F/F}$ mice using primers #1 and #2 located on opposite sides of the 5' loxP site. Only a smaller 392 bp amplimer was obtained from $RANK^{\Delta IEC}$ mice using primers #1 and #3 flanking the single remaining loxP site after deletion of exons 2 and 3.

Supplementary Figure 2

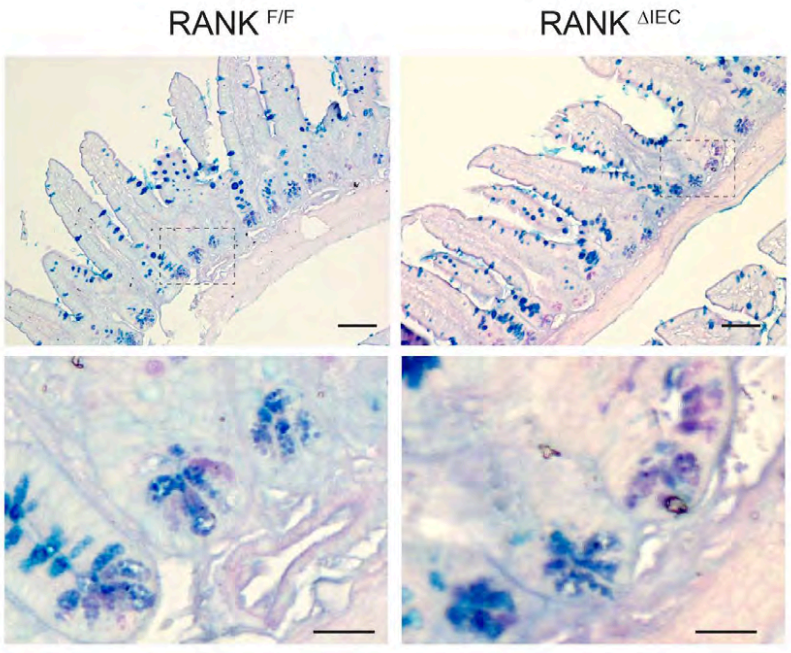

Normal Density, Distribution and Morphology of Goblet Cells and Paneth Cells in RANK$^{\Delta IEC}$ Mice

Small intestine tissue from 7-week-old RANK$^{F/F}$ and RANK$^{\Delta IEC}$ mice was fixed in formalin, embedded in paraffin and stained with a PAS-Alcian blue stain to identify mucin-containing goblet cells and granules within Paneth cells. The areas within the marked rectangles in the top set of panels are shown at higher magnification in the lower panels to better demonstrate the granules within Paneth cells at the base of the crypt. Goblet cells and Paneth cells are present at the same frequency in RANK$^{\Delta IEC}$ mice as in control RANK$^{F/F}$ mice, and there are no apparent morphological differences in any of the major enterocyte subsets. The scale bars represent 50 mM in the top panel and 10μM in the bottom panel.

Supplementary Figure 3

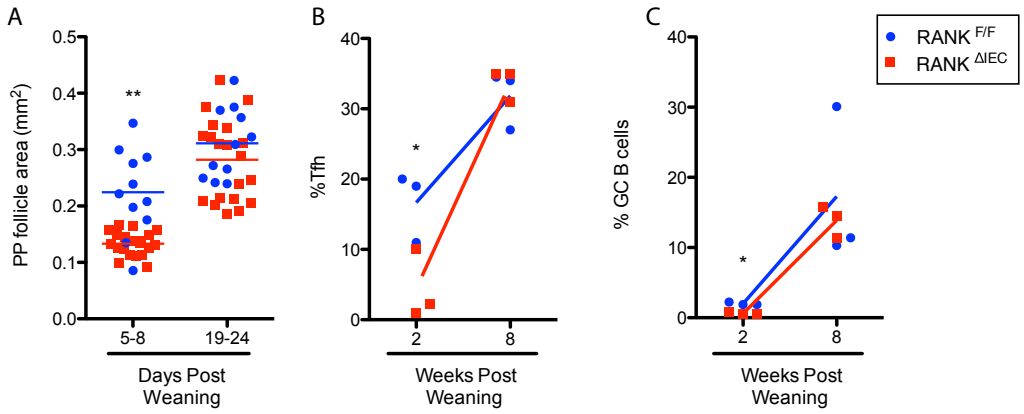

Peyer's Patches in RANK$^{\Delta IEC}$ Mice Have Smaller Follicles With Fewer Follicular Helper T Cells and Germinal Center B Cells

(A) Area of individual Peyer's patch follicles in RANK$^{\Delta IEC}$ and RANK$^{F/F}$ mice at 5-8 days after weaning and 19-24 days after weaning. The areas were calculated using major and minor radius measurements on PP follicles from 3 mice of each genotype in each age range. Data are summarized as mean ± SEM. (B) Frequencies of Tfh cells (CXCR5^{+} and PD-1^{+}) in Peyer's patches at 2 and 8 weeks after weaning.(C) Frequencies of germinal center B cells (CD19^{+} and GL7^{+}) in Peyer's patches at 2 and 8 weeks after weaning. *$p < 0.05$ (t-test), **$p < 0.01$ (t-test).

Supplementary Figure 4

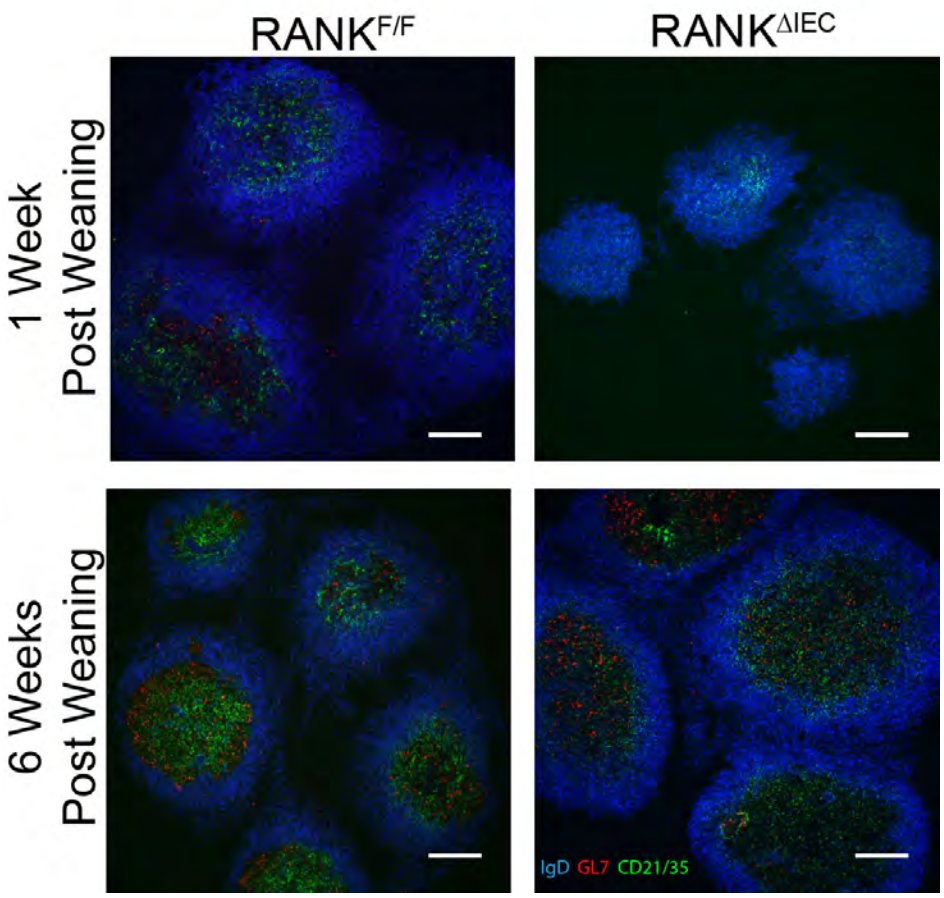

Peyer's Patch Germinal Centers from RANK$^{\Delta IEC}$ Mice Have a Normal Density of Germinal Center B Cells and Follicular Dendritic Cells at 6 Weeks after Weaning. Representative images of horizontal sections of PPs from RANK$^{F/F}$ and RANK$^{\Delta IEC}$ RANKΔIEC mice at 1 week (top row) and 6 weeks (bottom row) after weaning show that the density of GL7^{+} germinal center B cells and CD21/35^{+} follicular dendritic cells within the IgD^{-} region of Peyer's patch follicles is comparable in both strains at 6 weeks after weaning. The scale bars represent 100 μM.

Supplementary Figure 5

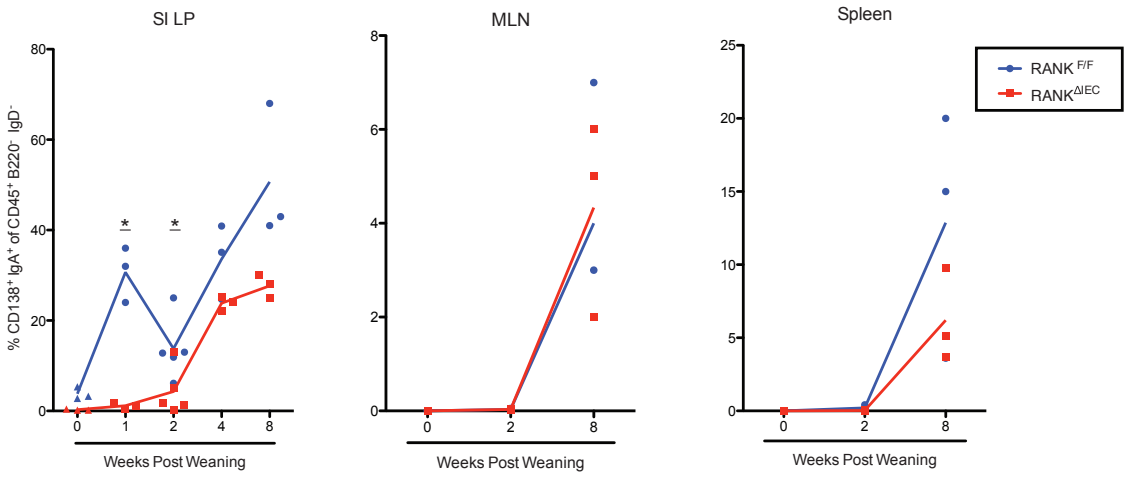

Frequency of IgA+ Plasma Cells is Reduced in the Small Intestinal Lamina Propria, But Not in the Mesenteric Lymph Node or Spleen.

Frequencies of IgA^+ plasma cells in the small intestinal lamina propria, mesenteric lymph node and spleen were determined at 0, 2, 4, and 8 weeks after weaning. Data are from 1 experiment with 3 mice per group at each time point examined. * $p < 0.05$ (t-test).

Supplementary Figure 6

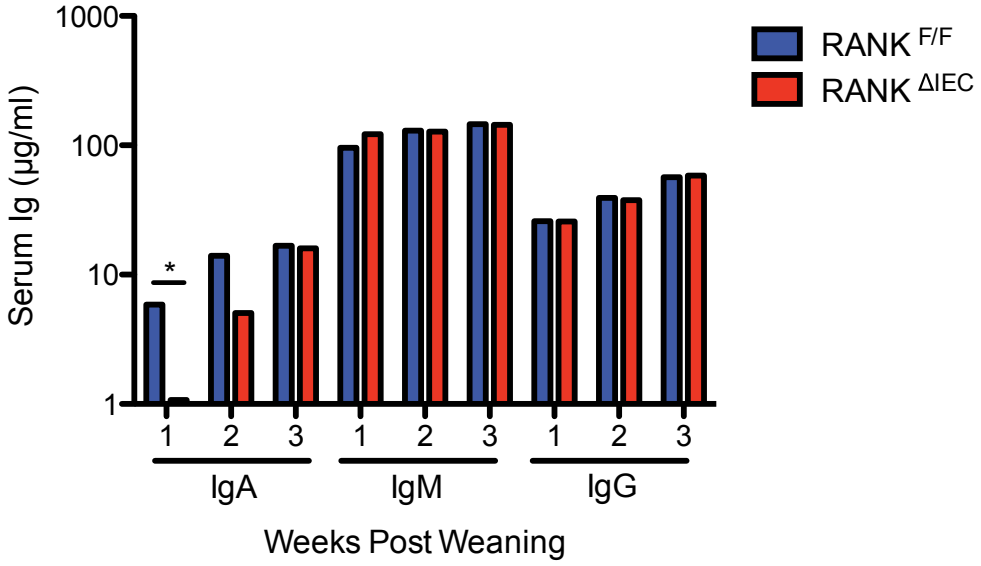

Serum IgA Concentrations Are Decreased in RANK$^{\Delta IEC}$ Mice at One and Two Weeks After Weaning.

Concentrations of serum IgA, IgM and IgG were determined by ELISA at 1, 2 and 3 weeks post weaning. Data are representative of 2 experiments with 3 mice per group. * $p < 0.05$ (t-test).

Supplementary Figure 7

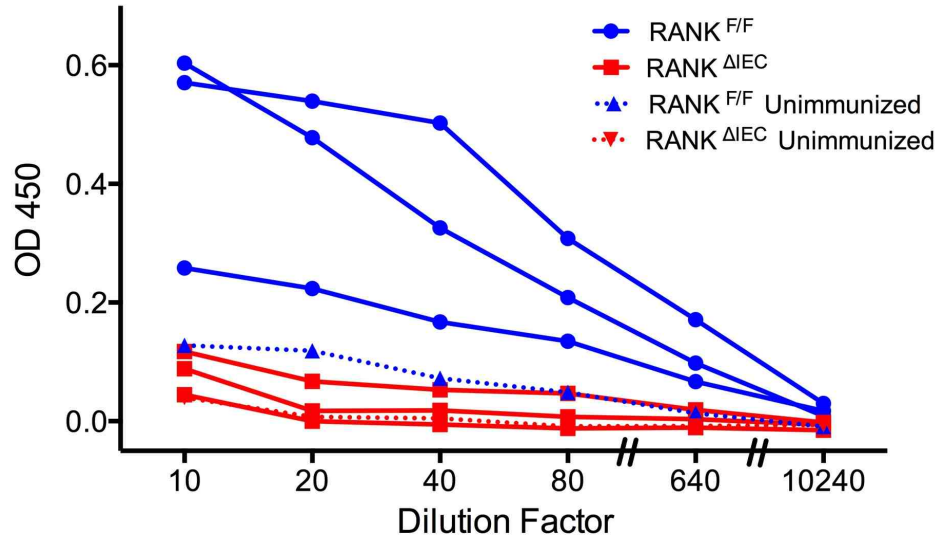

RANK$^{\Delta IEC}$ Mice Exhibit An Impaired Fecal IgA Response Following Oral Immunization With Horse Spleen Ferritin

Five-week-old RANK$^{\Delta IEC}$ mice and RANK$^{F/F}$ littermates (n=3 for both genotypes) were immunized with horse spleen ferritin by adding it to their drinking water on days 0-2 and then again on days 7-9. Two weeks after the initial immunization, serial dilutions of fecal supernatant from individual mice were tested for ferritin-specific fecal IgA by ELISA. The results are reported as the OD450 over a range of dilutions. Fecal supernatants from unimmunized age- matched control mice of both genotypes were used as controls.

Supplementary Figure 8

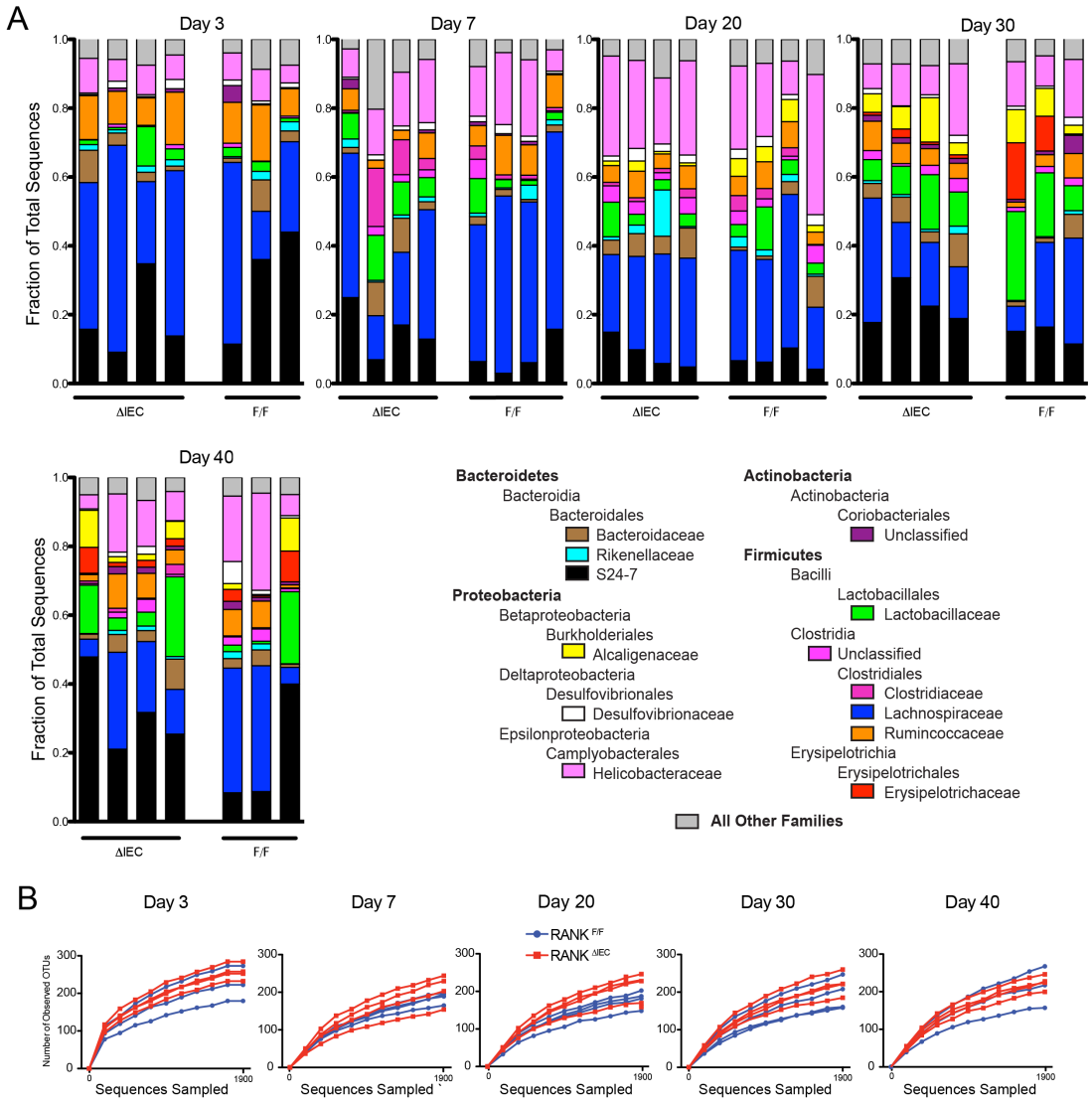

Fecal Microbiotas of RANK$^{F/F}$ and RANK$^{\Delta IEC}$ Mice Are Similar in Composition and Display Equivalent Alpha Diversity

Individual fecal samples from co-housed littermate RANK$^{\Delta IEC}$ and RANK$^{F/F}$ mice (n=3 or 4 for both genotypes) were collected at 3, 7, 20, 30, and 40 days after weaning. DNA was extracted from frozen fecal samples by bead beating. The V4 region of 16S rRNA genes was amplified with forward (515F) and reverse (806R) primers. PCR products pooled

from 4 independent amplifications were sequenced on an Illumina MiSeq and the sequences processed through a QIIME pipeline to yield OTU assignments and rarefaction curves. The results are displayed as stacked bar graphs showing the frequency of those bacterial families contributing 4% or more of the sequences in individual mice (A) and rarefaction curves for individual mice (B).

Supplementary Figure 9

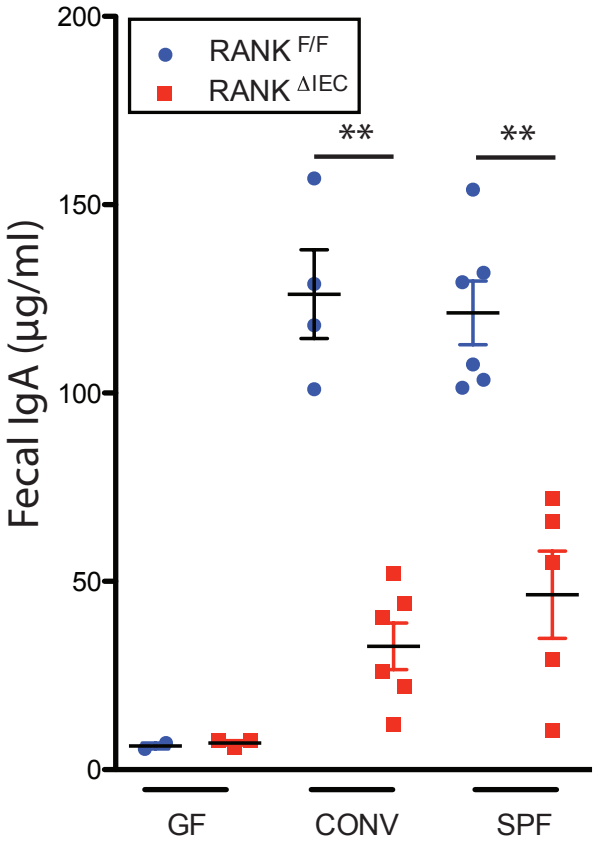

Achieving Normal Levels of Fecal IgA in Adult Mice Requires a Commensal Microbiota and Intestinal M Cells

Fecal IgA concentrations at 6 weeks after weaning were determined for litters containing both $RANK^{F/F}$ and $RANK^{\Delta IEC}$ mice that were maintained under germ-free (GF) conditions or born under germ-free conditions and conventionalized (CONV) with SPF flora at the time of weaning. These results are plotted alongside representative results from a litter maintained under standard SPF conditions. Data are summarized as mean ± SEM. **$p < 0.01$ (t-test).

Chapter 2

Differentiation and Function of Group 3 Innate Lymphoid Cells are Compromised in Mice Lacking Intestinal M cells

Rios D, Wood MB, Williams IR

Department of Pathology and Laboratory Medicine, Emory University School of Medicine, Atlanta, Georgia, USA.

Manuscript in Preparation

Abstract

Cryptopatches (CPs) are tertiary lymphoid structures found in the small and large intestine that can mature into isolated lymphoid follicles (ILFs), although the mechanisms by which this maturation occurs are poorly elucidated. Additionally, CPs serve as a primary physiological site at which group 3 innate lymphoid cells (ILC3) in the gut are located. Recent evidence suggests that both CPs and ILC3 are critical nodes in the IL-22 / IL-22R network and without either homeostasis is perturbed and responses to infection are attenuated. Despite the obvious linkage between CPs and ILC3 few studies have attempted to directly study their interdependence, instead opting to focus on the development of CPs or the role of ILC3 in mucosal immune responses independently. Here, we present data indicating that the maturation of CPs into ILFs and the development of ILC3 are partially dependent on the same pathways. We find that $RANK^{\Delta IEC}$ mice lacking intestinal M cells display stunted maturation of CPs into ILFs, have reduced frequency of ILC3 in intestinal tissues, and a reduced capacity for ILC3 to produce IL-22. These data indicate that antigen sampling by M cells is required for normal maturation of CPs into ILFs and the normal development of ILC3.

Introduction

The development of the mucosal immune system is dependent on crosstalk between host and microbiota. There are multiple established mechanisms by which antigen from the lumen of the intestine is sampled and transported into gut-associated lymphoid tissue (GALT) structures and the diffuse lamina propria of the small and large intestine. These mechanisms include the M cells in Peyer's patches (PPs) and isolated lymphoid follicles (ILFs) [1], mononuclear phagocytes in the lamina propria that can directly sample luminal contents via transepithelial dendrites [2-4], and goblet cells which have been recently shown to have the capacity to sample low molecular weight antigen.[5] However, the relative impact of each of these distinct pathways on the development of the various facets of the mucosal immune system remain poorly characterized.

Innate lymphoid cells (ILC) are newly described subset of the innate immune system.[6,7] At mucosal sites, group 3 ILC (ILC3) support epithelial cell proliferation and antimicrobial activity through the production of IL-22.[8] Developmentally these cells are reliant on the activity of the transcription factors T-bet, GATA3, RORγt and the aryl hydrocarbon receptor (AHR).[9-12] In the small intestine, these cells are found predominantly in cryptopatches (CPs), ILFs, and PPs, but are also found in the diffuse lamina propria.[13] It is well established that these cells are dependent on environmental stimuli, in the form of aryl hydrocarbon receptor ligands, for proper development. In mice lacking AHR frequencies of ILC3 in the intestinal lamina propria are dramatically reduced and the development of GALT structures, including PPs, CPs, and ILFs is ablated.[11,14] Many features of $AHR^{-/-}$ mice can be recapitulated by dietary restriction of AHR ligands indicating the primary source of AHR ligands is dietary in nature.[15]

Additionally, it appears that sensing of the microbiota is required for the normal development of CP and ILF, with multiple pattern recognition receptors contributing to this sensing.[16] Our current understanding of the relationship between the maturation of CPs into ILFs and the development of ILC3 is incomplete.

M cells are a specialized population of epithelial cells that are found exclusively on the follicle-associated epithelium of PPs and ILFs.[1] Previously, we reported that M cell development is dependent on RANKL-RANK signaling. In mice lacking the expression of RANKL, M cell development was blocked [17] and maturation of small intestinal CPs into ILFs was stunted.[18] In a subsequent study, we observed that tissue-specific abrogation of RANKL-RANK signaling in intestinal epithelial cells in $RANK^{\Delta IEC}$ mice resulted in complete loss of PP M cells. Furthermore, the loss of M cells resulted in the delayed initiation and persistent inhibition of secretory IgA responses.[19]

Based on our previous findings we hypothesized that M cells may play an important role in the development of CPs and their maturation into ILFs. Here we report that $RANK^{\Delta IEC}$ mice have stunted maturation of CPs in the small intestine associated with reduced frequencies of ILC3 in the lamina propria and decreased production of IL-22. These results suggest that M cells play an important, and previously unrecognized role in the development of CPs and ILFs and by extension are required for the full expansion and maturation of the ILC3 lineage.

Materials and Methods

Conditional RANK knockout mice. Derivation of mice with a conditional allele of *Tnfrsf11a* (the gene encoding RANK) featuring loxP sites flanking exons 2 and 3 was previously described [19]. These B6.Cg-Tnfrsf11a$^{tm1.1Irw}$/J mice were bred to villin-cre mice (Tg(Vil-cre)997Gum/J strain; The Jackson Laboratory) to produce mice homozygous for the floxed RANK allele that also carried the villin-cre transgene (villin- cre RANK$^{F/F}$ genotype; also designated RANK$^{\Delta IEC}$). Experimental mice used in experiments originated from breeding pairs of male RANK$^{\Delta IEC}$ and female RANK$^{F/F}$ mice and consisted of a mix of RANK$^{\Delta IEC}$ mice and RANK$^{F/F}$ littermates used as controls. Litters were weaned at either 21or 24 days after birth. All animal studies were reviewed and approved by the Emory University Institutional Animal Care and Use Committee.

Preparation of lamina propria cell suspensions for flow cytometry.To prepare intestinal lamina propria cells, PP were excised from the small intestine, the opened PP-free tissue was thoroughly washed in ice cold PBS to remove luminal contents, and the small intestine was cut into 10 approximately equal-sized pieces. The intestinal pieces were incubated for 15 min in PBS with 0.5 mM EDTA and 10 mM HEPES in a shaking incubator at 37^{o}C, and then strained though a large metal mesh strainer to remove epithelial cells. This step was repeated at until no epithelial cells were visible in the supernatant. The intestinal fragments were washed thoroughly with PBS to remove the EDTA, minced exactly 30 times with a small scissors in an microfuge tube and incubated in 20 ml of RPMI-1640 supplemented with 10% FBS, 0.25 mg/ml Collagenase D (Roche), 0.25 mg/ml Collagenase Fraction IV (MP Biomedicals) and 40 μg/ml DNase I (Roche) for 20 min at 37^{o}C, with constant agitation. After digestion intestinal fragments

were shaken vigorously by hand for 30 sec and passed through a 100 μm mesh cell strainer. The cell suspension was sedimented at 1000 g for 10 min and the resuspended pellet was further purified from the interface of a 30%/90% Percoll density gradient.

Intracellular cytokine staining after in vitro stimulation.Isolated cells were stimulated for 4 hr at 37^{o}C, in RPMI-1640 w/10% FBS and PMA (500 ng/ml)(Sigma) plus ionomycin (500 ng/ml) (Sigma) in the presence of recombinant IL-23 (20 ng/ml) (Biolegend) and brefeldin A (GolgiPlug, BD Biosciences).

Measurement of IL-22 secreted by organ-cultured ileal punch biopsies. Full-thickness punch biopsies of tissue from the terminal 2 cm of the ileum away from PPs were obtained with a dermal punch biopsy instrument. Two punch biopsies were cultured for 2 days in 150 μl of sterile filtered RPMI-1640 (Corning) containing 10% FBS (Atlanta Biologics), 10 mM HEPES (Corning), 100 U/ml penicillin (Corning), 100 μg/ml streptomycin (Corning), 100 μg/ml gentamycin (Corning) and 250 μg/ml amphotericin B (Corning) with or without rIL-23 (20 ng/ml) (BioLegend) for 48 hr at 37°C with 5% CO_2. IL-22 produced in the supernatant was then determined using the R&D Systems mouse IL-22 DuoSet kit according to the manufacturer's instructions.

Flow cytometry analysis. The directly conjugated antibodies included PE-anti-mouse IL-22 (Poly5164, BioLegend), PE-Cy7 anti-mouse-IL-17 (TC11-18H10.1, BioLegend), FITC anti-mouse-CD11c (N418, Tonbo), FITC anti-mouse-CD11b (M1/70, Tonbo), FITC anti-mouse-CD19 (1D3, Tonbo) APC anti-mouse RORγ (B2D, eBiosciences), PE NKp46 (294A1.4, eBiosciences), Alexa700 anti-mouse-CD4 (RM4-5, BioLegend), BV605 anti-mouse-CD45 (30-F11, BioLegend), violetFluor450 anti-mouse CD3 (17A2, Tonbo). Live/dead discrimination was done with Fixable Viability Dye eFluor 506

(eBioscience). Staining was carried out for 15 min at 20°C in PBS with 1% BSA and 0.02% NaN_3. After staining all cells were fixed for overnight at 4°C in FoxP3 / Transcription Factor Staining Buffer (Tonbo). To stain for intracellular cytokines and transcription factors, cells were permeabilized for 20 min at 20°C in BD Perm/Wash buffer, and then stained for 15 min at 20°C in BD Perm/Wash buffer. Stained cells were analyzed on an LSRII cytometer (BD Biosciences). Post-acquisition analysis of data was done with FlowJo v9.3.1 software.

Analysis of bacterial translocation by aerobic culture and 16S rRNA sequencing. Spleen, mesenteric lymph node (MLN), and liver were isolated under aseptic conditions. Tissue was mechanically homogenized by passage through a 40 μm mesh filter. Serial dilutions were plated on non-selective BHI agar (Gibco). For 16S rRNA analysis DNA extracted from tissue was amplified with forward F505 and reverse 806R primers flanking the V4 variable region. The products from 4 independent PCRs on each sample were purified and sequenced using an Illumina MiSeq sequencer as previously described [19].

Isolation of intestinal epithelial cell suspensions and staining with UEA-I.Intestinal epithelial cells (IEC) were isolated from $RANK^{F/F}$ and $RANK^{\Delta IEC}$ mice. Some of the mice were pretreated by i.p. injection of 1.5 μg of recombinant mouse IL-22 (BioLegend) 6 hr before tissue collection. The small intestinal tissue was incubated with 5 mM EDTA for 30 min at 37°C. Tissue fragments were passed through a 70 μm filter. Supernatant containing IEC was then pelleted by centrifugation at 650g for 10 min. The pellet was resuspended in 5 mM EDTA and vigorously pipetted to achieve a single cell suspension. The cells were then fixed overnight in 4% paraformaldehyde at 4°C. Cells were then

washed twice in PBS. Cells were then stained with 0.25 mg/ml FITC-UEA-I (Vector Labs) for 20 min at 20^{o}C. Stained cells were analyzed on an LSRII cytometer (BD Biosciences). For whole mount UEA-I staining of intestinal epithelial cells intestinal segments were isolated and fixed in 4% paraformaldehyde for 20 min at 20^{o}C. After fixation cells were incubated with 1% N-acetyl-L-cysteine (Sigma) for 15 min at 20^{o}C with constant agitation to remove mucus. Intestinal segments were then stained with 0.25 mg/ml FITC UEA-I (Vector Labs) for 20 min at 20^{o}C. The tissue was mounted in ProLong Gold anti-fade reagent (Invitrogen) and held for 1 hour at 4^{o}C in the dark prior to image acquisition using a Nikon 80i epifluorescence microscope.

Enumeration of lymphoid aggregates in the small and large intestine. The terminal 4 cm of the ileum or large intestine were harvested at the indicated time-points and placed directly into ice-cold PBS. The tissue was then fixed for 1 min at room temperature in 4% paraformaldehyde, and then briefly rinsed in PBS. Tissue was then placed in a solution of PBS with 10% sucrose (EMD Millipore) until it sank to the bottom of the vessel containing the solution. At this point tissues were opened via cutting along the mesenteric wall of the intestine and rinsed thoroughly in PBS to remove fecal matter. Tissues were then laid flat, embedded in OCT (TissueTek) freezing media and flash frozen. Three 5.0 μm sections were cut on a Leica 1510 cryostat at 100 μm intervals to ensure that suitable regions for the counting of CPs and ILFs were present throughout the section. Sections were then fixed for 20 min in acetone at -20°C and blocked for 10 minutes in StartingBlock buffer (Thermo Fisher Scientific). Sections were then stained for 2 hrs at room temperature or overnight at 4°C with PE anti-mouse Thy-1.2 (30-H12, BioLegend) and FITC anti-mouse B220 (RA3-6B2, Tonbo). Sections were then mounted in ProLong

Gold anti-fade reagent (Invitrogen) and held for 1 hr at 4^{o}C in the dark prior to image acquisition using a Nikon 80i epifluorescence microscope. The total number of lymphoid aggregates was determined manually,.

Classification of lymphoid aggregates in the intestine. Three types of CPs were identified based on Thy-1 and B220 staining of sections: CPs containing no B cells, CPs with 1-10 B cells and CPs with 10-50 B cells. Two types of ILFs were identified. Immature ILFs were identified as structures containing greater than 50 B cells and some follicular organization. Mature ILFs were identified as structures containing greater than 50 B cells, a central B cell follicle and most Thy-1 cells located peripherally. Representative images of each of the 5 categories are shown in Fig. S1.

RegIIIβ staining and imaging.Segments of the small intestine located 2-8 cm and 14-20 cm away from the ileo-cecal junction were harvested and immersion fixed in 4% paraformaldehyde for 30 minutes at room temperature. Tissue was mounted in "Swiss roll" orientation in OCT freezing media (TissueTek) and snap frozen. Sections with a thickness of 5.0 μm were cut on a Leica 1510 cryostat and allowed to equilibrate to room temperature. Slides were washed briefly in PBS, and then blocked for 10 min in StartingBlock buffer (Thermo Fisher Scientific). Slides were stained overnight with sheep anti-mouse RegIIIβ at 10 μg/ml (Cat #AF5110, R&D Systems). The next day slides were washed 3 times in PBS, and stained with rabbit anti-sheep FITC (Southern Biotech) at a 1:1000 dilution in PBS with DAPI for 1 hour at room temperature. Slides were washed 3 times in PBS mounted in ProLong Gold anti-fade reagent (Invitrogen) and held for 1 hr at 4^{o}C in the dark prior to image acquisition using a Nikon 80i epifluorescence microscope.

Quantitative real time PCR analysis of gene expression.Segments of small intestine located 0-2 cm and 12-14 cm away from the ileo-cecal junction were isolated. The segments were opened lengthwise and washed thoroughly in PBS to remove adherent feces. Cleaned SI segments were then placed in 1 ml of PBS with 5 mM EDTA for 30 min at room temperature and then vigorously shaken to dissociate epithelium from the underling lamina propria. The solution containing epithelial cells was centrifuged at 5000g to pellet intestinal epithelial cells. Intestinal epithelial cells were resuspended in 500 µl of RNALater (Sigma) and stored for 24 hours at 4^{o}C. RNA was isolated via the manufacturers instructions for the RNeasy Mini Kit (Qiagen). RNA concentrations were determined using a Nanodrop spectrophotometer. 500 ng of template RNA was used to generate cDNA using the iScript cDNA synthesis kit (BioRad). RT-qPCR was performed on a CFX Connect thermal cycler (Bio-Rad) using iTaq Universal SYBR Green Supermix (Bio-Rad). The primer pairs used to determine relative expression levels of genes of interest were: *Gapdh* 5'-TTCACCACCATGGAGAAGGC-3' and 5'-GGCATGGACTGTGGTCATGA-3'; *Reg3b* 5'-ATAGGGCAACTTCACCTCAC - 3' and 5'-CTGCCTTAGACCGTGCTTTC-3'; *Reg3g 5'*-TTCAGCGCCACTGAGCACAGAC-3' and 5'-CGTGCCTATGGCTCCTATTGCT-3'; and cryptdins 5'-GGTGATCATCAGACCCCAGCATCAGT-3' and 5'-AAGAGACTAAAACTGAGGAGCAGC-3' [20]. The relative expression of target genes was determined by normalization to *Gapdh* using the comparative Ct method.

Statistical analysis.Prism (GraphPad Software) was used to carry out statistical tests. Most comparisons of groups were done using a paired Student's t test. The other comparisons were done by using the nonparametric Mann-Whitney and log-rank tests. A

p of 0.05 was considered the threshold for significance.

Results

Cryptopatch maturation is impaired in RANK$^{\Delta IEC}$ mice

To assess the impact of the loss of M cells on the development of CPs, the terminal 4 cm of the ileum was harvested at 3, 4.5 and 10 weeks post birth from RANK$^{\Delta IEC}$ and control RANK$^{F/F}$ mice (Fig. 1). Frozen horizontal sections were taken from these intestinal fragments and stained with anti-Thy-1.2 and anti-B220 antibodies to visualize CPs and ILFs. These structures were assigned to 5 categories described in Methods based on the extent of maturation.

At day 3 weeks post birth we observed no differences in the number of lymphoid aggregates between RANK$^{\Delta IEC}$ and RANK$^{F/F}$ mice. There were very few lymphoid aggregates in both genotypes of mice, and all the observed aggregates contained no B220 positive cells indicating that they were immature CPs. By 4.5 weeks post birth, there were a greater number of total lymphoid aggregates in both types of mice, but differences in the maturation state of these aggregates were apparent. In control RANK$^{F/F}$ mice the majority of the aggregates began to incorporate B cells while the majority of aggregates from RANK$^{\Delta IEC}$ contained no B cells and were identified as immature cryptopatches. These differences persisted at 10 weeks post birth with many immature and mature ILF in RANK$^{F/F}$ mice while the majority of aggregates from RANK$^{\Delta IEC}$ still contained few B cells (Fig. 1A).

Interestingly, we observed that development of CPs into ILFs in the large intestine did not appear to be affected by the loss of RANK expression in the enterocytes of the colon. We observed an equivalent distribution of lymphoid aggregates in the terminal 4 cm of the large intestine in RANK$^{\Delta IEC}$ and RANK$^{F/F}$ mice (Fig. S2).

RANK$^{\Delta IEC}$ have reduced frequencies of ILC3

Previous studies indicate that CPs and ILFs are the physiological locations at which the majority of ILC3 reside.[14] We therefore hypothesized that the decreased total number of lymphoid aggregates and the stunted maturation of CPs into ILFs observed in RANK$^{\Delta IEC}$ mice would result in a reduced total frequency of ILC3 in the gut of these mice. The frequency of ILC3 was determined by flow cytometric analysis of lymphocytes from the small intestinal lamina propria at 27 days (Fig. 2B) and 56 days (Fig. 2C) of age. ILC3 were identified as cells that were CD45^{+}, CD11b^{-}, CD11c^{-}, CD19^{-}, CD3^{-}, CD4^{-}, RORγt^{+} and were either NKp46^{+} or NKp46^{-}. We observed a statistically significant reduction in the frequency of both NKp46^{-} and NKp46^{+} ILC3 from the lamina propria at both time points.

RANK$^{\Delta IEC}$ mice have reductions in IL-22 production from ileal tissue biopsies

Since previous data indicates that ILC3 are one of the major cellular sources of IL-22 in the gut [8,21,22], we hypothesized that the reduced frequencies of ILC3 we observed in RANK$^{\Delta IEC}$ mice might lead to reductions in IL-22 production in these mice. Punch biopsies from the terminal 2 cm of the ileum of 8-week-old RANK$^{\Delta IEC}$ and RANK $^{F/F}$ mice were cultured for 48 hours in the presence of rIL-23 to stimulate IL-22 production. Biopsy tissue isolated from RANK$^{\Delta IEC}$ mice produced 3- to 6-fold less IL-22 compared to equivalent samples from control RANK$^{F/F}$ mice (Fig. 3).

IL-22 dependent fucosylation of intestinal epithelial cells is lost in RANK$^{\Delta IEC}$ mice

Recent reports indicate that IL-22 signaling in intestinal epithelial cells initiates up-regulation of the fucosyltransferase FUT2 and induces protective fucosylation of intestinal epithelial cells.[23] Further investigation of this pathway has identified ILC3 as

the relevant population of IL-22 producing cells required for this fucosylation response [24]. Based on our observation that both production of IL-22 from ileal fragments and the frequency of ILC3 in the small intestinal lamina propria in $RANK^{\Delta IEC}$ were reduced, we hypothesized that IL-22-dependent protective fucosylation responses might likewise be affected. Intestinal epithelial cells were isolated from the proximal, middle and distal thirds of the small intestine of mice 8-10 weeks old under homeostatic conditions and stained with the lectin UEA-I, which binds to α-1-2 fucose linkages produced by FUT2. Flow cytometry revealed that there was a gradient of fucosylation present in intestinal epithelial cells from control mice (Fig. 4A, B), with the level of fucosylation being low in the proximal third of the small intestine and high in the distal third. This gradient, however, was absent in $RANK^{\Delta IEC}$ mice and instead these mice displayed low levels of fucosylation throughout the small intestine (Fig. 4C, D). Treatment of $RANK^{\Delta IEC}$ mice with rIL-22 for 6 hours was able to restore the gradient of fucosylation in intestinal epithelial cells, with the most dramatic increase in fucosylation apparent in the terminal third of the small intestine (Fig. 4E).

Endogenous expression of RegIIIβ and RegIIIγ is reduced in $RANK^{\Delta IEC}$ mice

In addition to inducing protective fucosylation IL-22 has been established as on of the key factors driving the production of anti-microbial peptides in intestinal epithelial cells.[25] RegIIIβ and RegIIIγ are two members of the Reg family of proteins. The bacteriostatic effects of RegIIIγ are able to attenuate infection from both gram-negative and gram positive bacteria [26], and promote the physical separation of the microbiota from intestinal epithelial cell [27] while the biological activity of RegIIIβ seems to only affect gram-negative microbes.[28] To follow up on our observation that protective fucosylation

in the terminal ileum was ablated in RANK$^{\Delta IEC}$ mice we investigated the expression of RegIIIβ and RegIIIγ in the small intestines of these mice via immunofluorescence and RT-qPCR. We found that there was a dramatic reduction in the expression of mRNA coding for both RegIIIβ and RegIIIγ in intestinal epithelial cells isolated from the middle of the small intestine and the terminal ileum (Fig. 5A,B). We then confirmed that protein expression of RegIIIβ was similarly reduced in tissues via immunofluorescence microscopy (Fig 5C). Additionally, we observed unaltered expression of cryptdins from epithelial cells of RANK$^{\Delta IEC}$ mice (Fig. S3).

IL-22 production by ILC3s in response to IL-23 stimulation is reduced in RANK$^{\Delta IEC}$ mice

We next assessed the functional capacity for the remaining ILC3 from RANK$^{\Delta IEC}$ mice to produce IL-22. Lymphocytes from the lamina propria and PPs were isolated from adult mice aged 8-10 weeks and stimulated for 4 hours with IL-23 (20 ng/ml) and PMA/ionomycin in the presence of brefeldin A. Intracellular cytokine stimulation was then carried out, and production of IL-22 was determined by flow cytometric analysis (Fig. 6A). We observed a significant reduction in IL-22 production from ILC3 isolated from the lamina propria or PPs of RANK$^{\Delta IEC}$ mice compared to RANK$^{F/F}$ mice (Fig. 6B).

RANK$^{\Delta IEC}$ mice are predisposed to develop systemic spread of intestinal bacteria

Approximately 10% of RANK$^{\Delta IEC}$ mice died within 10 days of weaning (21 days of age) in our facility at Emory University (Fig. 7A). Once past this 10-day post-weaning period, the remaining RANK$^{\Delta IEC}$ did not display any increased risk for mortality or other spontaneous manifestation of disease. We speculated that the cause of this mortality was

infectious in nature. To further investigate this phenotype we attempted to culture aerobic bacteria from the mesenteric lymph node, spleen, and liver. We found that there was increased bacterial translocation into systemic tissues in $RANK^{\Delta IEC}$ mice at 24 days of age (Fig. 7B). Fluorescent in situ hybridization of 24 day MLN samples with a probe (EUB338) detecting all Eubacteria 16S sequences confirmed increased bacterial translocation in $RANK^{\Delta IEC}$ mice by a culture-independent method (data not shown). We next sequenced the V1-V8 region of the 16S rDNA genes of the isolated aerobic bacteria and found that the predominant genera of bacteria that were translocating into systemic tissues were *Corynebacteria* and *Escherichia*. To confirm these results we performed 16S rRNA sequencing to identify the specific types of bacteria undergoing translocation (Fig. 7C). We found that the two dominant families of bacteria that were translocating to systemic tissues were *Enterobacteriaceae* and *Corynebacteriaceae*.

Discussion

The mechanisms underlying the maturation of CPs into ILFs are poorly understood. The observations that CPs are enriched for ILC3 suggests that there is a probable link between the maturation of CPs and ILC3; however, this possibility has not been investigated to our knowledge. Previously we reported that organized lymphoid structures including CPs, ILFs and PPs contained RANKL-expressing stromal cells and that this restricted bioavailability of RANKL mechanistically explained the restricted tissue distribution of intestinal M cells.[17,29] Furthermore, we reported that $RANKL^{-/-}$ mice had stunted maturation of CPs into ILFs and that in the absence of RANKL signaling the majority of CPs did not mature into ILFs.[18] However, these observations were made in mice with a global knockout of RANKL and it was impossible to determine if these CP maturation defects were a result of RANKL-RANK signaling in ILC3, populations of APCs or intestinal epithelial cells.

Here we report that the tissue-specific deletion of RANK in intestinal epithelial cells partially recapitulates the impaired small intestinal CP maturation phenotype of $RANKL^{-/-}$ mice. Based on our observations from $RANKL^{-/-}$ and $RANK^{\Delta IEC}$ mice, we conclude that RANKL-RANK signaling between cells in CPs as well as between CPs and adjacent RANK-expressing intestinal epithelial cells are both important for the maturation of CPs into ILFs. These results suggest a possible model in which RANKL produced locally in CP acts on developing intestinal epithelial cells to induce their terminal differentiation into M cells as well inducing other cells present in the maturing CPs to produce more RANKL. These CP-associated M cells could increase antigen sampling into CPs and facilitate their maturation into ILFs. The hypothesis presented

strongly suggests that M cells are the means by which total antigen and PRR ligands are acquired to drive maturation of CPs into ILFs.

The development of ILC3 is an area of intense debate, rife with seemingly contradictory and paradoxical observations. However, there are some facets of ILC3 development that have reached consensus. The transcription factors required for the development of ILC3 are the RAR-related orphan receptor RORγt [10] and the aryl hydrocarbon receptor.[11] Loss of either of these transcription factors leads to dramatic reductions in the population of ILC3 present in the intestinal lamina propria. The primary source of aryl hydrocarbon receptor ligands appears to be dietary in nature [15]; although some microbiome-derived metabolites have also been identified as AHR ligands.[30,31] Dietary restriction of food derived AHR ligands results in similar reductions in ILC3 to mice lacking AHR expression.[15] The functional maturation of ILC3 appears to be at least partially dependent on PRR signaling. Several reports indicate that ILC3 express functional a TLR2[32,33] and that the NK receptors NKp46 [34] and NKp44 [35], which are expressed on mouse and human ILC3 respectively, are able to sense unique bacterial products. Additionally, several cytokines produced either by intestinal epithelial cells or antigen presenting cells in response to PRR activation modulate ILC3 function including IL-7[36], IL-15[37], TSLP[38] and IL-23.[39]

The developmental relationship between CPs, ILFs and ILC3 appears to be very intimate. Many of the requirements for their development are shared. For example, mice lacking expression of AHR have reduced frequencies of ILC3 [11] and impaired development of CPs.[14] Similarly, in mice in which lymphotoxin signaling is interrupted either through genetic deletion or administration of blocking antibodies, the development

of CPs, ILC3 and ILFs is impaired.[40,41] Independent observations indicate that the microbiota is required for the maturation of CPs into ILFs [42] and the normal development of IL-22 producing ILC3.[8,43] Finally, altered expression of PRRs including TLRs and NLRs impedes the maturation of CPs into ILFs [16] while simultaneously impairing the function of ILC3.[44] Based on these observations we hypothesize that the development of both ILC3 and the maturation of CPs into ILFs are dependent on the same underlying biological factors.

We observed that a small fraction of $RANK^{\Delta IEC}$ mice died shortly after weaning. Furthermore, we found evidence for a breach in the containment of intestinal microbes and their subsequent escape into the systemic circulation in some apparently healthy $RANK^{\Delta IEC}$ mice shortly after weaning. While it is well established that IL-22 is a critical factor in the maintenance of barrier integrity at mucosal sites, we are not aware of any reports in which mice deficient in IL-22 or IL-22Rmice maintained under SPF conditions develop complications secondary to systemic spread of gut bacteria. Previously we reported that $RANK^{\Delta IEC}$ mice have a temporal delay in the initiation of intestinal IgA responses immediately after weaning. Thus, we hypothesize that $RANK^{\Delta IEC}$ mice are susceptible to developing systemic infections by commensal pathobionts because of a combination of poor IgA and IL-22 responses shortly after weaning. This hypothesis would indicate that simultaneous loss of IL-22 and IgA in the intestine (as a result of genetic deletions or antibody-mediated neutralization) may result in spontaneous escape of pathobiont bacteria from normal containment leading to systemic infection.

Our current study of $RANK^{\Delta IEC}$ mice indicates that the antigen sampling capacity of M cells is one contributing force behind both the development of ILC3 and the

maturation of CPs into ILFs. These findings add to our growing knowledge of how crosstalk between the microbiota and the mucosal immune system is achieved. It would appear that M cells play a central role in this process since we have now reported that M cells are required for the normal time-dependent development of IgA responses in the gut [19], the maturation of CPs into ILFs, and the development of IL-22-producing ILC3.

References

1. Mabbott, N. A., Donaldson, D. S., Ohno, H., Williams, I. R. & Mahajan, A. Microfold (M) cells: important immunosurveillance posts in the intestinal epithelium. *Mucosal immunology* **6**, 666-677, doi:10.1038/mi.2013.30 (2013).
2. Rescigno, M. *et al.* Dendritic cells express tight junction proteins and penetrate gut epithelial monolayers to sample bacteria. *Nature immunology* **2**, 361-367, doi:10.1038/86373 (2001).
3. Chieppa, M., Rescigno, M., Huang, A. Y. & Germain, R. N. Dynamic imaging of dendritic cell extension into the small bowel lumen in response to epithelial cell TLR engagement. *The Journal of experimental medicine* **203**, 2841-2852, doi:10.1084/jem.20061884 (2006).
4. Farache, J. *et al.* Luminal bacteria recruit CD103+ dendritic cells into the intestinal epithelium to sample bacterial antigens for presentation. *Immunity* **38**, 581-595, doi:10.1016/j.immuni.2013.01.009 (2013).
5. McDole, J. R. *et al.* Goblet cells deliver luminal antigen to CD103+ dendritic cells in the small intestine. *Nature* **483**, 345-349, doi:10.1038/nature10863 (2012).
6. Spits, H. & Di Santo, J. P. The expanding family of innate lymphoid cells: regulators and effectors of immunity and tissue remodeling. *Nature immunology* **12**, 21-27, doi:10.1038/ni.1962 (2011).
7. Spits, H. *et al.* Innate lymphoid cells--a proposal for uniform nomenclature. *Nature reviews. Immunology* **13**, 145-149, doi:10.1038/nri3365 (2013).

8. Satoh-Takayama, N. *et al.* Microbial flora drives interleukin 22 production in intestinal NKp46+ cells that provide innate mucosal immune defense. *Immunity* **29**, 958-970, doi:10.1016/j.immuni.2008.11.001 (2008).
9. Sciume, G. *et al.* Distinct requirements for T-bet in gut innate lymphoid cells. *The Journal of experimental medicine* **209**, 2331-2338, doi:10.1084/jem.20122097 (2012).
10. Sawa, S. *et al.* Lineage relationship analysis of RORgammat+ innate lymphoid cells. *Science* **330**, 665-669, doi:10.1126/science.1194597 (2010).
11. Qiu, J. *et al.* The aryl hydrocarbon receptor regulates gut immunity through modulation of innate lymphoid cells. *Immunity* **36**, 92-104, doi:10.1016/j.immuni.2011.11.011 (2012).
12. Zhong, C. *et al.* Group 3 innate lymphoid cells continuously require the transcription factor GATA-3 after commitment. *Nature immunology* **17**, 169-178, doi:10.1038/ni.3318 (2016).
13. Pabst, O. *et al.* Cryptopatches and isolated lymphoid follicles: dynamic lymphoid tissues dispensable for the generation of intraepithelial lymphocytes. *European journal of immunology* **35**, 98-107, doi:10.1002/eji.200425432 (2005).
14. Lee, J. S. *et al.* AHR drives the development of gut ILC22 cells and postnatal lymphoid tissues via pathways dependent on and independent of Notch. *Nature immunology* **13**, 144-151, doi:10.1038/ni.2187 (2012).
15. Kiss, E. A. *et al.* Natural aryl hydrocarbon receptor ligands control organogenesis of intestinal lymphoid follicles. *Science* **334**, 1561-1565, doi:10.1126/science.1214914 (2011).

16. Bouskra, D. *et al.* Lymphoid tissue genesis induced by commensals through NOD1 regulates intestinal homeostasis. *Nature* **456**, 507-510, doi:10.1038/nature07450 (2008).
17. Knoop, K. A. *et al.* RANKL is necessary and sufficient to initiate development of antigen-sampling M cells in the intestinal epithelium. *Journal of immunology* **183**, 5738-5747, doi:10.4049/jimmunol.0901563 (2009).
18. Knoop, K. A., Butler, B. R., Kumar, N., Newberry, R. D. & Williams, I. R. Distinct developmental requirements for isolated lymphoid follicle formation in the small and large intestine: RANKL is essential only in the small intestine. *The American journal of pathology* **179**, 1861-1871, doi:10.1016/j.ajpath.2011.06.004 (2011).
19. Rios, D. *et al.* Antigen sampling by intestinal M cells is the principal pathway initiating mucosal IgA production to commensal enteric bacteria. *Mucosal immunology*, doi:10.1038/mi.2015.121 (2015).
20. Nenci, A. *et al.* Epithelial NEMO links innate immunity to chronic intestinal inflammation. *Nature* **446**, 557-561, doi:10.1038/nature05698 (2007).
21. Cella, M. *et al.* A human natural killer cell subset provides an innate source of IL-22 for mucosal immunity. *Nature* **457**, 722-725, doi:10.1038/nature07537 (2009).
22. Luci, C. *et al.* Influence of the transcription factor RORgammat on the development of NKp46+ cell populations in gut and skin. *Nature immunology* **10**, 75-82, doi:10.1038/ni.1681 (2009).

23. Pickard, J. M. *et al.* Rapid fucosylation of intestinal epithelium sustains host-commensal symbiosis in sickness. *Nature* **514**, 638-641, doi:10.1038/nature13823 (2014).
24. Goto, Y. *et al.* Innate lymphoid cells regulate intestinal epithelial cell glycosylation. *Science* **345**, 1254009, doi:10.1126/science.1254009 (2014).
25. Zheng, Y. *et al.* Interleukin-22 mediates early host defense against attaching and effacing bacterial pathogens. *Nature medicine* **14**, 282-289, doi:10.1038/nm1720 (2008).
26. Loonen, L. M. *et al.* REG3gamma-deficient mice have altered mucus distribution and increased mucosal inflammatory responses to the microbiota and enteric pathogens in the ileum. *Mucosal immunology* **7**, 939-947, doi:10.1038/mi.2013.109 (2014).
27. Vaishnava, S. *et al.* The antibacterial lectin RegIIIgamma promotes the spatial segregation of microbiota and host in the intestine. *Science* **334**, 255-258, doi:10.1126/science.1209791 (2011).
28. Van Ampting, M. T. *et al.* Intestinally secreted C-type lectin Reg3b attenuates salmonellosis but not listeriosis in mice. *Infection and immunity* **80**, 1115-1120, doi:10.1128/IAI.06165-11 (2012).
29. Taylor, R. T. *et al.* Lymphotoxin-independent expression of TNF-related activation-induced cytokine by stromal cells in cryptopatches, isolated lymphoid follicles, and Peyer's patches. *Journal of immunology* **178**, 5659-5667 (2007).

30. Zelante, T. *et al.* Tryptophan catabolites from microbiota engage aryl hydrocarbon receptor and balance mucosal reactivity via interleukin-22. *Immunity* **39**, 372-385, doi:10.1016/j.immuni.2013.08.003 (2013).
31. Fukumoto, S. *et al.* Identification of a probiotic bacteria-derived activator of the aryl hydrocarbon receptor that inhibits colitis. *Immunology and cell biology* **92**, 460-465, doi:10.1038/icb.2014.2 (2014).
32. Takatori, H. *et al.* Lymphoid tissue inducer-like cells are an innate source of IL-17 and IL-22. *The Journal of experimental medicine* **206**, 35-41, doi:10.1084/jem.20072713 (2009).
33. Martin, B., Hirota, K., Cua, D. J., Stockinger, B. & Veldhoen, M. Interleukin-17-producing gammadelta T cells selectively expand in response to pathogen products and environmental signals. *Immunity* **31**, 321-330, doi:10.1016/j.immuni.2009.06.020 (2009).
34. Chaushu, S. *et al.* Direct recognition of Fusobacterium nucleatum by the NK cell natural cytotoxicity receptor NKp46 aggravates periodontal disease. *PLoS pathogens* **8**, e1002601, doi:10.1371/journal.ppat.1002601 (2012).
35. Esin, S. *et al.* Direct binding of human NK cell natural cytotoxicity receptor NKp44 to the surfaces of mycobacteria and other bacteria. *Infection and immunity* **76**, 1719-1727, doi:10.1128/IAI.00870-07 (2008).
36. Zhang, W., Du, J. Y., Yu, Q. & Jin, J. O. Interleukin-7 produced by intestinal epithelial cells in response to Citrobacter rodentium infection plays a major role in innate immunity against this pathogen. *Infection and immunity* **83**, 3213-3223, doi:10.1128/IAI.00320-15 (2015).

37. Cella, M., Otero, K. & Colonna, M. Expansion of human NK-22 cells with IL-7, IL-2, and IL-1beta reveals intrinsic functional plasticity. *Proceedings of the National Academy of Sciences of the United States of America* **107**, 10961-10966, doi:10.1073/pnas.1005641107 (2010).
38. Vonarbourg, C. & Diefenbach, A. Multifaceted roles of interleukin-7 signaling for the development and function of innate lymphoid cells. *Seminars in immunology* **24**, 165-174, doi:10.1016/j.smim.2012.03.002 (2012).
39. van Beelen, A. J. *et al.* Stimulation of the intracellular bacterial sensor NOD2 programs dendritic cells to promote interleukin-17 production in human memory T cells. *Immunity* **27**, 660-669, doi:10.1016/j.immuni.2007.08.013 (2007).
40. Taylor, R. T., Lugering, A., Newell, K. A. & Williams, I. R. Intestinal cryptopatch formation in mice requires lymphotoxin alpha and the lymphotoxin beta receptor. *Journal of immunology* **173**, 7183-7189 (2004).
41. Ota, N. *et al.* IL-22 bridges the lymphotoxin pathway with the maintenance of colonic lymphoid structures during infection with Citrobacter rodentium. *Nature immunology* **12**, 941-948, doi:10.1038/ni.2089 (2011).
42. Pabst, O. *et al.* Adaptation of solitary intestinal lymphoid tissue in response to microbiota and chemokine receptor CCR7 signaling. *Journal of immunology* **177**, 6824-6832 (2006).
43. Sanos, S. L. *et al.* RORgammat and commensal microflora are required for the differentiation of mucosal interleukin 22-producing NKp46+ cells. *Nature immunology* **10**, 83-91, doi:10.1038/ni.1684 (2009).

44. Van Maele, L. *et al.* Activation of Type 3 innate lymphoid cells and interleukin 22 secretion in the lungs during Streptococcus pneumoniae infection. *The Journal of infectious diseases* **210**, 493-503, doi:10.1093/infdis/jiu106 (2014).

Figures

Figure 1

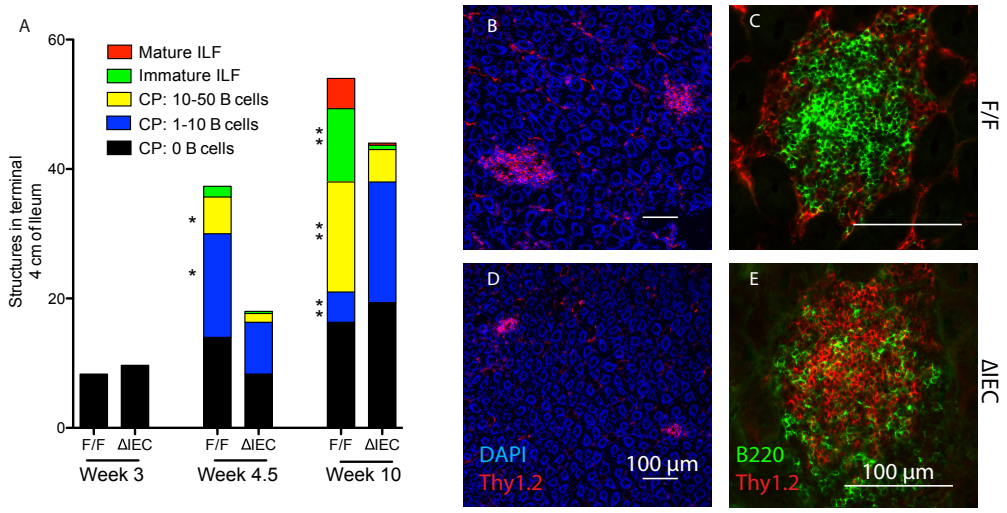

Impaired maturation of CPs into ILFs in RANK$^{\Delta IEC}$ mice

A, All lymphoid structures found in the terminal 4 cm of the ileum from RANK$^{F/F}$ and RANK$^{\Delta IEC}$ mice at 3, 4.5, and 10 weeks of age were assigned to 1 of 5 categories based on degree of maturation. Representative images of each of the five categories are shown in Fig. S1. Data at 3 weeks is from 1 experiment with 3 mice per group; data at 4.5 and 10 weeks is representative of 3 experiments with 3 mice per group. B, D, Representative low power immunofluoresence images (Thy-1.2 and DAPI) showing increased size of CPs in RANK$^{F/F}$ (B) compared to RANK$^{\Delta IEC}$ (D) mice at 10 weeks of age. C, E, Representative higher power images of ILFs of similar size from RANK $^{F/F}$ (C) and RANK $^{\Delta IEC}$ (E) mice showing more B cells and a greater degree of follicular organization in ILFs from RANK $^{F/F}$ mice at 10 weeks of age. *, $p \leq 0.05$ and **, $p \leq 0.01$ by Student's t-test

Figure 2

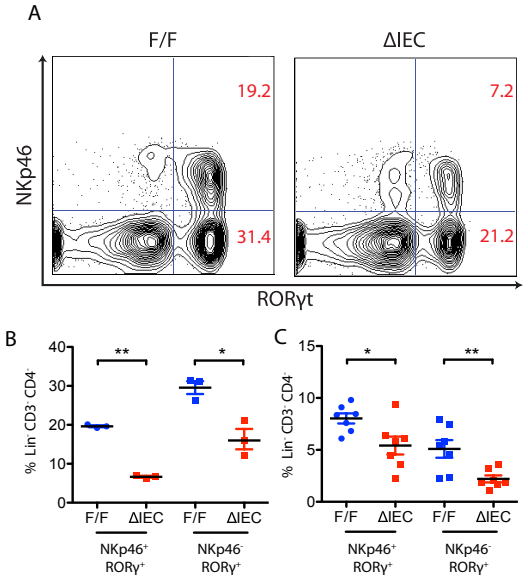

Frequency of ILC3 is reduced in the lamina propria of RANK $^{\Delta IEC}$ mice

A, Representative dot plots of the frequencies of RORγt^{+} ILC3 in RANK $^{F/F}$ and RANK $^{\Delta IEC}$ mice at 21 days of age. Plots shown were pre-gated on live CD45^{+} singlets that were negative for lineage markers (CD11b, CD11c, CD19, CD4 and CD3). B, C, Scatter plots showing the frequency of NKp46^{+} ILC3 and NKp46^{-} ILC3 from RANK$^{F/F}$ and RANK$^{\Delta IEC}$ mice at 28 days of age (B) and 70 days of age (C). The data in B is from 1 experiment with 3 mice per group and is representative of 2 experiments. The data in C is combined data from 2 separate experiments with a total of 7 mice per group. *, $p \leq 0.05$ and **, $p \leq 0.01$ by Student's t-test

Figure 3

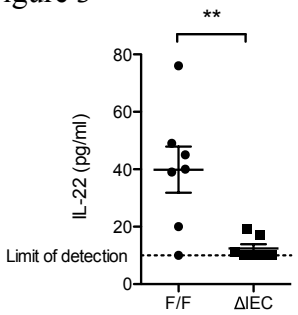

Production of IL-22 in the terminal ileum is reduced in RANK$^{\Delta IEC}$ mice

Punch biopsies harvested from the terminal 2 cm of the ileum from 8 week old RANK$^{F/F}$ or RANK$^{\Delta IEC}$ mice, were cultured for 48 hr in the presence of rIL-23 (20 ng/ml). IL-22 in culture supernatants was determined by sandwich ELISA. Data plotted is aggregated from 2 separate experiments with 3 and 4 mice per group. **, $p \leq 0.01$ by Student's t-test

Figure 4

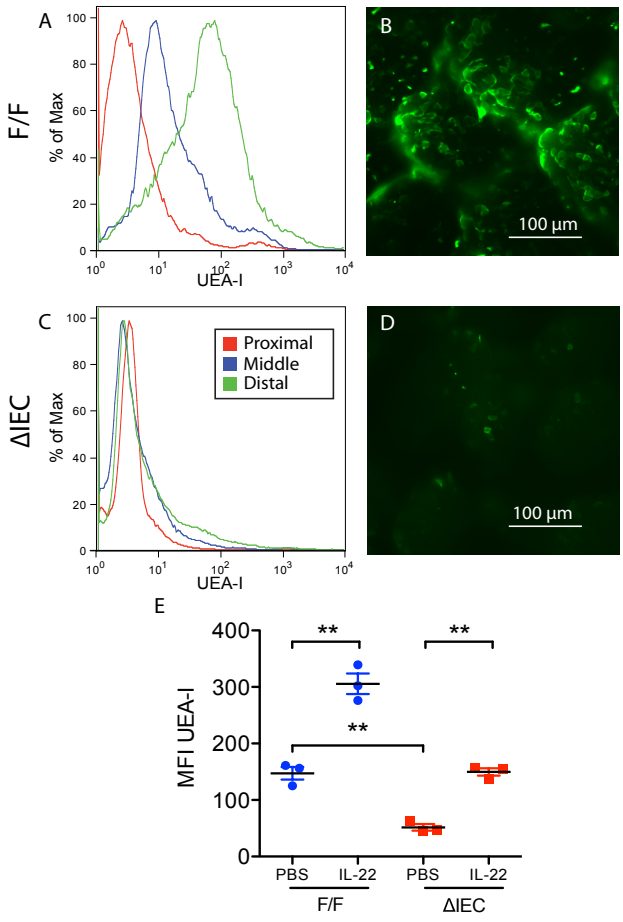

Endogenous IL-22 dependent fucosylation of the terminal ileum is reduced in RANK$^{\Delta IEC}$ mice

A, C, MFI of FITC-UEA-I staining of epithelial cells isolated from the proximal, middle or distal thirds of the small intestine from RANK$^{F/F}$ (A) or RANK$^{\Delta IEC}$ (C) mice. B, D Representative whole mount images of UEA-I staining of the terminal 1 cm of the ileum from RANK $^{F/F}$ (B) or RANK $^{\Delta IEC}$ (D) mice. E, Scatter plots of the MFI for FITC-UEA-I staining of ileal epithelial cells from RANK$^{F/F}$ and RANK$^{\Delta IEC}$ mice at baseline or 6 hours after a single IL-22 injection. Data shown is from 1 of 2 experiments using 3 mice per group, mice were 8-10 weeks old. **, $p \leq 0.01$ by Student's t-test

Figure 5

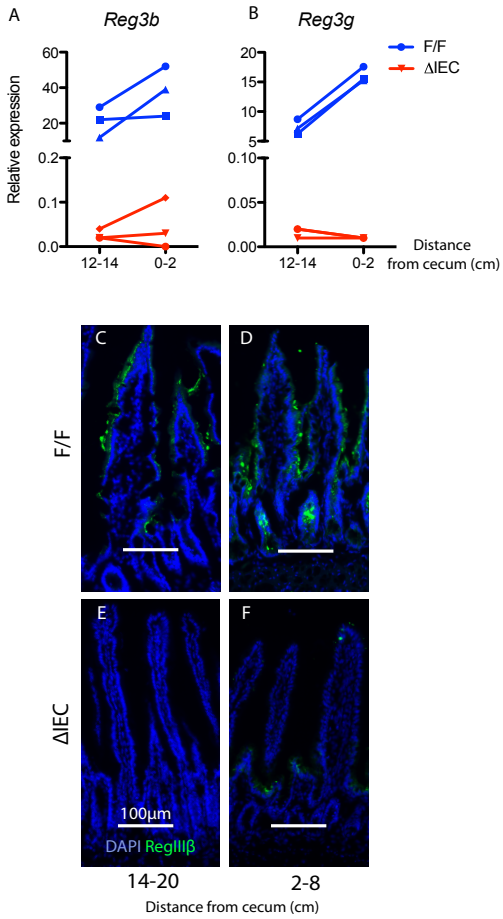

Endogenous expression of RegIIIβ and RegIIIγ in intestinal epithelial cells is reduced in RANK$^{\Delta IEC}$ mice

A, B, Intestinal epithelial cells were isolated from 2 cm long segments of the small intestine harvested from 0-2 cm and 12-14 cm away from the ileo-cecal junction. Expression levels of *Reg3b* (A) and *Reg3g* (B) mRNA relative to *Gapdh* were determined via real time quantitative PCR. C-F, Epithelial expression of RegIIIβ was detected via immunofluorescence microscopy on 5 µm sections of Swiss rolls prepared from segments of the small intestine harvested at 14-20 (C,E) and 2-8 (D,F) cm away from the ileo-cecal junction of RANK $^{F/F}$ (C,D) or RANK $^{\Delta IEC}$ (E,F) mice. All samples were taken from 8-week-old mice. Data is from 1 experiment with 3 mice per group.

Figure 6

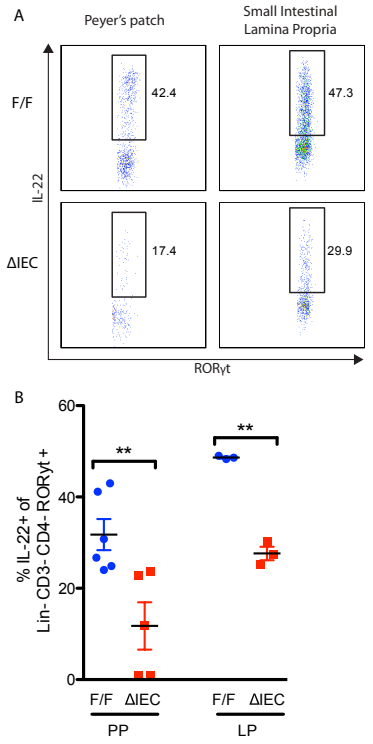

IL-22 production from ILC3 isolated from the lamina propria and Peyer's patches of RANK $^{\Delta IEC}$ mice is reduced

A, Representative dot plots of intracellular IL-22 in ILC3 isolated from the small intestinal lamina propria or PPs of RANK$^{F/F}$ and RANK$^{\Delta IEC}$ mice at 8-10 weeks of age. Cells were stimulated in vitro with 20 ng/ml rIL-23 in the presence of PMA, ionomycin and brefeldin A. Plots shown were pre-gated on live CD45^{+} and RORγt^{+} singlets that were negative for lineage markers (CD11b, CD11c, CD19, CD4 and CD3). B, Scatter plots showing the relative frequencies of IL-22 producing ILC3 in the indicated tissues. Data from PPs is representative of 2 experiments with 3 mice per group. Data from lamina propria is from 1 experiment with 3 mice per group. **, $p \leq 0.01$ by Student's t-test

Figure 7

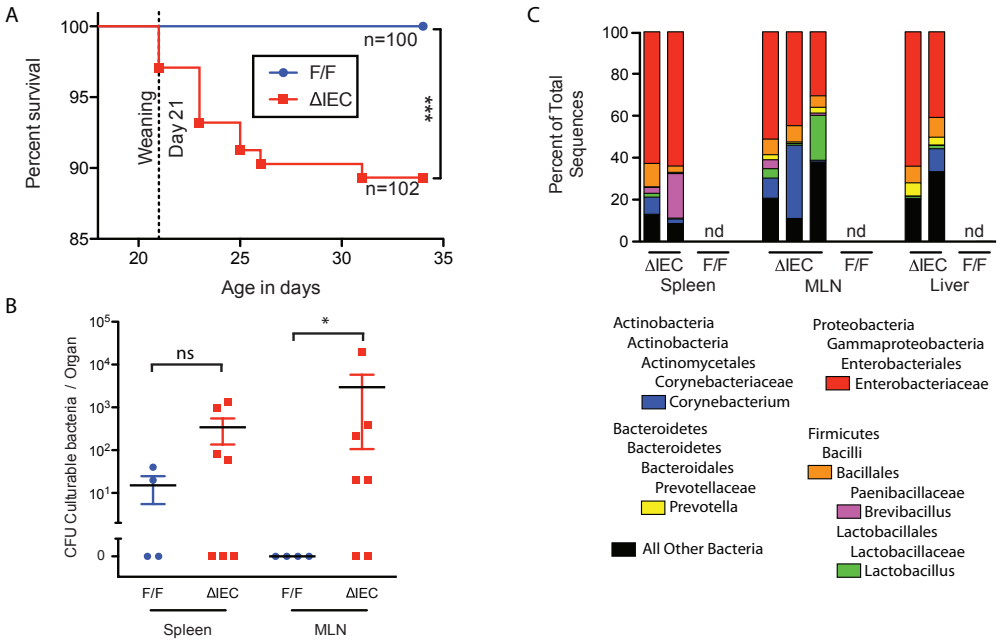

RANK$^{\Delta IEC}$ mice are susceptible to bacterial infection shortly after weaning

A, Kaplan-Meier survival curves for littermate RANK$^{\Delta IEC}$ and RANK$^{F/F}$ mice weaned at 21 days. The results are based on the outcome of 22 consecutive litters containing a total of 203 mice. ***, $p \leq 0.001$ by log-rank test. B, Frequency of bacterial colonies isolated from the MLNs and spleens of RANK$^{\Delta IEC}$ and RANK$^{F/F}$ mice based on samples obtained from 4 RANK$^{F/F}$ and 7 RANK$^{\Delta IEC}$ mice at 24 days of age. The data are representative of 1 of 2 similar experiments. *, $p \leq 0.05$ by Mann-Whitney test. C, Taxonomic classification of bacterial 16S rRNA sequences from MLN, spleen, and liver of RANK$^{\Delta IEC}$ mice at 24 days after birth. PCR amplimers were not detected (nd) using tissues from RANK$^{F/F}$ littermates.

Supplemental Figure 1

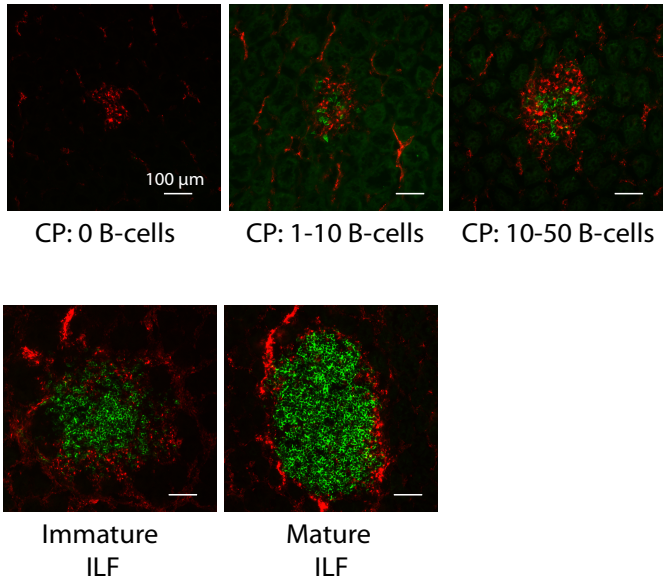

Representative images of 5 different categories of CPs and ILFs

Representative images demonstrating the characteristic appearance of each of the 5 classes of lymphoid aggregates distinguished on the basis of immunofluorescence staining for B220 (green) and Thy-1.2 (red). See Materials and Methods for a full description of the features of the 5 classes of lymphoid aggregates.

Supplemental Figure 2

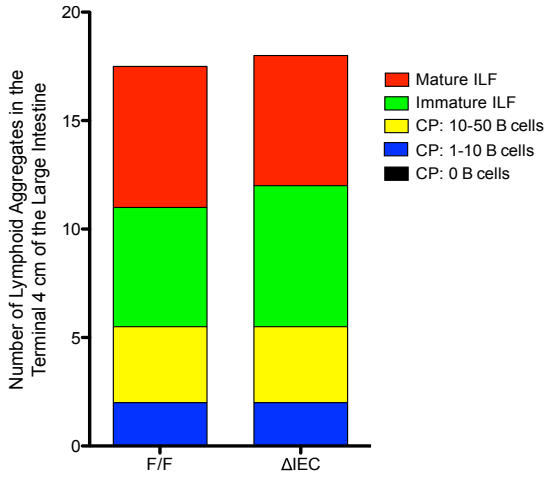

Development of lymphoid aggregates in the large intestine is unaffected in RANK$^{\Delta IEC}$ mice

Frequency of 5 classes of lymphoid aggregates in the terminal 4 cm of the large intestine from mice at 10 weeks of age.

Supplemental Figure 3

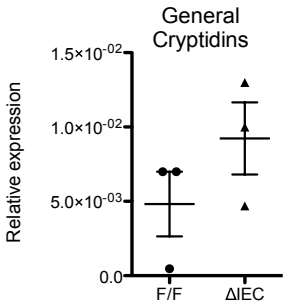

Expression of cryptdin mRNA is comparable in intestinal epithelium of RANK$^{\Delta IEC}$ and RANK$^{F/F}$ mice

Intestinal epithelial cells were isolated from the terminal 2 cm of the small intestine. Expression levels of cryptdins relative to *Gapdh* were determined via real time quantitative PCR. Data is representative of 1 experiment with 3 mice per group.

Discussion

The data presented in this thesis support a central role for M cells in mediating a dialogue between the host immune system and the intestinal microbiome. Our novel mouse model system of M cell deficiency has allowed for significant advances to be made in understanding M cell biology, and their role in the immune system. We find that M cells are critically required for the early initiation of IgA responses in the time shortly after weaning, priming of antigen specific responses against particulate model antigens, maturation of cryptopatches into isolated lymphoid follicles and, unexpectedly the development of and function of ILC3s. Our findings indicate that that M cells play an important, and non-redundant role, in the development of the mucosal immune system and maintenance of homeostasis in the intestine.

While there are several published models in which M cells are absent, these systems all have severe systemic defects. Mice lacking global expression of lymphotoxin β lack Peyer's patches (PP)[1], and as a result M cells. Similarly, *in utero* treatment of pregnant dams with soluble LT-βR-Ig at gestational days E14 and E17 results in selective developmental blockade of PP, while allowing for development of lymph nodes.[2] While these models allow for a dissection of the role of PPs in the context of mucosal and systemic immune responses, they do not allow for an isolated examination into the role of M cells into these processes. More recently our lab published data supporting a central role for the RANKL-RANK axis in the development of M cells. Mice lacking global expression of the co-stimulatory molecule RANKL lacked PP M cells, but still had intact

PPs. [3]. RANKL is a potent immunostimulatory molecule that plays critical roles in thymic selection of T cells [4] and osteoclast development [5] making these mice unsuitable for the study of M cells in normal immune responses. Using the Cre-loxP system we extended previous findings from our lab, that $RANKL^{-/-}$ mice lacked PP M cells, and generated a mouse in which RANK was deleted exclusively in intestinal epithelial cells. We found that specific deletion of RANK in tissues expressing Cre-recombinase under the villin promoter completely abrogated development of PP M cells. Using this model we were able to directly observe the consequences of loss of M cells on downstream immune outcomes without having to control for any off-target effects on the immune system.

There are multiple routes of antigen sampling postulated to play a role in facilitating crosstalk between host and microbiota. A fundamental question in mucosal immunology is what are the relative contributions of each of these discrete pathways to the maintenance of mucosal homeostasis, and how much redundancy can be found in these pathways. It has proven difficult to answer these questions, or even develop models in which these questions could theoretically be addressed. Our model represents the first example of a system in which a single pathway – the M cell route – of intestinal antigen sampling is removed, while the other pathways – enterocytes, goblet cells, mononuclear phagocytes – remain intact, thus allowing for the elucidation of the role of M cells in the generation of mucosal immune responses, relative to other antigen-sampling modalities.

The most striking feature of our model is the observed delay in the initiation of secretory IgA responses, and the reduction in the total quantity of IgA production in the absence of M cells. We believe that the capacity for M cells to sample large, complex

antigens, such as whole bacteria, mechanistically explain this observation. When M cell deficient mice were challenged intragastrically with 0.2 μm microspheres, or fluorescently-labeled bacteria, we observed dramatic reductions in the translocation of these model antigens into the PP indicating that M cells are required for efficient sampling of such forms of particulate antigen. It is important to note that sampling of these large particulate antigenic forms into PPs was not totally eliminated, thus indicating that while M cells are the most efficient means by which these antigenic forms can be acquired, other less efficient routes of acquisition also exist. Additionally we observed very little particulate antigen sampling in the diffuse villous epithelium in RANK $^{F/F}$ or RANK$^{\Delta IEC}$ mice, and no differences were observed in RANK$^{\Delta IEC}$ mice. The dramatic reduction in sampling of particulate antigens into PPs in the absence of M cells was directly linked to delayed formation of germinal centers in PPs. It is well established that PPs are the primary physiological location for IgA class switch recombination [6], however the relevant forms of antigen that initiate these responses, or how these antigens are acquired have remained poorly characterized. Our data suggest that M cell acquisition of large particulate antigen is a necessary first step in the efficient initiation of IgA class switch recombination in PPs, but in the absence of M cells other, less efficient routes of antigen sampling can still initiate IgA class switch recombination.

One paradoxical observation from our study is that even though initiation of fecal IgA responses are delayed in the absence of M cells, as a consequence of near total ablation of large particulate antigen sampling, they do in fact occur and reach levels only 2-3 fold less than normal controls in adulthood. There are several explanations for this apparent paradox. Other mucosal sites such as the nasal cavity and the urogenital tract

are thought to possess cells with similar particulate antigen sampling capacity to PP M cells, all of which would be unaltered in our model system. Recent evidence demonstrates the mouse nasal-associated lymphoid tissue (NALT) supports development and differentiation of epithelial cells that have functional properties similar to PP M cells, and share a differentiation program also characterized by the expression of the transcription factor Spi-B.[5] Homing to mucosal sites is controlled by interactions between the integrin α4β7 and the addressin MAdCAM-1.[7,8] All mucosal sites share this integrin-addressin pairing, such that responses primed at any mucosal sites can be disseminated to all mucosal sites. Therefore an undetermined quantity of the IgA found in the gut of M cell deficient mice may actually have been primed at a different mucosal site, potentially in response to particulate antigen sampling at these sites. Additionally, the specificity of IgA in M cell deficient mice may differ significantly from that of control mice. We observed that when fed the model particulate antigen equine ferritin, M cell deficient mice generated weaker antigen specific secretory IgA responses. Similarly we observed that the endogenous coating of the microbiota by IgA was reduced in M cell deficient mice. Taken together these observations suggest that the IgA repertoire being generated in M cell deficient mice may be very different from control wild-type mice. One factor confounding our study of the specificities of IgA in our model system is the relatively low level of affinity maturation observed in IgA and the high glycosylation levels of IgA. Compared to other isotypes of antibodies IgA generally has less accumulated mutations present in its CDR3,[9] thus conferring broad as opposed to highly targeted specificity. Additionally the high level of glycosylation of IgA allows for interactions between IgA and target antigen mediated by glycans instead of the immunoglobulin combining sites. A

full investigation of the IgA repertoire in M cell deficient mice would require high throughput techniques such as next-generation sequencing of the IgA repertoire in individual mice.

The majority of immune responses in the gut are induced by interactions with the commensal microbiota. As a result, mice reared under germ-free conditions have dramatic reductions in production of IgA.[10,11] The exact antigen being acquired, and subsequently priming IgA responses, by M cells have long been postulated to be commensal microbes. However, shortcomings in previous models of M cell deficiency have made investigation into this question essentially impossible. In our model system we observed that there were no differences in IgA responses between control and M cell deficient mice when housed in a germ-free setting. These results confirm that the primary antigenic targets M cells are acquiring are the bacteria compromising the intestinal microbiota.

In addition to PPs, M cells are also found on the FAE of isolated lymphoid follicles (ILF).[12] Previously our laboratory published data supporting a role for RANK-RANKL signaling in the development of small intestinal ILFs. $RANKL^{-/-}$ mice had a relative expansion of cryptopatches (CPs) and other immature forms of ILFs compared to more mature ILFs, although because a global knockout was used the exact mechanism behind these findings could not be determined.[13] Based on these previous findings, and the more recent findings described in chapter 1, we hypothesized that M cells may play a direct role in the processes underlying the maturation of CPs into ILFs.

Our findings that CP maturation into ILFs and the frequency and function of ILC3s are reduced in $RANK^{\Delta IEC}$ mice have interesting implications for the role of M cells

in the development of other parts of the mucosal immune system aside from IgA responses. Based on our current level of understanding of these processes we can only speculate as to the precise mechanisms by which M cell antigen sampling affect maturation of CPs into ILFs and the development and function of ILC3s. The observation that CP maturation into ILFs is partially dependent on the presence of M cells is similar to our observation that PPs from $RANK^{\Delta IEC}$ mice have delayed initiation of germinal center formation shortly after weaning. One critical difference between the development of PPs and ILFs is that PPs are permanent secondary lymphoid structures, while ILFs are transient tertiary lymphoid structures. Since PPs are permanent, the effect of loss of M cells on their maturation is manifest primarily as a kinetic delay as opposed to a different end-point. In contrast, it would appear that loss of M cells causes abortive maturation of CPs into ILFs, resulting in a deficiency in mature ILFs. Previous reports have indicated that loss of certain PRR signaling molecules [14], or lack of microbiota [15] have similar effects on the maturation of CPs into ILFs. Thus, it is likely that M cells are acquiring antigen that drives this maturation process and in their absence maturation is stunted.

Our observation that ILC3 are reduced in total frequency and in their functional capacity to produce IL-22 is more difficult to explain. CPs are composed primarily of ILC3s, and B cell trafficking to cryptopatches initiates maturation of CPs into ILFs.[16] Our data suggest that the maturation of CPs into ILFs has two distinct effects on the development of ILC3. First, maturation of CPs into ILFs causes expansion of the total ILC3 compartment. In the absence of M cells the maturation of CPs into ILFs is stunted and thus the total population of ILC3s is reduced. Second, we find that the remaining intestinal ILC3s isolated from M cell deficient mice produce less IL-22 than ILC3s

isolated from control mice. This observation indicates that maturation of CPs is required for ILC3s to attain their full effector function. Based on the composition of CPs and ILFs it is possible that ILC3-B cell interactions are required for full maturation of ILC3s, however this possibility has not been formally examined.

While our model system has provided valuable insights into the mechanistic workings of the mucosal immune, many questions still remain. These questions can be grouped into two categories: those pertaining to the basic workings of the immune system and those relating to pathogenesis of gastrointestinal infections. At this juncture it is unclear what role M cells play in shaping T cell responses in the intestine. Phenotypic characterization of Th17 and Tregs in mice lacking M cells did not reveal any significant perturbations when compared to control mice. Since T cells are primed by linear peptide fragments, it is possible that M cell sampling of complex large molecular weight antigens may have a relatively minor role in initiating T cell responses. Two other populations of cells that have been incompletely characterized in the absence of M cells are dendritic cells and macrophages. Phenotypic characterization of dendritic cell and macrophages in mice lacking M cells did not reveal any significant differences in population or tissue distributions. We hypothesized that the activation state of dendritic cells and macrophages would be reduced, particularly in PP, in mice lacking M cells due to a reduction in the total antigen load. However, we found no differences in the expression of MHC class I and class II molecules or the major co-stimulatory molecules (CD80 and CD86). Use of germ-free systems, paired with defined antigenic stimuli such as bacterial monocolonization, or intra-gastric administration of model antigens will be necessary to uncover the impact of M cells on dendritic cell and macrophage biology.

M cells are well known for their role in serving as a portal of entry for various gastrointestinal pathogens.[17-19] Much of this data has been generated by the observation that PPs serve as primary foci of infection, and many pathogens can be seen transiting through M cells to gain access to underlying tissues. However, data from mice lacking secondary lymphoid organs, including PPs and consequently M cells, indicates that M cells are not required for some infection as these mice generally have a similar or more severe phenotype compared to control mice.[20, 21] While currently available evidence seems to suggest that PPs may not be absolutely required for acquisition of a wide range of GI pathogens, these models do not preclude the development of structures other than PPs. Furthermore it is also possible that M cells may be absolutely required for some gastrointestinal infections, which, simply, have yet to be examined. Of course these comparisons come with a caveat – since these mice have severe systemic defects in priming immune responses the increased severity in GI infection in these models could be a consequence of a directly manipulated immune system. Use of our model system in an infectious setting will be necessary to understand the true role of M cells in GI infections. Obviously since our mice lack PP M cells, GI pathogens will be unable to gain access to the PPs via the M cell route. While this may restrict the ability of GI pathogens to cross the intestinal epithelium, the consequential effects this would have on the immune response are unclear. Since we have demonstrated that M cells are required for the initiation of total IgA responses and the generation of antigen specific IgA responses, we would speculate that M cell deficient animals challenged with a GI infection would have reduced production of anti-pathogen IgA and would be more sensitive to infection. The precise opposite argument could be made, that the reduction in crossing over the

epithelium would lead to a reduced disease burden thus making M cell deficient mice resistant to infection. Determination of the role of M cells in infection will require that M cell deficient mice are challenged with a wide range of gastrointestinal bacteria and viruses.

Since the success of the attenuated oral polio vaccine researchers have been striving to develop novel vaccines and therapies that can be delivered through the oral route. Unfortunately these attempts have given rise to very few additional licensed oral vaccines. Due to the massive total antigenic load present in the gut it is extremely difficult to generate specific immune responses to particular antigens at these sites. Our data, that equine ferritin is able to generate specific IgA responses in an M cell dependent manner, indicate that direct targeting of vaccines to M cells may be a required step in the generation of antigen specific responses in the gut. We speculate that it is the particulate nature of ferritin that confers its immunogenicity when given by the oral route. Based on these observations we believe that the use of technologies to encapsulate model antigens and potential vaccines into particulate forms may give rise to a new generation of oral vaccination and therapeutic strategies.

The data represented in this work represent a significant advancement in our understanding of the mucosal immune system. Here we have defined some of the critical non-redundant functions of M cells in the maintenance of mucosal homeostasis. At this juncture it is unclear what role M cells may play in human disease states because to date no disease phenotypes have been linked to absence or over-activity of Peyer's patch M cells. As M cells are positioned at the interfaces between the microbiome and the host immune system it is tempting to ponder the role that M cells may play a role in the vast

array of chronic diseases that plague mankind. Perturbations in mucosal homeostasis have been correlated to many chronic disease states and so it is not unreasonable to speculate that since M cells play a key role in the development of the mucosal immune system they may also be implicated as key players in the pathogenesis of chronic diseases. A fuller understanding of the biology of M cells will be required to fully understand the inner workings of the mucosal immune system, and may yield unexpected and valuable pathways for therapeutic interventions.

References

1 Alimzhanov, M.B. *et al.* Abnormal development of secondary lymphoid tissues in lymphotoxin beta-deficient mice. *Proc. Natl. Acad. Sci*., **94** , pp. 9302–9307 (1997)

2 Rennert, PD. *et al.* Lymph node genesis is induced by signaling through the lymphotoxin beta receptor. *Immunity* **1**, 71-79 (1998)

3 Knoop KA. *et al.* RANKL is necessary and sufficient to initiate development of antigen-sampling M cells in the intestinal epithelium. *J Immunology* **183**, 5738-47 (2009)

3 Rossi, S. W. *et al.* RANK signals from CD4(+)3(-) inducer cells regulate development of Aire-expressing epithelial cells in the thymic medulla. *J Exp Med* **204**, 1267-1272, (2007).

4 Boyce, B. F. & Xing, L. Biology of RANK, RANKL, and osteoprotegerin. *Arthritis Res Ther* **9 Suppl 1**, S1, (2007).

5 Mutoh, M. *et al.* RANKL regulates differentiation of microfold cells in mouse nasopharynx-associated lymphoid tissue (NALT). *Cell Tissue Res*, (2015).

6 Craig, W.S., Cebra, J.C., Peyer's patches: an enriched source of precursors for IgA-producing immunocytes in the rabbit. *J Ex Med.* **134**, 188-200 (1971)

7 Berlin, C. *et al.* Alpha 4 beta 7 integrin mediates lymphocyte binding to the mucosal vascular addressin MAdCAM-1. *Cell* **74**, 185-195 (1993).

8 Mestecky, J. The common mucosal immune system and current strategies for induction of immune responses in external secretions. *J Clin Immunol* **7**, 265-276

(1987).

9 Lindner, C. *et al.* Age, microbiota, and T cells shape diverse individual IgA repertoires in the intestine. *J Exp Med* **209**, 365-377, (2012).

10 Benveniste, J., Lespinats, G. & Salomon, J. Serum and secretory IgA in axenic and holoxenic mice. *J Immunol* **107**, 1656-1662 (1971).

11 Hapfelmeier, S. *et al.* Reversible microbial colonization of germ-free mice reveals the dynamics of IgA immune responses. *Science* **328**, 1705-1709, (2010).

12 Mabbot, N.A., Donaldson, D.S., Ohno, H., Williams, I.R. & Mahajan, A. Microfold (M) cells: important immunosurveillance posts in the intestinal epithelium. *Muc Immuno.* **4**, 666-677 (2013).

13 Knoop K.A., Butler B.R., Kumar N., Newberry R.D. & Williams I.R. Distinct developmental requirements for isolated lymphoid follicle formation in the small and large intestine: RANKL is essential only in the small intestine. *Am J Pathol* **179**. 1861-1871 (2011).

14 Bouskra, D., Brézillon, C., Bérard, M., Werts, C., Varona, R., Boneca, I.G. & Eberl G. Lymphoid tissue genesis induced by commensals through NOD1 regulates intestinal homeostasis. *Nature* **456**, 507-510 (2008)

15 Satoh-Takayama, N. *et al*. Microbial flora drives interleukin-22 production in intestinal NKp46+ cells that provide innate mucosal immune defense. *Immunity* **29**, 958-970 (2008)

16 Wang, C., McDonough, J.S., McDonald, K.G., Huang, C., Newberry, R.D. Alpha4beta7/MAdCAM-1 interactions play an essential role in transitioning

cryptopatches into isolated lymphoid follicles and a nonessential role in cryptopatch formation. *J Immunol* **181**, 4051-61 (2008)

17 Perdomo, O. J. *et al.* Acute inflammation causes epithelial invasion and mucosal destruction in experimental shigellosis. *J Exp Med* **180**, 1307-1319 (1994).

18 Jones, B. D., Ghori, N. & Falkow, S. Salmonella typhimurium initiates murine infection by penetrating and destroying the specialized epithelial M cells of the Peyer's patches. *J Exp Med* **180**, 15-23 (1994).

19 Nibert, M. L., Furlong, D. B. & Fields, B. N. Mechanisms of viral pathogenesis. Distinct forms of reoviruses and their roles during replication in cells and host. *J Clin Invest* **88**, 727-734, (1991).

20 Spahn, T. W., Eugster, H. P., Fontana, A., Domschke, W. & Kucharzik, T. Role of lymphotoxin in experimental models of infectious diseases: potential benefits and risks of a therapeutic inhibition of the lymphotoxin-beta receptor pathway. *Infect Immun* **73**, 7077-7088, (2005).

21 Nikitas, G. *et al.* Transcytosis of Listeria monocytogenes across the intestinal barrier upon specific targeting of goblet cell accessible E-cadherin. *J Exp Med* **208**, 2263-2277, (2011).